Clonal dynamics of TEL-AML1+ childhood ALL: an *in vivo* model

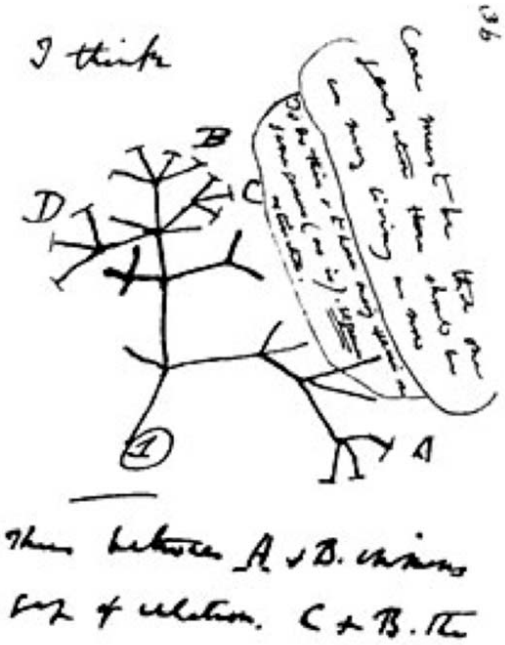

Virginia Turati

Molecular Haematology Unit
Weatherall Institute of Molecular Medicine
University of Oxford
Green Templeton College

A thesis submitted for the degree of Doctor of Philosophy 2014

DECLARATION

I hereby declare that this thesis is my own. Where other sources of information have been used, I confirm that these have been indicated in the thesis.

_____

ABSTRACT

ETV6–RUNX1 gene fusion is an early or initiating genetic lesion of Childhood Acute Lymphoblastic Leukaemia, followed, in disease progression, by a modest number of recurrent or ‘’driver’’ copy number alterations. Among patients diagnosed with this particular cytogenetic subtype of ALL cure rate reaches over 80%. However, treatment protocols are extremely demanding, and the molecular mechanisms driving drug-resistance and relapse in the remaining 10% of patient are still unknown. Recently a genetic signature of subclones arranged in a complex non-linear or branching architecture has been identified in this leukaemia, pioneering similar observations in many other cancer types. At present, most reports of this intratumor diversity represent static, in-depth snapshots of clonal diversity of tumours at a given time. “Real-time” longitudinal and spatial analysis of subclonal evolutionary dynamics is required to understand the functional characteristics of individual subclones. Such approach also promises to reveal the overall clinical relevance of this phenomenon.

This project therefore aims to understand whether genetically distinct subclones are also functionally different, particularly with respect to chemoresistance.

A mouse model that allows for the independent exposure of the same tumour to treatment multiple times, and the tracking of clonal dynamics by mean of a selected pool of genetic markers was established. While the analysis is still ongoing, preliminary data confirm that tumours generated from the same inoculum are highly similar in their genetic makeup across recipients, that multiple clones within a tumour can survive chemotherapy, but sensitivity of clones equally

represented within the bulk can vary, and unexpectedly that spatially segregated subclones can be identified in this model of liquid cancer. The complete analysis of the collected samples by mFISH as well as by single cell whole genome sequencing will provide unprecedented insight into the impact of cytotoxic treatment on intratumour genetic heterogeneity, and might reveal novel mechanisms of chemoresistance and relapse.

Additionally, a lentiviral overexpression system was designed to endogenously manipulate clonal interactions through the restored expression of *TEL* and *PAX5* in primary cells from patients, and evaluate their impact on clonal relationships and hierarchies and to validate the results obtained from the first part of the study. Lentiviral vectors for *TEL* and *PAX5* second hit overexpression were produced and tested by Western blot and qPCR. The TEL vectors were adopted in a preliminary *in vivo* experiment, showing no effect on overall engraftment ability.

TABLE OF CONTENTS

TABLE OF FIGURES

ABBREVIATIONS

AGM	intraembryonic aorta-gonad-mesonephros
2-ME	2-mercaptoehanol
ABL	Abelson murine leukaemia viral oncogene homolog 1
ABL1	Abelson murine leukaemia viral oncogene homolog 1
AKT	thymoma viral oncogene homolog
ALL	Acute Lymphoblastic Leukaemia
AML	Acute Myeloid Leukaemia
AML1	Acute myeloid leukaemia 1 protein
APC	Allophycocyanin
ASP	asparaginase
ATM	Ataxia telangiectasia mutated
B-ALL/B-LBL	B cell acute lymphoblastic leukaemia/lymphoma
BCL-2	B-cell lymphoma 2
BCL-X_L	B-cell lymphoma-extra-large
BCR	breakpoint cluster region
BLNK	B-cell linker
BM	Bone marrow
BMI1	polycomb ring finger oncogene
BMP	Bone morphogenetic proteins
BTLA	B- and T-lymphocyte attenuator
CBF	core binding factor
CDKN2A/CDKN2B	cyclin-dependent kinase inhibitor 2A/2B
CFU	colony-forming unit
CFU	Colony forming unit assay
ChIP	chromatin immunoprecipitation
CLL	chronic lymphoblastic leukaemia
CLPs	common lymphoid progenitors
CMPs	myeloid progenitor population
CNA	copy number alterations
CNS	central nervous system
CR	Complete remission
CSC	cancer stem cell
CSF	colony stimulating factor
DEPC	Diethylpyrocarbonate
DEX	Dexamethasone
DMEM	Dulbecco's Modified Eagle's medium
DMSO	Dimethyl sulfoxide
EBF-1	early B-cell factor 1
EDTA	Ethylenediaminetetraacetic acid
EFS	event-free survival
EPO	Erythropoietin
ERG	ETS-related gene

ETS	E-twenty six
ETV6	ETS translocation variant 6
FACS	fluorescence-activated cell sorting
FISH	Fluorescence in situ hybridization
FLT-3)	Fms-like tyrosine kinase 3
FOXO1	Forkhead box protein O1
GLI1	growth factor independence 1
GMPs	granulocyte/monocyte progenitors
GR	glucocorticoid receptor
HA	Hemagglutinin
HAT	Histone acetyltransferase
HCSs	Haematopoietic stem cells
HDACs	Histone deacetylases
hESCs	human embryonic stem cells
HLH	helix-loop-helix
HOXB4	Homeobox B4
HPCs	Haematopoietic progenitor cells
Hpgk	Human phosphoglycerate kinase eukaryotic promoter
HTLV	Human T-lymphotropic virus
iFISH	immune-fluorescence in situ hybridization
IFNs	Interferons
IgH	immunoglobulin heavy chain
IKZF1	IKAROS
IL	Interleukin
IL-2Rγ	interleukin-2 receptor gamma chain
IL-7R	IL-7 receptor
IT	Intrathecal
JAK	Janus kinase
KTLS	c-Kit^{+}/Thy1^{+}/lineage$^{-/lo}$/Sca1^{+}
LICs	leukaemia initiating cells
LMO2	LIM domain only 2
LMPPs	lymphoid-primed multipotent progenitors
LNGFR	low-affinity nerve growth factor receptor
LOH	loss of heterozygosity
LTRCs	long term reconstituting cells
MEPs	megacakaryotic/erythroid progenitors
MFI	Mean Fluorescence Intensity
mFISH	multiplex in situ hybridization assays
MLL	mixed-lineage leukaemia
MMP3	matrix metalloproteinase-3
MPLs	lymphoid progenitor cells
MPPs	multipotent progenitors
mTOR	mechanistic target of rapamycin
NK	natural killer
NOD/Lt	non-obese diabetic mice
p27^{KIP1}	cyclin-dependent kinase inihibitor 1B

PAX5	Paired box 5
PBS	Phosphate buffered saline
PBX1	pre-B-cell leukaemia homeobox 1
PcGs	polycomb group proteins
PDX	patient-derived xenografts
PI3K	Phosphatidylinositol 3-Kinase
PMTs	Phototomulipliers
pRb	retinoblastoma protein
PTEN	Phosphatase and tensin homolog
PU.1	purine box factor-1
PU.1	Transcription factor PU.1
PVDF	Polyvinylidenefluoride
qRT-PCR	quantitative Real-Time PCR
RAG1/2	recombination activating gene ½
RAS	Rat sarcoma
RBC	Red blood cells
RHD	Runt Homology Domain
RIPA	Radio-Immunoprecipitation Assay
RPMI	Roswell Park Memorial Institute
RUNX	Runt-related transcription factor
RUNX1	Runt-related transcription factor 1
SAM	sterile alpha motif
SB	Sleeping Beauty
SCID	severe combined immunodeficiency
shRNA	small hairpin RNA
SLAM	signalling lymphocyte activation molecule
SNP	single nucleotide polymorphism
SPIB	Spi-B transcription factor
STAT	signal transducer and activator of transcription
STRCs	short term reconstituting cells
TA	Transcriptional activating domain
T-ALL/T-LBL	T cell acute lymphoblastic leukaemia/lymphoma
TBS	Tris-buffered saline
TCF3	Transcription factor 3
TEL	translocation–Ets-leukemia
TPO	Thrombopoietin
VCR	Vincristine
VPREB1	Immunoglobulin iota chain
VXL	Vincristine/Dexamethasone/L-Asparaginase
WBC	white blood cells

ACKNOWLEDGEMENTS

I would like to thank my PhD supervisor, Prof. Tariq Enver for hosting me in his lab over the past four years. I especially value the intellectual freedom given to me during this time, offering the best possibility to grow my independence as a scientist.

I am also very grateful to all of the Enver lab members, for the support they have shown me along the path. I'm particularly thankful to Bernadett, Anja, Sara, Simon, Eli, Flo and Duncan for sharing with me the best and the worse of these years.

I'm also grateful to my co-supervisor, Prof. Sten Eirik Jacobsen, and to all the members of his lab, for always having made me feel "at home" during the frequent work commuting from London to Oxford.

Additionally, I'd like to thank Yanping, Petter and Oni for their patience and helpfulness as teachers, as well as Rachel and Gill for their key feedback.

My deepest thank you goes to my parents and my brother, for always being the best supporters anyone could desire!

Last but not least, a heartfelt thank you to Maurizio.

CHAPTER 1

INTRODUCTION

1.1 Haematopoiesis

Blood is a tissue that has very high turnover, with around one trillion (10^{12}) cells produced daily in the bone marrow (BM) (Rieger and Schroeder, 2012). Blood cells belong to a variety of distinct blood cell types, which can be classified into two major subgroups: red and white blood cells (RBC and WBC). Red blood cells, also called erythrocytes, are the most highly represented cells in the blood. Their primary functions include delivery of oxygen to and removal of carbon dioxide from the tissues. White blood cells can further be classified into granulocytes (myeloid cells such as neutrophils, basophils and eosinophils) and agranulocytes (like lymphoid cells and monocytes). There are two different types of lymphocytes: B cells, responsible for the antibody–mediated immune response, and T cells, responsible for the cell-mediated immune response. In the blood, lymphocytes account for only 1% of the total volume while erythrocytes represent 45%. The process that supplies the human body with all of these different cell types, and in the correct relative amount both to maintain normal homeostasis and in response to environmental stress, is called haematopoiesis. Despite being incredibly diverse, all blood cells are derived from a common precursor cell type called the haematopoietic stem cell (HSC). HSCs sit at the top of a hierarchy of multipotent lineage progenitors that progressively become restricted to single lineages as they differentiate, and eventually give rise to mature cells (Doulatov et al., 2012; Orkin, 2000). As the hematopoietic system must be able to respond to environmental and physiological challenges by adapting the volume and ratios of blood cells it produces, haematopoiesis is a dynamic process that is tightly controlled by a wide variety of regulatory signals involving cell-cell communication via the production of secreted proteins called cytokines. In addition to being

responsible for the production of differentiated blood cells, HSCs carry out a second fundamental job: they self-renew in order to maintain a constant pool of HSCs. Validation of a stem cell as such therefore requires that it operationally displays both extensive self-renewal and differentiation abilities when transplanted into sublethally irradiated mice. Stem cells that possess these abilities are extremely rare, representing less than 0.05% of bone marrow cells (Spangrude et al., 1988). In the mouse model it has also been possible to subclassify the HSCs into two different categories: long-term reconstituting cells (LTRCs), which can repopulate the mouse immune system for longer than 12 weeks, and short term reconstituting cells (STRCs), which are capable only of transient engraftment.

The original pool of HSCs is produced during embryogenesis in different embryonic tissues and sites (the yolk sac, the aorta-gonad-mesonephros region, the placenta and the foetal liver) at different times during development. The first blood cells, mostly erythrocytes and macrophages, are produced in the extraembryonic yolk sac in specific structures called “blood islands” (Moore et al., 1973). These cells are part of a transient population of progenitors responsible for the so-called “primitive haematopoiesis”. The erythroid cells generated by this first hematopoietic wave differ from adult cells in that they are bigger, rounder, nucleated and express embryonic globin proteins. Their role is to enable tissue oxygenation in the rapidly growing embryo. No lymphoid cells are produced by these progenitors. The second and “definitive” wave of haematopoiesis produces different progenitor cells detectable in the foetal liver at mid-gestation, and subsequently in the bone marrow. Foetal haematopoiesis must concomitantly meet the dual requirements of generating differentiated blood cells necessary for the growth and survival of the developing embryo and producing a stock of HSCs

outside of the yet to be formed specialized postnatal haematopoietic niches. Given the complexity of the task, while the liver is the main site of foetal haematopoiesis, other regions are involved. Several studies have shown that the intraembryonic region called aorta-gonad-mesonephros (AGM) gives origin to clusters of HSCs forming the definitive haematopoietic stem cell population (Dieterlen-Lievre and Martin, 1981; Dzierzak and Medvinsky, 1995). This region consists of the dorsal aorta, its surrounding mesenchyme and the urogenital ridges, and HSCs emerge asymmetrically from a functional niche localized in the ventral region of the AGM (Ivanovs et al., 2014). Within a short time from their emergence in the AGM, HSCs can be found also in the yolk sac, placenta and foetal liver. Several studies have suggested that HSCs can in fact independently originate from the yolk sac, placenta and AGM, from which they then migrate to the foetal liver. By week 5 post-conception haematopoiesis fully resides in the foetal liver, while following birth the bone marrow represents the main site of HSC-derived homeostatic haematopoiesis in the human (Wang and Wagers, 2011) (Figure 1-1).

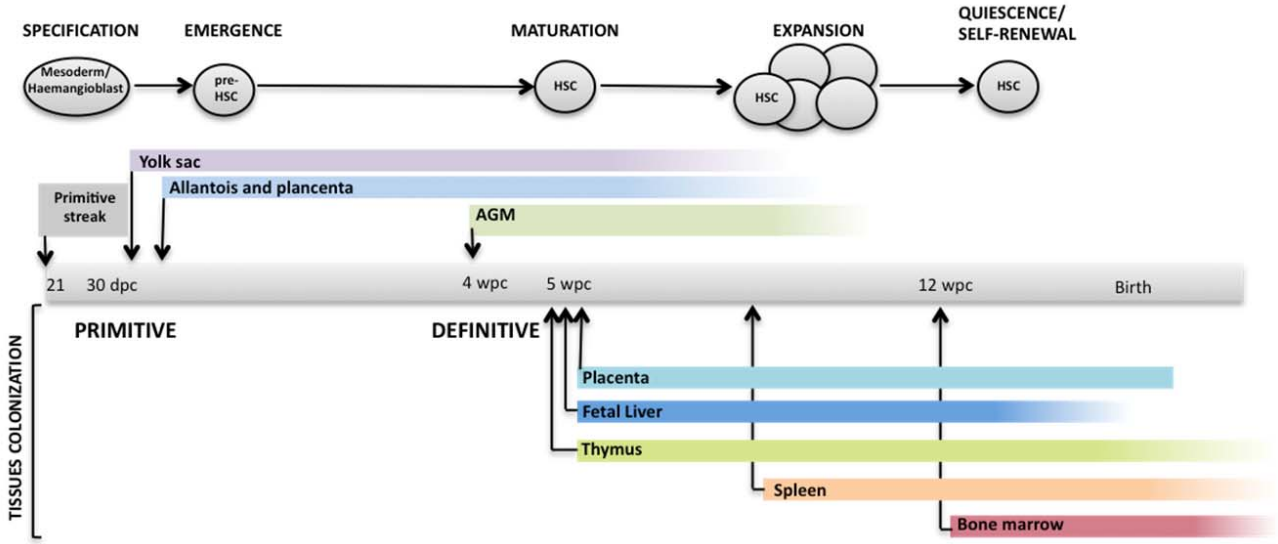

Figure 1-1: Detailed timeline of primitive and definitive haematopoiesis in human embryos [Adapted from (Wang and Wagers, 2011)]. Embryonic haematopoiesis is a multistep process characterized by two main waves: primitive and definitive. While primitive haematopoiesis mainly generates red blood cells, a pool of HSCs responsible for the lifelong production of blood cells is the output of definitive haematopoiesis. The development starts at specification of primitive streak mesoderm into hematopoietic and vascular fates. Emerging HSCs undergo a maturation process that allows them to home, survive and self-renew in different anatomical niches. Subsequently, fetal HSCs expand rapidly, until they home into the bone marrow and enter a state of relative quiescence. AGM: aorta–gonad–mesonephros; dpc: days post-conception; wpc: weeks post-conception.

The relationship between the primitive and definitive stages of human haematopoiesis is still debated. It is possible that the first HSCs that colonise the liver hail from the yolk sac and that all blood cells in the embryo, foetus and adult are actually derived from a single small pool of cells during development. These cells would then be replaced by the AGM-derived cells, which colonise the spleen, and, at birth time, the bone marrow, the thymus and all the other regions known as haematopoietic organs. However, only the direct imaging of the cells migration would definitively prove this hypothesis.

Some cells, such as maturing lymphoid cells, complete their maturation in the lymphoid tissues, including the lymph nodes and the spleen, while erythroid cells undergo differentiation in the bone marrow and get released into the circulation only once this process is fully completed.

As the sites of haematopoiesis change during embryonic development, the environment to which stem cells are exposed in each is likely to differ. The importance of understanding the key characteristics of these sites has become very clear after it was shown that stem cells, both during primitive and definitive haematopoiesis, are highly dependent on inputs from the cellular microenvironment. Microenvironments that are able to support HSC survival, self-renewal, quiescence and differentiation, are called niches (Schofield, 1978). The niche concept includes the specific cell types, anatomical locations, soluble molecules, signalling cascades and gradients, as well as physical factors, such as shear stress, oxygen tension and temperature, that sustain homeostatic HSC self-renewal at different stages of their ontogeny.

In vivo imaging of individual HSCs arising from the AGM strongly supports the *haemogenic endothelium* hypothesis, which postulates that HSCs arise directly from committed endothelial cells (ECs). This theory is only partially related to the previously suggested haemangioblast hypothesis, which posited the existence of a shared common bipotent precursor for both vasculature and blood cells. The studies additionally suggested that the ECs that do not convert into HSCs can provide those that do, and that rather than entering aortic circulation remain embedded within the endothelium, with their first niche. When distinct somatic endothelial precursors colonize the AGM its haematopoietic potential is revoked. The molecular mechanisms that then allow the production of HSCs by the yolk sac and placenta are not yet defined, but by analogy with the AGM, it is possible that these also originate from heamogenic endothelium. The factors responsible for the homing of HSCs to the foetal liver have not yet been fully defined either. However, the chemokine CXCL12, expressed by stromal cells, and its G-protein coupled receptor CXC chemokine receptor 4 (CXCR4 or CD184), expressed by haematopoietic cells, have been shown to be required for proper HSCs functioning and migration, not just to the foetal liver. Similarly, the signalling cascade activated by the cytokine SCF, secreted by stromal cells, and its receptor KIT (also called CD117), expressed on the membrane of multipotent haematopoietic cells, is not only crucial to HSCs activity, but is also enhances foetal HSC responsiveness to CXCL12. Additional factors capable of activating WNT signalling (e.g. α4 integrin, neural cadherin (N-cadherin), and osteopontin) and other key pathways are also likely to be involved in these processes.

To date the adult bone marrow remains the best-characterised human HSC niche. Haematopoiesis relocation to this specialized tissue only occurs following

the development of osteoblast and chondrocyte precursor cells, which enable the formation of the HSC niche. This observation further supports a co-developmental model of HSCs and niche cells mediated by their interaction throughout ontogeny. The departure of HSCs from the foetal liver and their homing to the newly formed bone marrow niche is at least partially mediated by the CXCL12-CXCR4, SCF-KIT, TIE2-angiopoietin, integrin and CD44-epithelial cadherin (E-cadherin) adhesion signalling cascades. The bone marrow is structurally complex, and data collected so far recognize the existence within it of multiple microenvironments suitable to host HSCs in postnatal life. The trabecular regions of the bone marrow are home to many HSCs, which reside in, or in proximity to the endosteum (a thin layer of tissue lining the medullary cavity), adjacent to the osteoblasts (Suda et al., 2005). This represents the so-called ‘‘endosteal niche’’. Additionally, HSCs have also been found to reside in proximity to the sinusoidal blood vessels (Kiel et al., 2005), within the so-called “”vascular niche””. If canonically the different niches were though to be anatomically isolated and home to specific cell types uniquely suitable to produce key factors necessary to local HSCs maintenance, recent advances suggest that perhaps these sites are interlaced, and provide the cells with redundant sources of microenvironmental cues. Imaging data have for example recently demonstrated that although following transplantation LT-HSC preferentially reside by the endosteal region of the BM both in the calvarium and in the long bones, this area is also located in close proximity to perivascular cells, concomitantly exposing the HSCs to the two microenvironments. However, transplantations models might not reflect the true physiology of endogenous HSCs, and it is possible that each niche represent a discrete entity, to which,

depending on the type of locally released factors, HSCs with different functional abilities are homed.

Significant progress has been made in understanding the composition of the adult bone marrow HSC niches. Genetic manipulation, for example, showed that the Bone morphogenetic proteins (BMP) pathway, responsible for an increase in the number of osteoblasts, also impacts HSC production, highlighting the fundamental role of this cell type in HSC maintenance (Calvi et al., 2003; Zhang et al., 2003). This is not entirely surprising since osteoblasts not only secrete cytokines which support HSC survival and differentiation, such as granulocyte colony-stimulating factor (G-CSF), granulocyte-macrophage CSF (GM-CSF) and interleukin-6 (IL-6), but also express factors like angiopoietin, thrombopoietin, WNT, Notch, N-cadherin, and osteopontin, which can directly affect HSC production. However, the ability of HSCs to self-renew and differentiate during foetal development, even before the formation of the trabecular bone marrow, shows that during most of gestation these cells are maintained in the absence of osteoblast cells. Interestingly, studies showing that Casr (calcium sensing receptor) knockout mice are unable to establish proper BM haematopoiesis suggest that HSCs engrafting the endosteal bone surface can sense Ca^{2+}(Adams et al., 2006). Within the perivascular niche several cell types, like mesenchymal stem cells (MSCs), CXCL12-aboundant reticular cells (CAR cells) and neural cells have been shown to regulate HSC function.

The overall picture is that the regulation of self-renewal, proliferation and differentiation of a system as dynamic as the haematopoietic is likely equally driven by cell-intrinsic processes, such as cell cycle regulators (i.e., Bmi1, p53, p21) and the PI3-kinase signalling pathway (e.g. ATM, PTEN, mTOR, FoxO),

microenvironmental cues, requiring complex interactions between multiple stromal cell types, and non-cell autonomous developmental pathways such as TGF-β, Wnt, Hedgehog and Notch. A better comprehension of the mechanisms of niche-dependent regulation of HSC activity is particularly important in light of the observation that blood malignancies can arise though alterations of the niche (Wang and Wagers, 2011). These can be responsible for the haematopoietic dysregulation, to which mutations in the HSC population contribute only as secondary events. A compelling example of this phenomenon is the development of myelodysplasia (in few cases with the progression of the same to myeloid leukaemia) induced by the disruption of miRNA processing in the osteoblast population (Raaijmakers et al., 2010). Additionally, changes in the cells that form the microenvironment (e.g. increased mTOR signalling and ROS production) were shown to synergize with HSC-intrinsic modifications in the insurgence of aging-induced alterations into the HSC population, including the accumulation of phenotypic HSCs with reduced repopulating abilities and a differentiation bias towards myelopoiesis rather than lymphopoiesis (Chen et al., 2009; Wagner et al., 2008).

Most of our knowledge of haematopoiesis comes from the mouse, as functional repopulation assays were once the only technique allowing the identification and quantification of HSCs, making the study of human HSCs extremely challenging. More recently however, the development of xenotransplantation models and of more reliable *in vitro* clonal assays, as well as the identification of surface markers for the purposes of cell sorting have facilitated enormous progresses towards the understanding of human blood formation (Orkin and Zon, 2008). Although the gold standard technique to validate the stem cell

nature of a cell remains the mouse repopulation assay, thanks to technologies like monoclonal antibodies and fluorescence-activated cell sorting (FACS) it is now possible to prospectively isolate HSCs on the basis of their unique signature of cell surface markers.

Even though there are many similarities between human and mouse haematopoiesis, HSC activity in the two species lies within populations identified by different surface markers. Mouse HSCs were first defined as a population of bone marrow cells marked by $cKit^{+}/Thy1^{+}/lineage^{-/lo}/Sca1^{+}$ (KTLS) (Morrison and Weissman, 1994). This heterogeneous KLTS population is composed of LTRCs, STRCs, and multipotent progenitors (MPPs), which lack any self-renewal potential. These three subpopulations can be further distinguished with the use of additional surface markers. KTLS cells that are also $CD34^{-}$ correspond to LTRCs, and can be alternatively defined through the use of lymphocyte activation molecules (SLAM family) as $CD150^{+}/CD48^{-}$ (Kiel et al., 2005). LTRCs correspond to 1 in 2/3 of the KTLSs. In contrast, a heterogeneous population enriched for human HSCs can be purified from umbilical cord blood, foetal liver, foetal bone marrow, adult bone marrow, placenta and mobilised peripheral blood as $CD34^{+}/Thy1^{+}/cKit^{low}/CD38^{-}$ (Baum et al., 1992). However, a higher purity population of human HSCs can be found within the $Lin^{-}/CD34^{+}/CD45RA^{-}/CD90^{+}/Rhodamine123^{low}/CD49f^{+}$ population (Notta et al., 2011a). Both these signatures have however been challenged by a recent paper suggesting that an even more primitive population of human HSCs can be detected in the bone marrow as $CD34^{-}$, similar to the mouse (Anjos-Afonso et al., 2013).

The self-renewal properties and multilineage potential of HSCs gradually disappear as cells proceed through various multilineage, oligolineage and

unilineage stages and eventually commit to erythroid, myeloid or lymphoid identity. According to the classical model of haematopoiesis, the first population to arise from HSCs is a subset of multipotent progenitors (MPPs) that retain transient multi-lineage differentiation potential, but are distinguishable from their HSC ancestors in that they lack self-renewal ability (Reya, 2003). This population has been described both in human and mouse. MPPs subsequently further originate two distinct populations of strictly separated progenitors. The first one, an early lymphoid progenitor cell population, the common lymphoid progenitors (CLP) ($Lin^{-}IL7R\alpha^{+}SCA\text{-}1^{lo}KIT^{lo}$), is restricted towards the lymphoid lineage. The second one, the common myeloid progenitor population (CMP) ($Lin^{-}SCA\text{-}1^{-}KIT^{+}IL7R\alpha^{-}Fc\gamma R^{lo}CD34^{+}$), gives rise to GMPs and megakaryocyte/erythroid progenitors (MEPs), which can in turn commit towards the granulocyte/monocyte (GM) and erythrocyte/megakaryocyte (MegE) lineages respectively (Doulatov et al., 2012).

More recently however, evidence that the separation into common myeloid and lymphoid pathways might not be the first lineage commitment step of hematopoietic stem cells (HSCs) has been obtained through the identification of myelo-lymphoid commitment within the MPP fraction of LSK cells that express FMS-like tyrosine kinase 3 (FLT3) at high levels (Buza-Vidas et al., 2011). Such analysis has proven the existence of a CMP-CLP-independent pathway for lymphoid lineage commitment, proving the existence of a population with robust and combined B and T lymphoid, as well as GM potential, but little or no MkE potential. MLPs/LMPPs can hence produce B and T lymphocytes and natural killer (NK) cells, as well as granulocyte/monocyte progenitors (GMPs) or fully differentiated myeloid cells (Adolfsson et al., 2005), implicating a close

developmental relationship between the lymphoid and GM lineages. The population, first defined in the mouse, has been named lymphoid-primed multipotent progenitors (LMPPs), while its human counterpart is termed MLPs (multipotent lineage progenitors).

MPPs, have since then been further characterised as a heterogeneous population composed of distinct subfractions with different lineage differentiation potentials. Through the combined use of VCAM-1 and Flt3, Lai and Kondo further subdivided the MPP population into 3 distinct subsets, $Flt3^{lo}VCAM\text{-}1^{+}$, $Flt3^{hi}VCAM\text{-}1^{+}$, and $Flt3^{hi}VCAM\text{-}1^{-}$ MPPs, with variable *in vivo* differentiation potentials (Lai and Kondo, 2006; Lai et al., 2005). $Flt3^{lo}VCAM\text{-}1^{+}$ MPPs represent true multilineage progenitors, with the ability to give rise to MegE, GM, and lymphoid lineages, $Flt3^{hi}VCAM\text{-}1^{+}$ MPPs have lost MegE differentiation potential, but retain high GM and T/B differentiation potential both *in vitro* and *in vivo,* while Flt3hi MPPs are endowed with small MegE potential residing in a subset of cells that that expresses the thrombopoietin receptor (Lai and Kondo, 2006).

1.1.1 Molecular basis of haematopoiesis

Transcription factors play key roles during haematopoiesis as intrinsic determinants of stem cell maintenance, lineage commitment and differentiation. A full understanding of their mechanisms of action would therefore provide an insight into how HSCs develop during embryogenesis and how lineage-restricted differentiation works (Orkin, 2000). Even though they are maintained in undifferentiated state, HSC are not fully lacking of elements linked to maturation; and in a process defined as lineage-priming they are maintained responsive to

environmental cues promoting differentiation through low-level expression of lineage-associated genes and activating epigenetic markers (van Galen et al., 2014). Relevant data collected so far are mainly derived from gene knockout experiments in mice, from overexpression experiments and from the analysis of other model organisms (e.g. Zebrafish, Drosophila, Xenopus). Among the transcription factors identified as key to the formation and proper function of HSCs are SCL/Tal1, IM domain only 2 (LMO2), mixed lineage-leukaemia gene (MLL), Runt-related transcription factor 1 (RUNX1), and E-twenty six (Kheifets et al.) translocation variant 6 (TEL/ETV6). SCL/tal-1 and LMO2 are extremely important for both primitive and adult haematopoiesis as they are required for the specification of haemangioblasts, the embryonic precursors of hematopoietic cells, and in their absence blood cells are not produced (Kim and Bresnick, 2007). MLL and RUNX1 are required for the production of HSCs in the AGM (Orkin, 2000). Lack of *Runx1* affects the formation of HSC clusters in the dorsal aorta of mouse embryos. This observation is consistent with other findings, as this factor lies downstream of the NOTCH signalling cascade, activity of which was shown to be key in triggering haematopoiesis in Zebrafish (Burns et al., 2005). MLL is involved in supporting Homeobox (HOX) gene activity once it is switched on, and HOXB4 (and possibly other HOX genes) induce its expression during HSC specification. When overexpressed in mouse HSCs, HOXB4 can push cells towards symmetric division and increases stem cell production by around 1,000-fold on its own (Antonchuk et al., 2002). Unfortunately, the transduction of human $CD34^+$ cells with HOXB4 overexpression vectors is not sufficient to reproduce a similar effect (only a 4-fold expansion is observed) (Amsellem et al., 2003; Buske et al., 2002).

The decision making process begins with extracellular stimuli in the shape of hematopoietic growth factors (cytokines), secreted from stromal cells as well as other hematopoietic cells. These signalling molecules bind to surface receptors (composed of homo or heterodimers) on the HSCs and progenitors to activate a cascade of intracellular signal transduction pathways that influence and regulate lineage commitment. Cytokines usually work in combination, as the integration of signals coming from multiple cytokines is required to convert their stimuli into gene expression changes that regulate cell fate choices (Rieger and Schroeder, 2012). The majority of cytokines function via the Janus kinase (JAK)-signal transducer and activator of transcription (STAT) pathways (JAK-STAT), although some of them directly activate receptor tyrosine kinases (Orkin, 1995). Individual cytokines can be lineage-specific or can broadly control multipotent cells acting on multiple lineages. Moreover, the same cytokines are involved in basal and emergency haematopoietic cell proliferation. In normal conditions several cytokines are secreted at low levels to produce multiple blood cell types, while in response to stress an additional dose of cytokines is released for a short period of time. Other than stimulating proliferation and survival of target cells expressing the right receptor, cytokines are also involved in mediating adhesion and migration in more mature cells (Pixley and Stanley, 2004). Two hypotheses have been formulated to address the role of cytokines during haematopoiesis. According to the permissive (or stochastic) model cytokines do not have a directing role in stem cell differentiation. Lineage commitment is seen as intrinsically driven by key transcription factors controlling specific gene expression programs, while cytokine action is limited to allowing the survival and multiplication of these cells. The instructive model instead proposes that cytokines also play a role in transmitting

specific signals to multipotent haematopoietic cells to regulate their lineage commitment choices (Cantor and Orkin, 2001; Orkin, 2000). Evidence in favour and against both of these theories has been reported, suggesting that both scenarios are likely to reflect aspects of reality. It is now therefore becoming of fundamental importance to gain a better understanding of how these two elements of the decision making process are integrated with each other.

Among the best-characterised cytokines of the haematopoietic system are interleukins (ILs), colony-stimulating factors (CSFs), interferons (IFNs), erythropoietin (EPO) and thrombopoietin (TPO). A key member of the interleukin family is IL-7, a cytokine fundamental to lymphoid commitment. IL-7 and IL-7 receptor (IL-7R) knockout mice do in fact exhibit severely impaired B and T lymphopoiesis due to a dramatic depletion in lymphoid progenitors (CLPs) (Peschon et al., 1994; Puel et al., 1998; Tsapogas et al., 2011; von Freeden-Jeffry et al., 1995). The CSF family of cytokines on the other hand is mostly in charge of myeloid lineage commitment. Four CSFs with different colony-stimulating activities have been described. In *in vitro* colony forming unit (CFU) assays GM-CSF (CSF2) stimulates granulocyte and macrophage colony formation, M-CSF (CSF1) stimulates macrophage colony formation, G-CSF (CSF3) stimulates granulocyte colony formation, and multi-CSF (IL-3) stimulates a broad range of haematopoietic cell colony types (Metcalf, 2010).

1.1.2 B-cell development

B-lymphocyte cells and the antibodies these produce are key to humoral immunity and can fight a countless variety of pathogens. They originate from

multipotent haematopoietic stem cells as part of a tightly controlled multistep process of maturation and selection. Most our knowledge on B-cell specification has been derived from the use to mouse mutant models. Multipotent MPPs take their first step towards the lymphoid-cell lineage by giving rise to lymphoid-primed multipotent progenitors (LMPPs) capable of differentiating into common myeloid progenitors (CMPs) as well as into common lymphoid progenitors (CLPs), but lacking erythroid and megakaryocyte potential. CLP cells arising from the LMPPs are further restricted in their potential and can generate B and T cells, but not myeloid cells. Subsequently, the first B cell-committed progenitor that is generated from CLPs is named the pro-B cell. Pro-B cells are fully restricted to the B cell lineage as they activate the recombination activating gene 1 (RAG1) and recombination activating gene 2 (RAG2) and begin the rearrangement of the immunoglobulin heavy chain (IgH) locus. Successful IgH gene rearrangement generates pre-B cells that express the pre-B-cell receptor (pre-BCR). These then undergo the rearrangement of the Ig light chain loci, which marks further differentiation towards mature B cells. In this way a repertoire of antibody-expressing cells is generated (Pieper et al., 2013).

The lineage progression and maturation of B cells requires the involvement of a pool of transcription factors and signal transduction molecules that orchestrate each step of this process (Figure 1-2). Reduction in the expression of genes associated with stemness and multilineage-priming, in favour of expression of factors linked to, in this case, B cell fate underlies the commitment of each lineage-specific progenitor. Among the most important transcription factors relevant to B cell commitment are IKAROS (IKFZ), PU.1 (PU.1), E2A, which are in charge of controlling the lymphoid versus myeloid fate choice, and early B-cell

factor 1 (EBF) and Paired box 5 (PAX5), which promote progression toward B cell specification. IKAROS is an N-terminal conserved zinc-finger transcription factor of the *IKAROS*, *AIOLOS* and *HELIOS* family. It is involved in suppressing the expression of stem cell-associated genes at very early stages of haematopoietic differentiation, while also inducing lymphoid specific genes (Ng et al., 2009). The amino (N)-terminal domain of these factors mediates the binding to the DNA, while the carboxy (C)-terminal domain is involved in the formation of homo- and heterodimers. Ikaros, like other members of the family, controls gene expression by binding to the promoters of its target genes and recruiting specific chromatin remodelling or repression complexes (Kim et al., 1999). Although only a few genes have been identified as direct targets of IKAROS, this transcription factor is fundamental for the further commitment of CLPs (Sabbattini et al., 2001). *Ikzf1*$^{-/-}$ mice are in fact completely deficient in NK cells, T cells, and B cells, lacking the pre-pro-B cell transitional population (Georgopoulos et al., 1994; Wang et al., 1996a). These data were further confirmed by the analysis of homozygous mutant mice expressing a hypomorphic *Ikzf1* allele (Kirstetter et al., 2002). Another essential regulator of the early stages of lymphoid specification is the ETS family transcription factor PU.1. *Pu.1* knock down mice die at day 18.5 (E 18.5) of embryonic development due to lack of B cells, T cells and granulocytes. The foetal liver of these mice exhibits impaired production of MPPs, with the few cells that are being unable to differentiate towards the B-lineage. B cell differentiation in *Pu.1*$^{-/-}$ mice can be partially rescued by the expression of the α chain of the interleukin 7 receptor (IL-7rα), the transcription of which is normally induced by PU.1 binding (DeKoter et al., 2002). PU.1 levels are crucial in inducing progenitors to differentiate towards either the lymphoid or myeloid lineages, and therefore

need to be tightly regulated during development (DeKoter and Singh, 2000). E2A, a member of the E protein (class I) family of HELIX-LOOP-HELIX (HLH) transcription factors (Dias et al., 2008), has three main roles during haematopoiesis. Early it is required for HSC production, maintenance, and lymphoid priming, later it is necessary for LMPPs generation and their restriction to myeloid priming, and finally it has a key role in B cell differentiation via EBF, PAX5 and Forkhead box protein O1 (FOXO1). Among all of the cell types in which *E2A* is expressed, B-lymphocytes show the most severe phenotype caused by defects in the functioning of this gene. This is because in B cells E2A mainly acts via homodimerization, while in other cell types it forms heterodimers with different E-box factors. The expression of important factors required for B-cell commitment, such as IL7Rα, RAG1, NOTCH and others, is impaired in *E2a*-deficient LMPPs. As a consequence these cells are unable to differentiate into pro-B cells and cannot complete the rearrangement of their IgH gene segments (Peschon et al., 1994; von Freeden-Jeffry et al., 1995; Zhuang et al., 1994). As *Ebf1* expression is controlled by E2A, this protein is absent in aberrant *E2a*$^{-/-}$ pro-B cells or Ikz1$^{-/-}$ mice. In contrast, *E2a* expression is not affected in *Ebf*$^{-/-}$ B cells (Reynaud et al., 2008; Seet et al., 2004; Smith et al., 2002). EBF1 is a transcription factor uniquely expressed by pro-B, pre-B and mature B cells in which, together with PAX5, it plays a key role in controlling B lineage specification. B-cells of *Ebf1*$^{-/-}$ mice are blocked in their differentiation at the pre-pro-B stage and show no or reduced expression of B lineage specific genes such *as Pax5, Pou2af1 and Mb-1* (Lin and Grosschedl, 1995). In normal conditions, *Ebf1* activation induces the downstream expression of *Pax5* gene in pro-B cells (Fuxa and Busslinger, 2007). This protein is, in turn, expressed in B-cells as well as in the nervous system. PAX5 is key to

the expression of many B-cell specific genes, like CD19, Igα and lymphoid enhancer binding factor-1 (LEF). Beyond being implicated in B-cell differentiation and in the rearrangement of V_H gene segments, PAX5 is also critical for the repression of genes associated with other lineages, allowing the cells to maintain a B cell identity (Nutt, 1998). Interestingly, PAX5 regulates different targets during early and late B lymphopoiesis (Revilla et al., 2012). *Pax5* mutant cells can't complete their differentiation into B cells and *Pax5* deficient embryos lack B lymphopoiesis in the foetal liver, whereas in the bone marrow B cell development in the absence of the protein proceeds to a progenitor-cell stage, suggesting a differential requirement for *Pax5* in foetal and adult B lymphopoieisis (Nutt et al., 1997; Urbanek et al., 1994). However, pro-B cells generated in the absence of *Pax5* do acquire a high level of plasticity, allowing them to aberrantly differentiate into different blood cell lineages when grown *in vitro* in the presence of selected cytokines (Nutt et al., 1999).

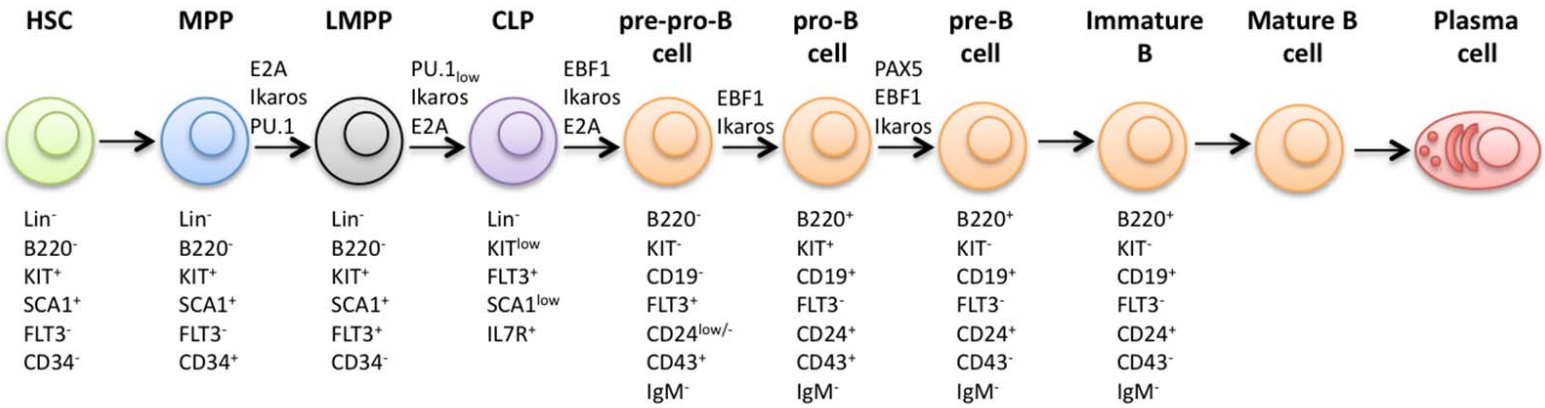

Figure 1-2: B cell differentiation from HSC [Adapted from (Zhu and Emerson, 2002)]. The diagram illustrates the current model for B cell differentiation from HSCs. B and T cells derive from a common lymphoid progenitor (CLP), which can then differentiate into distinct B cell progenitor intermediates before completion of B cell commitment. Establishment of B cell fate is marked by the sequential expression of key transcription factors that orchestrate Ig gene recombination, as well as the expression of B cell-specific surface markers and concomitant repression of genes associated with other lineages.

1.2 Acute lymphoblastic leukaemia

Defects in the complex regulatory mechanisms that control haematopoiesis can lead to many common and serious diseases. And in fact, almost every gene encoding a transcription factor contributing to this regulatory network has been shown to be involved in leukaemogenesis (via chromosomal translocations, amplifications and deletions).

Acute lymphoblastic leukaemia (ALL), in particular, is a malignant disorder of early lymphoid cells, and is characterized by the clonal accumulation of immature blood cells in the bone marrow (BM). ALL leukaemic cells, while arrested at an immature stage of differentiation, concomitantly undergo continual **proliferation**, and are responsible for suppression of normal lymphopoiesis and haematopoiesis within the BM (Inaba et al., 2013). Under normal conditions, the blasts, or immature cells of each blood lineage represent less than 5% of all cells in the tissue. However, in ALL patients their frequency increases to 20% or more, pushing these cells to abandon the marrow, enter the blood stream and become abnormally detectable in the peripheral blood (Harris et al., 1999). According to the World Health Organisation ALL is to be diagnostically classified as precursor B cell acute lymphoblastic leukaemia/lymphoma (B-AL/B-LBL) or as precursor T cell acute lymphoblastic leukaemia/lymphoma (T-ALL/T-LBL) (Teitell and Pandolfi, 2009). Most patients present with a pre-B-cell phenotype (80-85%), characterised by normal expression of pre-B cell surface markers, although approximately 20% of individuals also exhibit aberrant expression of myeloid lineage-specific cell surface antigens on the B cells (Firat et al., 2001).

ALL occurs in both children and adults, but with a peak incidence between 2–5 years of age, it is mainly a paediatric disease. It represents the most common childhood cancer, accounting for 35% of all cancers in children and its incidence in developed countries has been increasing by approximately 1% per year over the past two decades (Linabery and Ross, 2008). Thanks to improvements in diagnosis and treatment, overall cure rates for children with acute lymphoblastic leukaemia currently approach 90%, but it still remains one of the main causes of cancer deaths in children (Pui et al., 2011). Furthermore, the current treatment of childhood ALL involves a very demanding 2-3 years long protocol, and it is now recognized that further refinements, including the introduction of additional risk-adapted therapeutic protocols, may improve cure rates for patients at high risk of relapse, while limiting the toxicity of for patients with low risk.

Although a few cases of ALL (<5%) are associated with inherited predisposing genetic syndromes (e.g. Down syndrome, Bloom syndrome, and Fanconi anaemia) or exposure to ionising radiation and chemotherapeutic drugs, the pathogenic events leading to ALL remain largely unknown (Buffler et al., 2005; Kheifets et al., 2010). Two parallel infection-based theories supported by relevant epidemiological data were formulated a few years ago, and are still recognized as the most plausible hypotheses. Both infer that the disease could arise in susceptible individuals as a result of an abnormal or deregulated immune response to one or multiple common infections. According to the “delayed-infection theory” of Greaves, ALL might derive from the lack of exposure to infectious agents in young age. Later, this deficiency could result in an abnormal immune response to otherwise common infections, creating a favourable environment to promote leukemic transformation. In contrast, according to Kinlen’s

"population mixing" theory, ALL could arise as a consequence of exposure, through population movement and mixing, of non-immune children to unknown infection(s) (Greaves, 2006a, b; Kinlen, 2004).

Regardless of its actual causes, malignant transformation in ALL is widely recognized as a complex process, typically requiring at least two leukaemogenic events (or hits) of various kinds that affect the properties of blood progenitors of the lymphoid lineage or of haematopoietic stem cells with multilineage properties. According to microarray-based genome-wide profiling, genes with altered expression in ALL often encode important regulators of lymphoid commitment (e.g., *PAX5*, *IKZF1*, and *EBF1*), other key transcription factors [*ETV6*, ETS-related gene (*ERG*)], lymphoid signalling molecules [B- and T-lymphocyte attenuator (*BTLA*), CD200, B-cell linker (*BLNK*), Immunoglobulin iota chain (*VPREB1*)], cell cycle regulators and tumour suppressors [cyclin-dependent kinase inhibitor 2A/2B (*CDKN2A/CDKN2B*), Ataxia telangiectasia mutated (*ATM*), retinoblastoma protein (*RB1*), Phosphatase and tensin homolog (*PTEN*)], and more rarely regulators of drug-responsiveness (e.g., the glucocorticoid receptor (Pui et al., 2004)). The majority of initiating lesions in this leukaemia are classified as chromosomal translocations that cause constitutive activation of kinase genes and alterations to the function of critical transcription factors. ALLs are classified into specific karyotype subtypes based on the nature of these translocations (e.g., ETV6-RUNX1 Transcription factor 3 (TCF3)- pre-B-cell leukaemia homeobox 1 (PBX1), breakpoint cluster region (BCR)- Abelson murine leukaemia viral oncogene homolog 1 (ABL1), and rearrangements of MLL) (Yeoh et al., 2002). Additionally, numerical chromosome copy number aberrations, especially hyperdiploidy, and

gene-specific mutations, are also frequently detected among patients (Chen et al., 2010) (Figure 1-3).

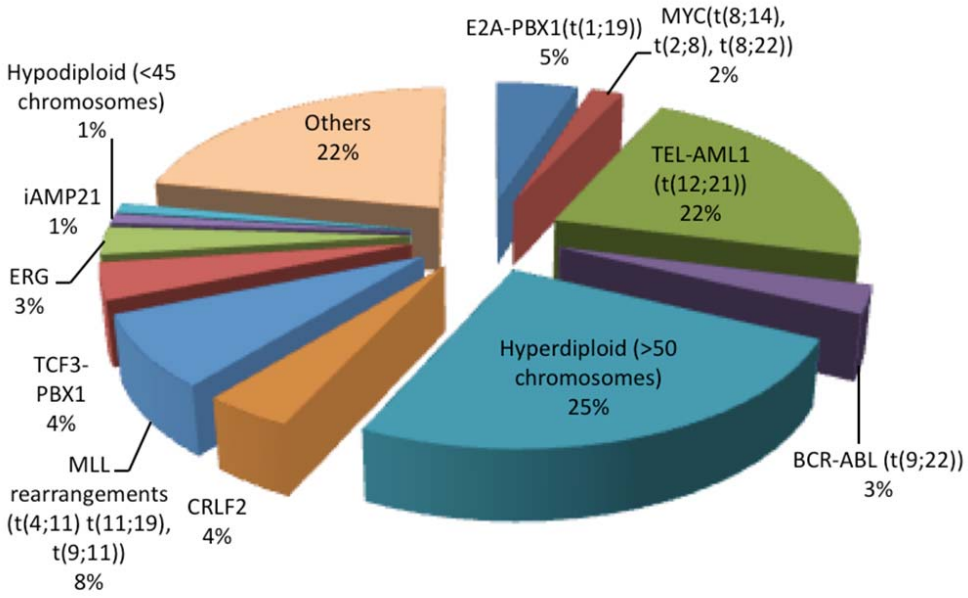

Figure 1-3: Frequency of abnormalities in paediatric Acute Lymphoblastic Leukaemia [Adapted from (Mullighan, 2012)]. The chart shows the relative frequencies of incidence of the most common genetic alteration detected in paediatric ALL. The most frequent abnormality is the t(12;21) translocation.

1.2.1 Treatment of newly diagnosed Acute Lymphoblastic Leukaemia

Treatment of childhood acute lymphoblastic leukaemia (ALL) typically involves 2 to 3 years of chemotherapy. The recommendations for newly diagnosed patients include induction, consolidation and maintenance therapy alongside nervous system (CNS) prophylaxis.

In the induction phase of chemotherapy patients are administered a combination of either three or four drugs, depending on the treatment protocol and on which risk group they belong to. The treatment core is composed of vincristine,

a corticosteroid (prednisone or dexamethasone) and L-asparaginase, in conjunction with intrathecal (IT) therapy. Vincristine is a vinca alkaloid agent that binds tubulin dimers to disrupt the assembly of microtubule structures. This particularly affects the formation of the mitotic spindle, and consequently arrests mitotic cells in metaphase. Most treatment protocols prescribe the administration of this drug with a dosage of 1.4 to 2 mg/m^2 on a weekly basis. For children weighing 10 kg or less the starting dose is 0.05 mg/kg administered by weekly intravenous injection. Dexamethasone is a potent synthetic member of the glucocorticoid class of steroid drugs. Like prednisone, it binds intracellularly to the glucocorticoid receptor (GR), inducing cell death by apoptosis. In children and young adults undergoing the induction course, dexamethasone is typically administered 6 mg/m^2 orally, with a maximum weekly dose of 10 mg. L-asparaginase is an enzyme isolated from the bacterium *Escherichia coli* or *Erwinia carotovora*, and it catalyses the hydrolysis of L-asparaginase to L-aspartic acid and ammonia, depleting the cell of asparagine. Leukemic cells are unable to synthesize this amino acid de novo, due to the lack or defective expression of the enzyme asparagine synthase. L-asparaginase administration, usually at 25 000 IU/m^2 per dose, does therefore inhibit protein synthesis of the susceptible leukemic cell populations, inducing their arrest in the G1 phase of cell cycle, and consequently their apoptosis. Overall, complete remission (CR) rate following induction treatment is greater than 95%, and response rapidity, measured as bone marrow clearance at days 7 and 14 of treatment, is considered an informative prognostic marker. Patients with slow or absent bone marrow response by day 14 or 15 after treatment initiation have poorer prognosis, and are often transferred to more aggressive treatment regimens. Similarly, patients presenting with high-risk

features do benefit from a more intensive induction regimen (four or five agents), typically including an anthracycline compound (e.g., daunorubicin). Strikingly, even after complete remission is achieved, further treatment is required, as in its absence, over 90% of patients would present with recurrent leukaemia within weeks or months.

The so-called consolidation or intensification therapy involves additional systemic treatment in conjunction with CNS sanctuary therapy. The intensity of this regimen varies considerably depending on risk group assignment and on national protocols. Several countries are however attempting to limit, where possible (standard-risk patients), the use of anthracyclines and alkylating agents, responsible for increased side effects. Treatment for children at high risk of relapse is often additionally coupled to autologous or allogeneic stem cell transplantation.

The final step of treatment, or maintenance chemotherapy, lasts until 2-3 years of continuous remission are achieved. In most protocols the recommendation is for daily oral mercaptopurine and weekly oral or parenteral methotrexate. Additionally, many treatment regimens also prescribe the continuation of intrathecal chemotherapy targeting the CNS sanctuary. Pulses of vincristine and corticosteroid are also frequently added to the standard maintenance backbone (Figure 1-4).

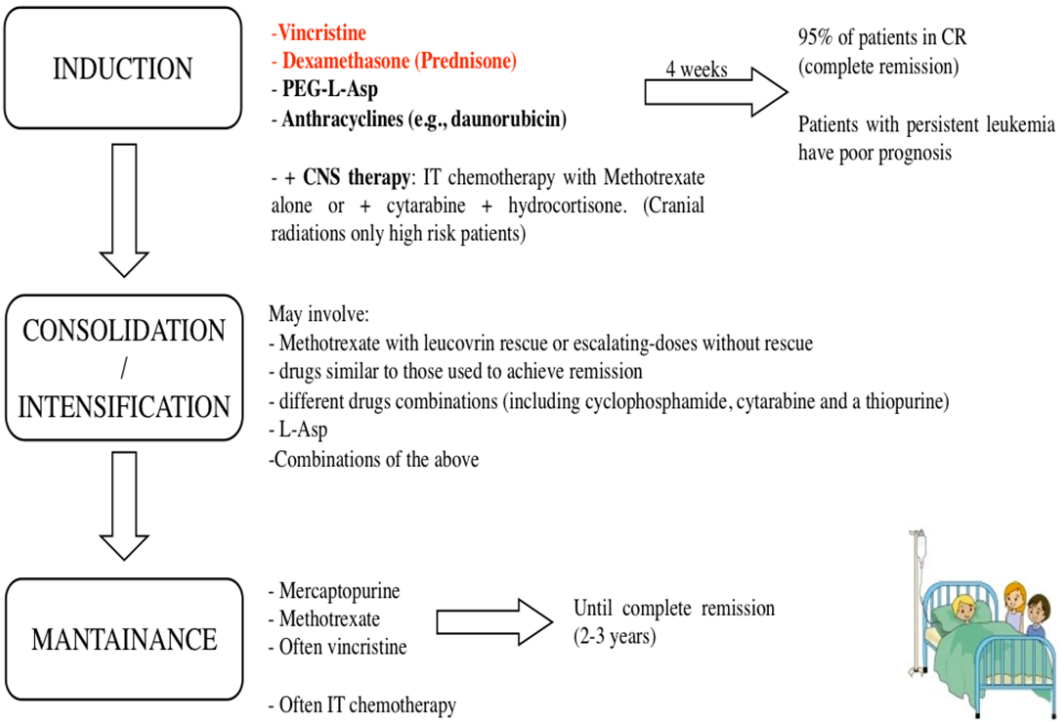

Figure 1-4: Treatment of childhood acute lymphoblastic leukaemia (ALL): guidelines of the National Cancer Institute. Treatment of childhood acute lymphoblastic leukaemia (ALL) involves three major phases: induction, consolidation or intensification, and maintenance. Treatment protocols can wildly differ between countries, both in terms of drugs of choice and duration of each phase. The figure summarises the National Cancer Institute (U.S.) treatment guidelines.

1.2.2 t(12;21) Acute Lymphoblastic Leukaemia

Emerging in about one quarter of patients, the t(12; 21)(p13; q22) 9TEL-AML1) translocation is the most common chromosomal abnormality in childhood B-cell precursor ALL (Mullighan, 2012) (Figure 1-3). By contrast, this fusion gene is only rarely detected in adult ALL patients (3%). Event free survival (EFS) rates among TEL-AML1 pre-B-ALL patients reach over 90%, unlike other karyotypic ALL

subtypes. The rearrangement is therefore widely believed to associate with rather favourable prognosis (Borkhardt et al., 1997; Kebriaei and Larson, 2003; Rubnitz et al., 1997). A few years ago this notion was however challenged by multiple studies showing similar incidence of the translocation at diagnosis and relapse (Loh and Rubnitz, 2002; Seeger et al., 1998), and raising the concern that, because of characteristic late onset of relapses among TEL-AML1+ patients, inadequate follow-up times could have biased the results of previous studies. Nevertheless, in 2004 the analysis of epidemiologic data for 372 patients, 94 of which were TEL-AML1 positive cases, allowed a study, led by the Austrian Berlin-Frankfurt-Münster group, to definitively prove that prognosis of TEL-AML1+ patients is significantly more favourable than that of TEL-AML1- patients. In particular, TEL-AML1+ blast cells are characterized by a higher sensitivity to corticosteroids, as indicated by the higher proportion of patients showing good responsiveness at early stages of the treatment protocol (Attarbaschi et al., 2004).

The t(12; 21)(p13; q22) rearrangement is a submicroscopic reciprocal translocation involving chromosomes 12 and 21. The translocation fuses the 5' terminus of the *TEL* gene (residues 1-336) in frame with almost the entire coding sequence (residues 21-480) of the *AML1* gene. The genomic breakpoint most frequently occurs between intron 5 of *TEL* and intron 1 of *AML*. However, in another common translocation variant exon 5 of *TEL* and exon 3 of *AML1* are fused together in frame. The rearrangement gives rise to TEL-AML1 (ETV6-RUNX1) fusion protein. Both TEL (ETV6) and AML1 (RUNX1) are transcription factors essential to normal haematopoiesis, and both are involved in other leukaemia-associated gene translocations.

AML1 (*RUNX1*) gene is located on chromosome 21 at 21q22.3. It encodes a key component of the core binding factor (CBF) complex (i.e. CBFα/RUNX1), expressed almost uniquely in cells of the haematopoietic lineage (Corsetti and Calabi, 1997). Although AML1 protein on its own is able to regulate the expression of various target genes, recruitment of the co-factor CBFβ (core binding factor β) enhances its DNA binding affinity and protects it from ubiquitin-proteasome-mediated degradation (Huang et al., 2001). Both AML1 binding to DNA and its heterodimerization with the partner protein CBFβ are mediated by the "Runt homology domain" (RHD), an evolutionarily highly conserved region of 128 amino acids shared by all the members of the RUNX gene family (*RUNX1*, *RUNX2* and *RUNX3*). AML1 binding either activates or represses expression of its target genes, depending on the specific promoter and/or cell context. Its activity is dependent upon the recruitment of non-DNA binding co-activators and co-repressors that participate in the formation of a transcriptional complex. Among AML1 partner co-activators are p300/CBP and HAT (histone acetyltransferase), while mSIN3A, Groucho/TLE and HDAC (histone deacetylase) are some of the co-repressors (Imai et al., 1998; Kurokawa and Hirai, 2003). As clearly demonstrated by the observation that *Aml1* deficient mice never develop definitive haematopoiesis, AML1 is essential for generation of HSCs in the embryo (Wang et al., 1996b). By contrast, adult *Aml1* conditional knockout mice display impairment in the maturation of megakaryocytes and differentiation of T and B cells, while their HSC pool is unimpaired (Ichikawa et al., 2004). These data were supported also by a recent study showing that in B cell progenitors AML1 binds to enhancer regions of genes critical for pre-B-cell transition (Niebuhr et al., 2013).

TEL (ETV6) is a nuclear protein of the ETS (E-26 transforming specific) family of transcription factors. All members of this family share an 88 amino-acids-long, evolutionarily highly conserved domain, called *ETS* domain. This is involved in DNA binding as well as in protein-protein interactions (Oikawa and Yamada, 2003; Wasylyk et al., 1993). A second highly conserved region of the gene is the N-terminally pointed domain, also known as HLH domain or sterile alpha motif (SAM), which is shared by several members of the family. This is implicated in protein-protein interactions such as homo- and heterodimerization and in transcriptional repression via binding to nuclear receptors such as SMRT, mSin3A, and N-CoR co-repressors, as well as histone deacetylase 3 (Chakrabarti and Nucifora, 1999; Irvin et al., 2003b; Kwiatkowski et al., 1998). Little is known about the regulation and downstream signalling of TEL. PAX6, the only known upstream regulator, represses TEL expression. Few downstream targets have been reported, and only matrix metalloproteinase-3 (*MMP3*) and B-cell lymphoma-extra-large ($BCL\text{-}X_L$) promoters have been shown to be directly bound by TEL (Boily et al., 2007; Cao et al., 2009; Fenrick et al., 2000; Irvin et al., 2003a). Even so, multiple *in vivo* studies have suggested a fundamental role for TEL in several key developmental pathways (Irvin et al., 2003). *Tel* knockout mice die at embryonic day 10.5 (E10.5) due to a severe defect precluding them from maintaining the developing vascular network of the yolk sac; haematopoiesis is however unaffected. In contrast, this protein is a key regulator of post-natal HSCs within the bone marrow, where it is required for the establishment of all blood lineages. HSCs and progenitors are in fact dependent on this molecule for their migration from foetal liver to the bone marrow, and for their ability to home and survive within the new niche (Hock et al., 2004; Wang et al., 1997; Wang et al., 1998).

Congruently with its key role in normal haematopoiesis, more than 40 translocations involving *TEL* have been reported so far in cancer, often coupled with a concomitant deletion of the non-rearranged allele.

Several studies on twins (Greaves et al., 2003) and on cord blood from newborns (Mori et al., 2002b) have demonstrated that TEL-AML1 lesion arises in utero, with a frequency in the population ~100 fold higher than the risk of leukaemia. Furthermore, TEL-AML1 translocation only generates a pre-leukemic clone that requires acquisition of secondary mutations in order to induce malignant transformation (Mori et al., 2002a). Over the years, other studies have challenged these findings, suggesting that perhaps TEL-AML1 initiating event is indeed as rare as the disease itself, and that therefore a high proportion (possibly 100%) of babies born with the fusion will eventually develop leukaemia (Lausten-Thomsen et al., 2011). Even though the two different mechanistic models are still being debated, the “two hit” model best explains the biology of the disease, and is supported by the observations that this leukaemia is typically not overt until the third or fourth year of life, and that TEL-AML1 fusion gene can be detected in the blood of some healthy adults (Olsen et al., 2006) (Figure 1-5).

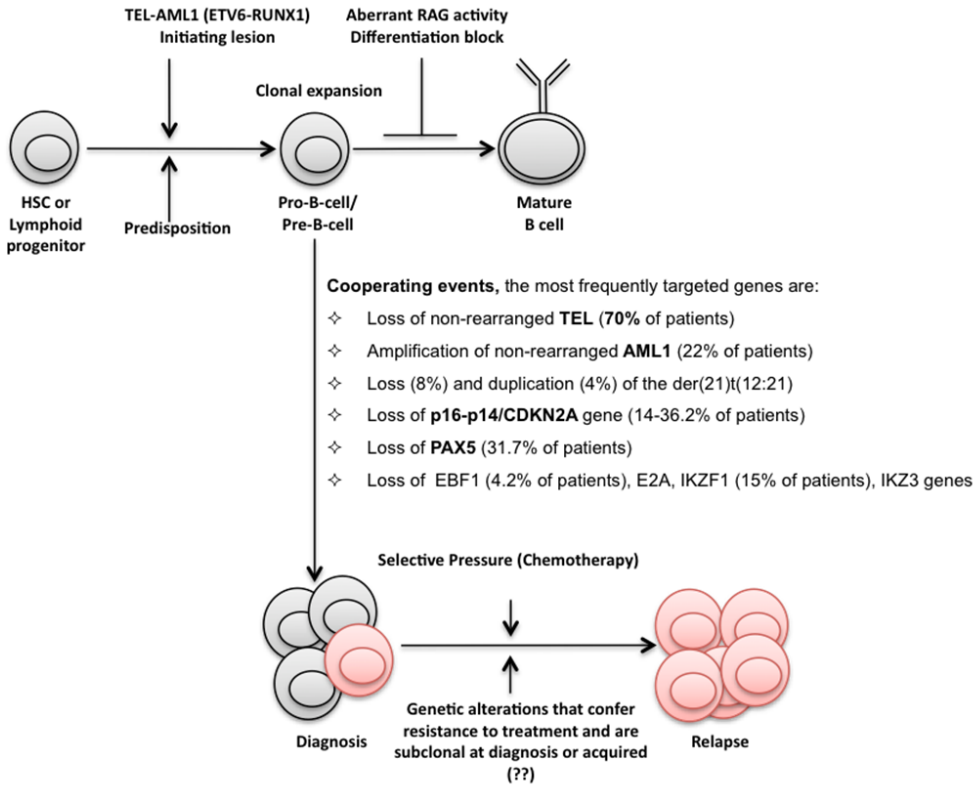

Figure 1-5: TEL-AML1+ Acute lymphoblastic leukaemia is a multistep disease [Adapted from (Inaba et al., 2013)]. The pre-LSC and its more differentiated pro-B-like progeny form a pre-leukaemic pool prone to the accumulation of additive mutations required to generate frank leukaemia. TEL-AML1 forced expression alone does not translate into the emergence of a leukemic clone until after a second hit is delivered (Hong et al., 2008). Additional mutations in ALL impact key biological functions, acting (i) at the stem cell level itself, (Cicalese et al., 2009) or (Hashimoto et al.) on more differentiated cells by endowing them with stem cell-like properties (Huntly et al., 2004) (Krivtsov et al., 2006).

TEL-AML1-positive leukemic cells are aberrantly arrested at the pro-B stage of differentiation: they initiate, but fail to complete immunoglobulin gene rearrangement (Panzer-Grumayer et al., 2005; Pui et al., 2004; Sloma and Eaves, 2009). This is probably due to a TEL-AML1-dependent down-regulation of the

transcription factors Spi-B (*SPIB*) and *IKZF3*, key regulators of pre-B transition (Niebuhr et al., 2013). Indeed, an aberrant immature B cell population, identified by the expression of $CD34^{+}CD38^{-}CD19^{+}$ surface markers, is linked to TEL-$AML1^{+}$ expression in pre-leukemic cells (Hong et al., 2008). Additionally, lines of evidence from both human and mouse models of *TEL-AML1* transduction suggest that the fusion might promote self-renewal of the differentiation-arrested early B cells, causing accumulation of pre-B cells in the marrow (Ford et al., 1998; Hong et al., 2008; Morrow et al., 2004). The biology of this pre-leukemic clone is however far from being fully understood, and regardless of the timing and mode of *TEL-AML1* expression, no mouse model of t(12;21) leukaemia has yet been able to fully recapitulate the disease. When Gilliland and colleagues first established a *TEL-AML1* transgenic mouse model, in which the fusion gene was placed under the control of the immunoglobulin heavy chain enhancer/promoter, not only did the mice not develop leukaemia, normal haematopoiesis was also unaffected. Subsequently similar results were obtained transplanting irradiated mice with HSCs transduced with a retrovirus expressing the fusion gene (Andreasson et al., 2001). In a different setting however, over-expression of the fusion in bone marrow transplant experiments caused leukaemia in two out of nine transplanted mice (a T-lineage ALL and a B-precursor ALL) and accumulation of both multipotent and B-cell progenitors in additional two mice (Bernardin et al., 2002; Fischer et al., 2005; Tsuzuki et al., 2004). Similarly, in Morrow's experiments, transduction of foetal haematopoietic cells caused an increase in BM repopulation by myeloid and B cells, without perturbing differentiation of TEL-$AML1^{+}$ cells (Morrow et al., 2004). Knock-in mouse models, in which *TEL-AML1* expression was driven by the endogenous *Tel* promoter, produced enhanced self-renewal of HSCs and foetal B

progenitors and a predisposition to development of leukaemia following mutagenesis (Schindler et al., 2009; van der Weyden et al., 2011). This observation was consistent with the hypothesised role of TEL-AML1 in creating a persistent pre-malignant clone, prone to the accumulation of additional genetic lesions prior to the progression to overt leukaemia. Finally, by means of a TEL-AML1 *Sleeping Beauty* (SB) transposase randomly inserting in the genome, Van der Weyden and colleagues were able to induce B-ALL leukaemia in about 20% of study mice (Schindler et al., 2009; van der Weyden et al., 2011).

TEL-AML1 fusion protein lacks the DNA binding activity of TEL, but retains its ability to form homo- and heterodimers with wild-type TEL and other members of the ETS family. For this reason the translocation is thought to convert AML1 from transcriptional activator to transcriptional repressor, imposing an altered pattern of constitutive inhibition on its target genes (Chakrabarti and Nucifora, 1999; Chakrabarti et al., 2000; Irvin et al., 2003a). This hypothesis was validated in a number of studies showing that the activity of haematopoietic-specific gene reporter constructs is repressed upon transient over-expression of the fusion protein (Fears et al., 1997; Hiebert et al., 1996; Uchida et al., 1999). This function appeared to be largely mediated by the PNT domain and the central region of TEL portion of the fusion protein, which, as for wild-type TEL, can recruit nuclear receptor/histone deacetylase (HDACs) complexes (Petrie et al., 2003; Wang and Hiebert, 2001). A more recent study has however found preliminary evidence for a possible role of TEL-AML1 in promoting the expression of particular downstream target genes. In particular the Phosphatidylinositol 3-Kinase/ thymoma viral oncogene homolog/ mechanistic Target Of Rapamycin (PI3K/AKT/mTOR) pathway, as well as HSC gene expression signatures were highly enriched in the

list of genes down-regulated upon shRNA-mediated knockdown of TEL-AML1 in human leukemic cell lines (Fuka et al., 2011). The PI3K/AKT/mTOR signalling pathway was subsequently shown to be critical for the survival of TEL-AML1 leukaemia, suggesting that, along with its function as wild-type RUNX1 antagonist, the fusion might act to up-regulate this, and possibly other oncogenic pathways (Fuka et al., 2012).

1.2.3 Cooperating mutations t(12;21)in Acute Lymphoblastic Leukaemia

As shown by array comparative genomic hybridization, SNP microarrays and high-resolution genome–wide analysis studies, at the time of diagnosis the majority of ALL patients carry a mean of 6-8 DNA aberrations or copy number alterations (CAN) in addition to the first mutagenic hit, and even more (up to 14.0) at relapse (Mullighan et al., 2007; Mullighan et al., 2008) (Figure 1-6). MLL-rearranged patients, who in contrast harbour very few additional genetic lesions, represent an exception to this observation (Mullighan et al., 2007). Carried out mainly in 2007-2008, these high-throughput studies have described more than 50 recurrent mutations. The nature and frequency of these lesions is highly dependent on the cytogenetic subtype. Overall however, most of these secondary events represent deletions targeting genes involved in lymphoid development (e.g. *PAX5*, *IKZF1*, *EBF1*, and *LMO2*) or in cell cycle and tumour suppression pathways (e.g. *CDKN2A/CDKN2B*, *PTEN*, and *RB*) (Bateman et al., 2010). Others target genes act in a variety of additional key cellular pathways including lymphoid signalling (*BTLA*, *CD200*, *TOX*, and the glucocorticoid receptor *NR3C1*), and transcriptional regulation and coactivation (*TBL1XR1*, *TEL* and *ERG*). Several

genes were found altered in different ways, including through copy number abnormalities, translocations and, less commonly in this disease, sequence mutations (Mullighan, 2012). In the context of TEL-AML1+ pre-B-ALL, *PAX5* (~31.7% of cases) *EBF1*, *E2A*, *IKZF3* and *IKZF1* (~15%) are recurrently deleted B-cell differentiation-related genes (Kuiper et al., 2007; Mullighan et al., 2007). In mice, complete absence of *Ebf1* or *Pax5* results in arrest of B-cell development at the early pro-B- or pre-pro-B-cell stage, while loss of Ikzf1 leads to an arrest at an even earlier stage (Georgopoulos et al., 1994; Lin and Grosschedl, 1995; Mullighan et al., 2007; Nutt et al., 1999). In adult haematopoiesis the expression of the transcription factor *PAX5* is switched on during the transition from pre-pro-B cells to committed pro-B cells, and switched off again when B cells differentiate into plasma cells. During these stages the protein acts to concomitantly down-regulate genes “inappropriate” for B lineage differentiation and up-regulate lineage-specific genes (like *CD19*, *CD79A*, *BLNK* and *CD72*) (Busslinger, 2004). Four different patterns of *PAX5* deletion were identified in a study published in 2007: focal deletions, most frequently involving only a subset of exons (intragenic), broader deletions covering *PAX5* as well as additional flanking genes, large deletions of chromosome 9p, and deletions encompassing the whole arm of the chromosome or even the whole chromosome (Mullighan et al., 2007). *EBF1* and *E2A* genes cooperate with *PAX5* to orchestrate B cell development, which is therefore arrested in absence of either of the two (Cobaleda et al., 2007).

Interestingly, loss of non-rearranged *TEL* allele is the most frequent second hit of TEL-AML1+ leukaemia (70% of patients), leading to the speculation that the function of the wild-type gene might be that of a tumour suppressor, possibly acting during cell-cycle to arrest cells in G_1 phase (Kempski and Sturt, 2000;

Raynaud et al., 1996; Rompaey et al., 2000). The extent of the deletion is highly variable among patients, ranging from a clearly detectable chromosomal deletion or other abnormalities of 12p, to submicroscopic lesions (Raynaud et al., 1996). Patients carrying an intragenic deletion, which can only be identified by FISH (Fluorescence in situ hybridization), do however represent only a small proportion of cases. In cases where LOH (loss of heterozygosity) is due to larger deletions, a few other genes have been shown as often concomitantly deleted with TEL. Among them is cyclin-dependent kinase inihibitor 1B ($p27^{KIP1}$), previously implicated in other types of cancer (Kobayashi et al., 1994). In a high percentage of patients (22%), amplification of the non-rearranged allele of AML1 is also involved in TEL-AML1+ ALL leukemic transformation (Woo et al., 2005), while trisomy 21 appears to be a second hit with higher frequency at relapse than at diagnosis. In contrast the role played by the fusion reciprocal transcript is still unclear. Several studies have reported that AML1-TEL can be detected only in a small proportion of cases (about 13%) (Aguiar et al., 1996; Kempski and Sturt, 2000; Shurtleff et al., 1995). However, both deletion (8%) and duplication (4%) of der(21)t(12:21) have been identified among ALL patients in a study which postulated that, being detected in all of leukemic cells, the der(21)t(12:21) deletion does likely occur at the same time as the translocation. Duplication of AML1-TEL was instead proposed to be a secondary event resulting from mitotic recombination errors, and is believed to almost exclusively be detectable in patients at relapse (Loncarevic et al., 1999). This observation was contradicted by a more recent study by Al-Shehhi and colleagues (Al-Shehhi et al., 2013).

Finally, the *CDKN2A* gene, encoding both $p16^{INK4a}$ and $p14^{ARF}$, is often deleted (14% - 36.2% depending on the study) in ALL patients (Mullighan et al.,

2008; Quesnel et al., 1995). Its inactivation neutralizes both the TP53 and the retinoblastoma pathways (Pui et al., 2004).

Even though the above described genetic aberrations clearly play a role in leukaemogenesis, whether or not any of these is involved in determining the likelihood or timing of relapse of B-ALL is still object of study. Alterations of *p16* (Heerema et al., 1999) and *IKZF1* have so far been proposed as adverse prognostic factors. In particular, alterations of *IKZF1* have been shown to triple the risk of treatment failure. *PAX5* aberrations, on the other hand, are yet to be linked to patient outcome (Mullighan et al., 2009), and the prognostic impact of *TEL* deletion has long been debated. In 2004 Attarbaschi et al. reported that deletion of the non-translocated *TEL* allele confers worse prognosis in patients, while in 2011 Ko et al. described it as linked to favourable prognosis. However, only the 2011 study did discriminate between true native *TEL* deletion and monosomy 12, possibly explaining the different conclusions reached by the two groups (Attarbaschi et al., 2004; Ko et al., 2011).

It is therefore clear that the biology of genetic alterations in t(12:21) ALL is only superficially uncovered, and greater efforts will be required to fully understand the role played by the different lesions in the development, diagnostics and progression of the disease, both individually and as cooperating mutations.

1.2.4 Intratumour genetic heterogeneity and t(12;21) Acute Lymphoblastic Leukaemia

Virtually every tumour displays wide intratumour cell-to-cell heterogeneity of distinguishable phenotypic traits, including activation of signalling pathways,

evasion of antitumour immunity, induction of senescence, production of secreted factors, migration, metastasis, angiogenic capacity, genetic makeup, response to anticancer agents, and activation of metabolic pathways. Even though this phenomenon has been recognized since the early days of cancer research, the role and cooperation of genetic diversity and non-genetic sources of heterogeneity has only recently started to be elucidated, and the implications of both for cancer development and treatment are still largely unknown (Almendro et al., 2013; Marusyk and Polyak, 2010).

Tumours have historically been seen from a gene-centric perspective as the result of a stepwise sequential accumulation of multiple genetic alterations occurring in single cells and leading to the clonal expansion of the fittest clone to the detriment of less competitive ones. Such a model equates cancer cells to asexually reproducing unicellular quasi-species subject to Darwinian evolution, and was first introduced by Peter Nowell in 1976 (Nowell, 1976). According to this classic view of tumour evolution, the stochastic process of the acquisition of driving mutations is constantly coupled to a strong positive and negative selection process driven by the microenvironment, and it is also paired to accumulation of innumerable passenger alterations that are neutral to tumour cell selection. In other words, as for organisms, cancer clones are invariably competing for space and resources. As a result, tumours at any stage of their progression are expected to be homogenous for mutations that functionally matter, and simply represent serial clonal expansions and outgrowths (‘selective sweep’) of the most competitive clone (monoclonal evolution) (Figure 1-6a).

This longstanding model has recently been challenged by the much more complicated image of tumour genetic architectures returned to us by modern high-

resolution genome-wide studies. Such studies have led to a number of modified clonal evolution theories, including models in which multiple clones of similar fitness evolve simultaneously, and models in which coevolution of subclones with potentially cooperative relations occurs. According to data collected in the past 3-4 years the majority of individual tumours are in fact characterized by a multitude of clones related to each other via complex and branching Darwinian-like speciation trajectories (polyclonal evolution) (Figure 1-6b); rather than the 'textbook' model of linear somatic evolution, as proposed by Nowell.

The first evidence of the unexpected clonally heterogeneous nature of tumours came from the pioneer work of two research groups investigating cytogenetically distinct subtypes of childhood ALLs. Anderson et al. characterized a set of TEL-AML1+ ALL samples, while Notta et al. worked with a pool of Ph+ (Philadelphia chromosome+) ALL samples (Anderson et al., 2011; Notta et al., 2011b).

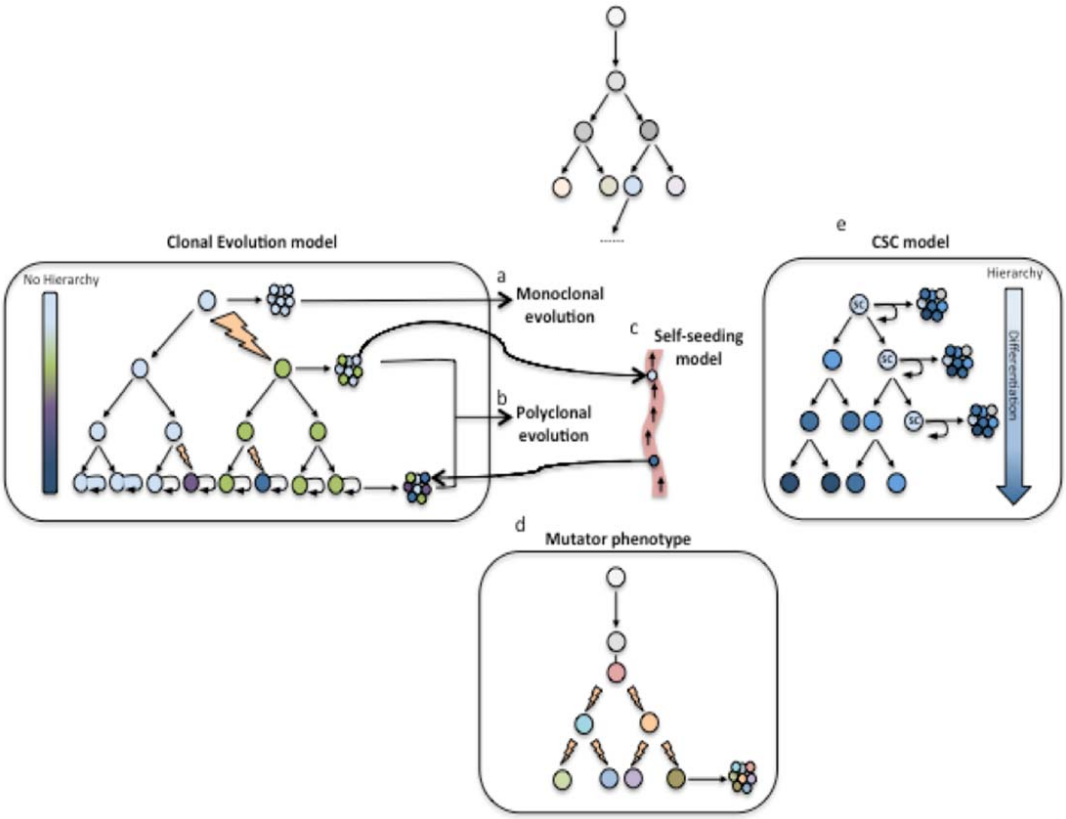

Figure 1-6: Different Models of tumour progression [Adapted from (Navin and Hicks, 2010)]. (a-e) proposed models of tumour progression. (a) In the classic model of monoclonal evolution a monogenomic, uniform, tumour is formed. (b) Polygenomic tumours generated by a tumour evolving in polyclonal way. (c) Self-seeding originates distant tumours with divergent genomic characteristics. As a reinterpretation of the "seed and soil" theory of Paget, the self-seeding model also proposes that the circulating tumour cells responsible for metastasis formation and growth might eventually make a comeback to their site of origin attracted by intrinsic homing mechanisms. (d) In the mutator phenotype generated tumours are highly heterogeneous, (e) In the cancer stem cell model the tumour is sustained by a minority of cells with self-renewal characteristics.

Both groups clearly described the coexistence of many genetically diverse subclones within the tumour bulk (up to 10 subclones), the former through multiplex in situ hybridization assays (Martinez et al.), and the latter by single cell single nucleotide polymorphism (SNP) arrays. Evolutionary trees showed complex architectures in which subclones “late” in the branching were not necessarily the dominant ones. The survival of clones with ancestral genomes alongside those occupying the newest branches of the genealogic tree made it possible the fully reconstruct the complex evolutionary processes that had played all along the neoplasms’ progression without the need to infer intermediate clones. Moreover, the observation of Anderson at al. that common or highly recurrent CAN were not acquired in any preferential order and could arise more than once independently, suggesting that their potency as oncogenic mutations may not had been contingent upon other CAN, raised the possibility that some key mutated loci in ALL might be targets of DNA damage. Evidence in favour of this hypothesis is the recent identification of *RAG* recognition sequences near the breakpoint junctions of many of the structural variants characteristic of TEL-AML+ ALL (Papaemmanuil et al., 2014).

As challenging as the interpretation of the described polyclonal intra-tumour genetic heterogeneity might seem, a possible explanation lies in the requirement for consecutive mutations to occur within a larger time frame than that needed for a clone to take over the tumour and promote linear evolution. Moreover, even in the absence of particular time constrains, mathematical modelling of data collected from primary tumours seems to suggest that the impact of driving mutations on clonal selection and tumour homogenization is likely to be incredibly small, and therefore insufficient to promote any selective sweeps (Bozic et al., 2010). Finally,

it is very probable that in case of subsequent mutation arising independently in two competitor clones, a phenomenon known as ‘clonal interference’, and described as a growth restrain on both clones as a result of the mutual competition among them, is triggered (Greaves and Maley, 2012). Spatial constraints therefore promote tumour differentiation, as the competition among tumour clones would not be equally fierce if these were topologically separated.

The data collected by Anderson et al. and Notta et al. are particularly interesting in light of the fact that a relatively small number of genetic alterations and driver mutations characterize ALL, and that the sequence of events leading to overt leukaemia is broadly known, making the collected data an ideal model for the analysis of cancers characterized by even more complex dynamics. Branched evolution has since been in fact documented in a wide range of primary and metastatic tumour types, including adenoma-to-carcinoma transition of the colon (Thirlwell et al., 2010), secondary acute myeloid leukaemia (AML) (Walter et al., 2012), chronic lymphoblastic leukaemia (CLL) (Landau et al., 2013), pancreatic cancer (Campbell et al., 2010), renal clear-cell carcinomas (Gerlinger et al., 2012), metastatic medulloblastoma (Wu et al., 2012), and breast cancer (Nik-Zainal et al., 2012; Shah et al., 2012). Additionally, the investigation of solid tumours has allowed the analysis of spatially separated and regionally separated cancer samples through different sequencing technologies, including single-nucleus sequencing and single-cell sequencing and immune-fluorescence in situ hybridization (iFISH) (Almendro et al., 2014b; Campbell et al., 2010; Navin et al., 2011; Navin et al., 2010; Yachida et al., 2010). By sequencing multiple distant biopsies from the same primary clear renal carcinoma, glioblastoma, breast cancer, pancreatic cancer or medulloblastoma, researchers showed the presence

of spatially separated tumour subclones, harbouring different genetic alterations. In this scenario metastatic clones from distinct distant sites were profoundly different from each other, in some cases to the point that the mutational landscape of a single biopsy was more closely related to metastasis from different primary tumours than to adjacent biopsies of the same mass (Martinez et al., 2013). Yet, clonal ancestry was not always traceable to the primary tumour, or only to low frequency populations (Shah et al., 2009). These observations may suggest that tumours progress following a self-seeding model, in which metastases are the result of the early or late (parallel versus linear progression model) migration of a single cell from the primary tumour into the vasculature, followed by its offsite expansion (Ashworth et al., 2011; Klein, 2009) (Figure 1-6c). As it is likely that many more cells are involved in similar migratory attempts without being equally successful, it is possible that metastatic clones are derived from a restricted number of genetic subclones in the tumours of origin (Yachida et al., 2010). Once the founding clone has reached the metastatic sites, the new microenvironment, together with the selective pressures imposed by the process of metastasis formation itself, will promote its additional genetic diversification prior to its outgrowth, creating a large phylogenetic distance between the original subpopulation in the primary tumour and the re-seeded clones (Navin and Hicks, 2010; Yates and Campbell, 2012). Indeed, the evaluation of genotypes across longitudinal samples of breast cancer analysed at the single cell level by immune-fluorescence in situ hybridization (iFISH) shows that overall genetic diversity of distant metastasis is higher than that of lymph node metastasis, which in turn are more heterogeneous than primary tumours. Moreover, the analysis of a limited cohort of pre-treatment primary tumours and matching lymph node metastasis

showed that while post-treatment lesions within the same patient were concordant, clear genetic divergence could be detected between treatment-naïve specimens (Almendro et al., 2014b). In some tumours, like pancreatic cancer, genomic instability has also been shown to hugely contribute to this process of continuous genetic evolution from the early stages of the neoplasia to tertiary metastasis (mutator phenotype model) (Figure 1-6d) (Campbell et al., 2010; Navin and Hicks, 2010). That said, some of the data collected so far describe a much more similar genetic composition between primary and metastatic lesions, and report that seeding clones can subsist at metastatic sites with fewer *de novo* driver mutations beyond those found in the primary tumours (Burrell et al., 2013; Ding et al., 2010).

Additionally to providing evidence of the inadequacy of the clonal succession model to describe the genetic evolution of cancer cells in ALL, both of the mentioned leukaemia studies made use of xenograft models to test the ability of genetically distinct clones to engraft NSG mice. The purpose of such experiments was to functionally test the link between the leukaemia-initiating property of some cancer cells and their underlying genetics and ascertain whether the sub-clonal architecture of cancer is generated and sustained by genetically distinct propagating cells with stem cell-like potency (Greaves, 2010). The cancer stem cell (CSC) model (Figure 1-6e), alternative to the classical theory of clonal evolution, proposes that cancer cells with similar genetic backgrounds but distinct phenotypes can be hierarchically organized according to their tumourigenic potential. According to this theory, similarly to normal tissues, at the apex of the cell differentiation hierarchy in the tumour sit so-called cancer stem cells (CSCs), or leukaemia initiating cells (LICs) in the case of haematological malignancies. CSCs are the subset of the tumour endowed with self-renewal and extensive or

indefinite replication potential, capable of giving rise to different types of transit-amplifying cells as well as to more differentiated cancer cells. These cells are functionally defined by their ability to produce long-term engraftment in the mouse and sustain the tumour's growth *in vivo*. According to this model of cancer progression only mutations hitting the CSC population can survive long-term, and any alteration at the expense of transit-amplifying cells is diluted out by the inability of these cells to persist within the tumour and be material for the selective process. For this reason alterations to cells further down the differentiation hierarchy can only partially account for the heterogeneity detected in a snapshot analysis of a tumour. This is true unless the acquired mutation is capable *per se* to confer self-renewal potential to the target cells, allowing it to *de novo* acquire stem cell-like properties. Given their proposed correspondence to stem cells in normal tissues, CSCs would be expected to represent a rare population within the tumour, and the high frequency of cells with CSC-like functional properties within certain types of cancers has previously made the CSC perspective waver. Although the two hypotheses, clonal evolution and CSCs model, have often been treated as mutually exclusive models of cancer development, they can be easily reconciled as complementary explanations of tumour evolution and generation of heterogeneity (genetic and phenotypic) (Michor and Polyak, 2010). What is still unclear about the CSCs model is whether the CSC activity of cells classified as such reflects non-genetic functional variation and even stochastic stem cell plasticity of cancer cells fluctuating among different differentiation states, or whether it is the deterministic and intrinsic property of specific genetically dominant subclones (Greaves, 2010). This is especially challenging to assess since the CSC compartment has so far been defined as such solely based on the

experimentally described phenotypic heterogeneity of cancer cells in the context of natural selection (in shape of cancer progression or resurgence post-treatment), and both genetic heterogeneity and tumour cell plasticity provide reasonable explanations to the observation that only a particular subset of cells (CSCs) has the ability to propagate a tumour in the xenograft model. The concept of tumour cell plasticity, introducing the idea that the majority of tumour cells can display some degree of stemness depending on the environmental cues and/or intrinsic (cell-autonomous) stochastic mechanisms influencing them, as opposed to the CSC model, seems in fact to fit well the observations regarding the complex evolutionary progression of cancer. Further evidence for this idea comes from the observation that in some types of cancer, for example acute myeloid leukaemia, leukaemia initiating cells can be identified among the undifferentiated as well as among more differentiated compartments of the tumour (CD34- and CD34+) (Taussig et al., 2010). Moreover, experimental evidence in favour of rigid differentiation hierarchies is poor even in the context of normal tissue, reinforcing the importance of considering a model in which genotypes on their own cannot specify strictly defined phenotypes, but only a range of phenotypic manifestations within a norm of reaction, allowing cells to behave distinctly even within a genetically homogeneous population (Hill, 2006). Once more, it is however important to stress that the concepts of cancer stem cells and phenotypic plasticity are not necessarily mutually exclusive, and that genetic heterogeneity could be important in both. It seems quite reasonable to imagine a scenario in which oncogenic transformation is capable of increasing the plasticity of cancer cells, (Chaffer et al., 2011), possibly explaining the differences in CSC numbers among different tumours, and at different stages of a tumour's progression. Similarly, the

ability of cancer stem cell to self-renew could be enhanced by an aberrant genotype or aberrant epigenetic features, and the kind of genetic variation described in leukaemia might confer adaptability on certain cancer stem cells in addition to their intrinsic drug- and irradiation-resistance, allowing for their selection via microenvironmental or therapeutic pressures (Greaves and Maley, 2012) (Figure 1-7). Given the current difficulty in directly interrogating the genome of single CSCs from primary samples, so far the genetic heterogeneity of this subset of cells has been inferred by comparing the subclonal architecture of cancers pre- and post-transplantation. When Anderson et al. injected NSG mice with either bulk or LSC-enriched subpopulations of leukemic cells, multiple genetic clones repopulated the bone marrow; showing that CSCs in ALL are unambiguously genetically diverse.

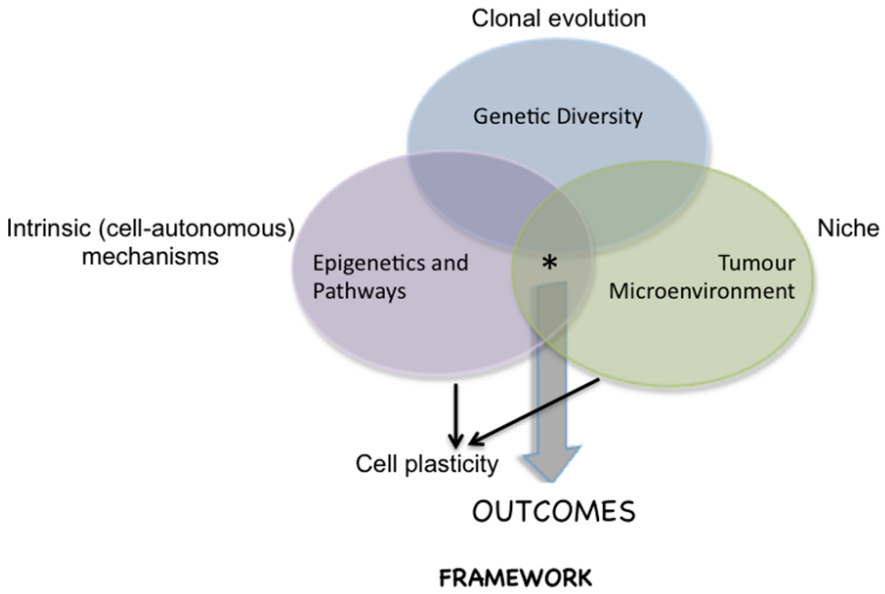

Figure 1-7: Sources of tumour heterogeneity [Adapted from (Kreso and Dick, 2014)]. Diversity within tumours can arise from stochastic genetic and epigenetic changes responsible for the multistep co-evolution of phenotypically and functionally distinct cancer populations. Different clones constitute material for the selection and clonal outgrowth of the fittest cell population. Heterogeneity can also originate in response to extrinsic environmental differences within the tumour. Phenotypic differences induced by interaction with the niche might be reversible or cause irreversible changes to cancer cell properties. In cancers that follow the CSC model tumour heterogeneity is driven by the presence of hierarchically organised populations of cells in different states of stemness or differentiation within the tumour. According to this model cells can only transit from CSC-to–non-CSC and not vice versa. CSCs can be serially transplanted, re-establishing phenotypic heterogeneity at each passage. The plastic cancer stem cell theory instead proposes the possibility of bidirectional conversions between non-CSCs and CSCs. In any case, cancers organised according to the CSC model are subject to clonal evolution and microenvironment-induced phenotypic heterogeneity. Therefore none of these sources of heterogeneity are mutually exclusive and together they all contribute (to a different extent in each individual cancer type) to the creation of a substrate for tumour evolution in response to treatment, therefore influencing patient outcome.

However, if in some cases the regenerated patterns of subclonal variation were highly concordant with the diagnostic sample, accurately reflecting the same composition of the original leukaemia, this was not true for all of the patient samples. In this regard additional data from Notta et al. seem to suggest that xenografts concordance with the diagnostic sample can be reconnected to specific genetic events in cancer (*CDKN2A/B* and *PAX5* deletion) gearing some cells for clear competitive superiority, while the reduced competitive fitness of minor subclones within the leukaemia possibly indicated the requirement for additional genetic events in order for these cells to increase their aggressiveness. More recently, Kreso and colleagues have carried out a similar study by tracing the fates of lentivirus-marked single-cell derived clones of colorectal cancer across serial xenograft repopulation assays. After having shown that in this type of malignancy clones did remain stable upon serial transplantation, the group observed that, despite the apparent genetic stability, proliferation and persistence properties were variable among colorectal cancer clones. This provided additional indirect evidence (via CNA profiling and sequencing of the bulk) of genetic heterogeneity among cancer initiating cells, and described notable genetics-independent differences in their behaviour. In fact, other than persistent and extinguishable clones, clones with fluctuating proliferative properties were also identified, showing that not all CSCs within the tumour contribute to its growth at any given time (Kreso et al., 2013).

Mutation profiling studies also have the potential to delineate the evolutionary history of relapse in cancers. This is particularly true for haematological malignancies, in which spatial heterogeneity does not represent a concern to sampling. However, not many studies on intra-tumour heterogeneity at

diagnosis have ventured to complementary characterization of clonal composition post-treatment. Deep sequencing of the whole genome of eight matching diagnosis and relapse AML samples has recently allowed the identification of two major patterns of clonal evolution across relapse. Both of these implied the existence of an ancestral tumour-initiating pre-diagnostic clone from which at least two distinct clonal lineages separately evolved through the acquisition of different genetic lesions. In the first scenario, the founding clone at diagnosis drove relapse following the acquisition of additional relapse-specific alterations. In the second, a subclone of the founding clone at diagnosis escaped chemotherapy and continued to evolve into the relapse clone. In any case, treatment in this setting clearly proved inadequate to achieve the complete eradication of the disease. Furthermore, as every relapse sample carried additional genetic abnormalities, it is likely that chemotherapy plays an active role in leukaemia progression, by increasing the rate of new mutations occurring within the founding clone or in its subclones, therefore creating additional substrate for selection and expansion (Figure 1-8c) (Ding et al., 2012). However, the suggestion is that at least some genetic populations in AML seem to be sensitive to treatment, as in four out of eight cases, specific primary subclones were lost at relapse, implying that genetic heterogeneity might indeed play a role in drug resistance. Limited data of similar nature where previously obtained for ALL (Anderson et al., 2011; Mullighan et al., 2008; van Delft et al., 2011). When Mullighan et al. carried out a genome-wide copy number analysis of bulk cells from 61 matching diagnostic and relapse paediatric B-ALL and T-ALL samples, the inferred primary and relapse clones displayed distinct patterns of copy number alterations (CNAs), pointing to the existence of a bottleneck selection and evolution process during treatment (Figure

1-8b). Once again, in the majority of the cases, relapse clones were recognized as evolutionary products of minor diagnostic subclones, while only in a small percentage of cases of relapse was driven by the major diagnostic clone, or a clonal descendent of the same. Of note, the most frequently acquired additional genetic lesions where, in this order, deletions of *CDKN2A/B* (mostly biallelic covering p16, p14 and p15), *TEL* and regulators of B cell development (*PAX5*, *IKZF1*, *IKZF2*, *IKZF3*, *TCF3*, *RAG1/2* and *EBF1*). In few cases, however, it was impossible to detect the ancestral clone within the diagnostic specimen. Identical results were obtained by the group of Mel Greaves in the analysis of subsets of TEL-AML1+ ALL samples (Anderson et al., 2011; van Delft et al., 2011). In these studies SNP arrays were coupled to single cell FISH analysis, of one and five samples respectively, in order to fully characterize the subclonal evolutionary relationships linking genetic clones characteristic of TEL-AML1+ ALL in late relapse, to those detected in the diagnostic specimens. Overall the data collected in these studies suggest that relapse originates from the survival of chemotherapy by likely multiple genetically distinct leukaemia propagating cells present at diagnosis as either major or minor subclones, which generate a reservoir for further diversification during treatment and remission. However, these data are discordant with the recent work of Kreso et al. and Almendro et al. showing that genetic diversity is not affected by chemotherapy in either colorectal cancer or breast cancer. In mice engrafted with lentiviral-labelled colorectal cancer cells, subsequent treatment with oxaliplatin, a common chemotherapeutic agent, reduced the tumour burden but had no effect on either the number of clones present or on their proportions within the bulk (Figure 1-8a) (estimated via CNA arrays). However, through the transplantation of oxaliplatin-treated cancer cells

into secondary recipient mice, the authors observed that chemotherapy had altered the growth properties of the CSCs, preferentially eliminating persistent (serially transplantable) clones and selecting for clones present below the detection threshold in the diagnostic specimen. Having previously demonstrated that behavioural differences of the CSC clones were not linked to their genotype, these experiments provided indirect evidence of the role of non-genetic cellular heterogeneity (stochasticity in gene expression and signalling pathways) and/or epigenetic modulation in driving key phenotypic differences (Kreso et al., 2013; Marusyk and Polyak, 2013). This innovative interpretation is in counter-current with the widely accepted idea that relapse is either driven by relevant genetic alterations or by preferential survival of dormant cancer stem cells (Lutz et al., 2013). Similarly, Almendro and colleagues observed the lack of a detectable treatment-driven bottleneck clonal selection process when assessing the effect of neoadjuvant therapy on intratumour heterogeneity of breast cancer (47 samples spanning the four major subtypes). Interestingly though, samples displaying lower diagnostic genetic heterogeneity were more likely to reach complete pathologic response to treatment.

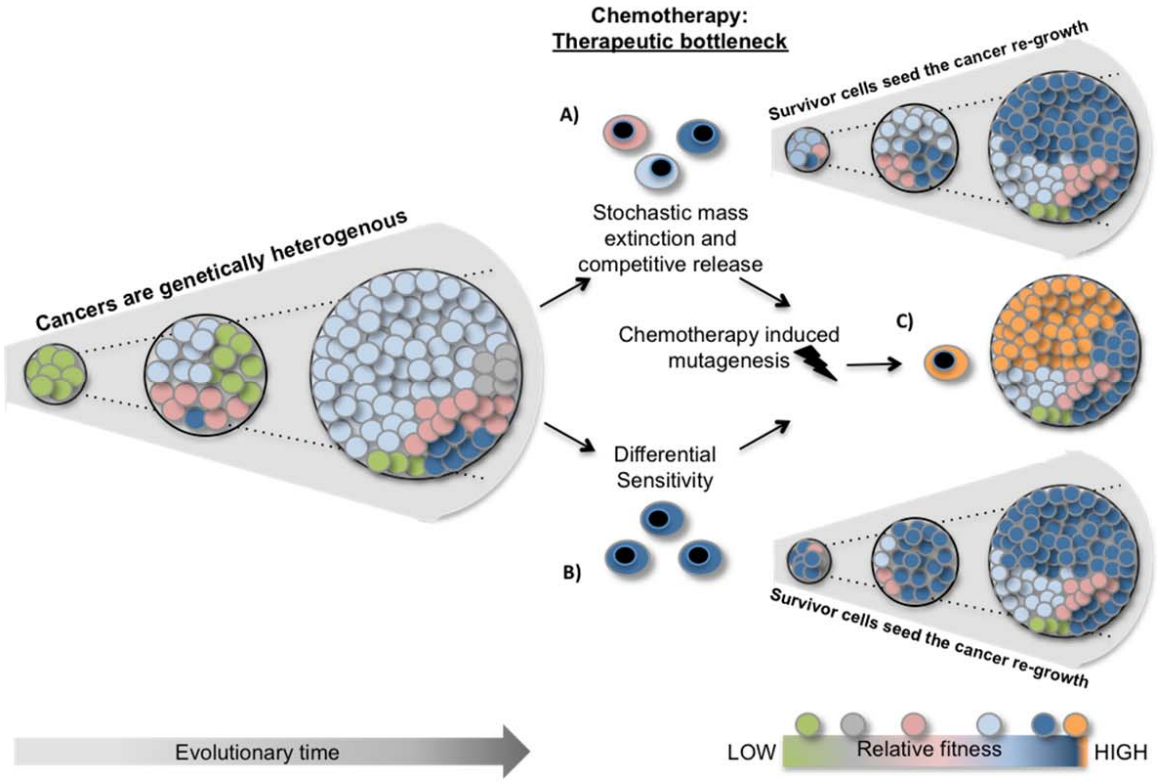

Figure 1-8: Models of treatment impact on clonal evolution [Adapted from (Landau et al., 2014)]. Three alternative ways in which chemotherapy could promote clonal evolution are presented. (a) First, assuming a similar sensitivity of all clones to treatment, drugs would be expected to equally affect these; and their proportions within the bulk, before and after cytoreduction, should be unaffected (b) Second, therapy can select for a clone (blue) containing a mutation that confers resistance to the therapeutic agent used, therefore drastically reducing genetic heterogeneity of the post-cytoreduction tumour. (c) Finally, cancer treatment, especially genotoxic agents, can induce novel mutagenesis, creating new clones detectable only at relapse.

Moreover, making use of a technique named immune-fluorescence in situ hybridization (iFISH), which allows for tracking of both phenotypic and genotypic diversity of hundreds of single cells simultaneously, the researchers described significant longitudinal changes in the tumours' phenotypes. Most of the samples displayed a shift in the cells' phenotype from more differentiated ($CD24^+$ / $CD44^-$) at diagnosis to more immature post-treatment ($CD24^-$ / $CD44^+$). This observation, in concomitance with the recorded decrease in cell proliferation rate, is compatible with the possibility that chemotherapy preferential eradicates highly proliferative cells (Almendro et al., 2014a). Therefore, unlike in colorectal cancer, phenotypes seem to play a fundamental role in breast cancer treatment-resistance insurgence. Overall, even though a limited number of studies have begun to dissect the role of genetic diversity in treatment response, further work combining cytogenetic and genomic tools is required to fully understand the role it plays in development of chemo-resistance on its own and through interplay with phenotypic heterogeneity (Navin et al., 2011). To complicate things, data collected so far in different types of cancers are conflicting. While in AML and ALL preliminary evidence points towards a possible relevance of genetic heterogeneity in influencing treatment response, as displayed by the post-treatment emergence of minor subclones with resistance-specific lesions, study of breast cancer in contrast highlights a greater importance of phenotypes in driving the insurgence of drug resistance in presence of rather stable genetic traits. Additionally, the analysis of colorectal cancer samples calls the attention to the need of fully understand those non-genetic mechanisms that are the sources of cellular and functional heterogeneity of tumour cells. It is likely that drug-resistance and post-therapeutic tumour reappearance are influenced not just by genetic heterogeneity and the stem-cell characteristics of some cells, but

also by different alternative sources of diversity, such as epigenetic regulation, noise in gene expression and variability in the microenvironment.

1.3 Aim of the study: a mouse model for ALL treatment and investigation of Intratumour genetic heterogeneity

As stated in the introduction, the role of second hits in TEL-AML1 pre-B-ALL is poorly understood. Our current knowledge is limited to the observation that TEL-ALML1 by itself is not sufficient to give rise to overt leukaemia. A number of additional genetic alterations are required for disease progression. However, how and when these second hits arise, what pathways they deregulate, and more importantly, what their role is in drug-resistance, is still to be clarified. Furthermore, the recent discovery of an unexpected high degree of intra-tumour genetic diversity within the leukaemia has added new challenges to these tasks and raised numerous important questions. One among these, namely whether it is possible that coexisting subclones within the leukaemia are endowed with distinct functional abilities dictated by their underlying genetic lesions, is the subject of this thesis. Answering this question would allow a better understanding of the roles played by different recurrent second hits in crucial phases of the disease (e.g. tumour formation and treatment response), concurrently shedding light onto the reason behind their coexistence. Such knowledge is also expected to provide better insight into the clinical implications of genetic tumour heterogeneity. As to whether these recent data should or should not influence the way the disease is handled from a therapeutic point of view is not yet clear. We approach these queries using two different experimental design strategies. Underlying both is the idea that to

and understand whether different genetic lesion are responsible for characteristic clonal behaviours, the tumour must be challenged.

1) The first approach makes use of chemotherapy to test the influence of genetics on the clones' sensitivity/resistance to it. After a trial experiment with $CD34^+$ cord blood cells, TEL-AML+ patient were injected into NSG mice. Mice were then treated with a combination of drugs normally used in the induction phase of treatment, and the ability of distinct leukemic clones to survive chemotherapy was analysed.

2) Additionally, as TEL deletion and PAX5 deletions represent the most common second hits in the context of TEL-AML1-positive leukaemia (Mullighan et al., 2007), lentiviral vectors have been generated to restore the expression of one or both in primary leukaemia cells. Upon transduction cells have been transplanted into several recipient mice in order to test the effect of the genes' restored expression on engraftment ability and clonal dominance. The subsequent characterization of the molecular pathways activated and/or repressed by the two genes is the interest of a separate project in the laboratory.

3) In a combination of the two original approaches, genetically modified cells have been treated with chemotherapy to test whether the drug-sensitivity of clones is affected by the expression of the selected genes.

Given that there are multiple ways in which the selective pressure exercised by the drugs could influence tumour diversity, these functional assays have numerous possible outcomes. Chemotherapy might succeed in eliminating all of the cancer cells no matter regardless of their underlying genetics, or it might simply create a population bottleneck followed by the expansion of resistant

clones, and lastly it might leave tumour heterogeneity unaffected. The current consensus is that drug-resistance is the property of a minority of cells that differ from the others in their genotype and/or phenotype (CSS) (Lutz et al., 2013). According to this theory cells harbouring the “wrong” genotype or phenotype are sensitive to treatment, and therefore preferentially eliminated by it, while, resistant clone/s survive and are responsible for the eventual regrowth of the tumour. However, whether or not the genomic makeup in reality affect responsiveness to treatment is difficult to establish from data collected so far. Evidence in favour of preferential elimination of specific genetic clones in leukaemia is preliminary, with not many samples of matching diagnosis and relapse having been analysed at the single cell level. Moreover, these observations are in direct contrast with what has been described for other kinds of malignancies. In breast cancer, for example, cell diversity (genotypic or phenotypic) is unaffected by treatment, suggesting that most of the cells could be resistant to chemotherapy (Almendro et al., 2014a). Even though it is possible that different cancers respond differently to chemotherapy, and maybe even to different drugs, it can’t be excluded that the analysis of a single late time point in the disease’s eradication history might not be informative enough. After a brief period of bottleneck selection tumour cells might re-diversify as part of the process of regrowth of the tumour mass, and this kinetic might very well elude us by the sole investigation of relapse samples. Additionally, only exposure to treatment of the same clone multiple times would provide clear link between genetic makeup and resistance. However, given the well characterised extent of intertumour heterogeneity, only extensive analysis of a large cohort of matching diagnostic, minimal residual disease (MRD), and relapse samples could provide evidence of post-treatment bottleneck genetic selection of

specific clones. These samples are however in very limited supply and often of small size. Our *in vivo xenotransplant* model of paediatric acute lymphoblastic leukaemia therefore offers a unique alternative platform for the study of genetic basis of tumour resistance.

CHAPTER 2

MATERIALS AND METHODS

2.1 Molecular biology

2.1.1 Transformation of bacteria

Chemically competent sub-cloning efficiency NEB 5-alpha and library efficiency NEB 5-alpha cells (New England BioLabs) were used to transform bacteria. 50 µl of cells were pipetted into a 1.5ml eppendorf tube placed on ice, and 1-5 µl of plasmid (0.5-1µg) DNA were added. The transformation mix was incubated on ice for 30 minutes, heat shocked at 42°C for exactly 30 seconds, and incubated on ice for additional 5 minutes. Subsequently 950µL of SOC outgrowth medium (New England BioLabs) were added and the mixture incubated at 37°C for 1 hour in a shaker (250 rpm). Following, a 10-fold dilution was plated onto pre-warmed selection plates prepared with LB agar (1.5g Bacto Agar (BD Bioscience) per 100ml LB broth (1% w/v Bacto Tryptone (BD Bioscience), 0.5% w/v Bacto Yeast Extract (BD Bioscience), 1% w/v Sodium Chloride (NaCl), [pH 7.0]) and 100µg/ml Ampicillin (Sigma-Aldrich) and incubated at 37°C overnight.

2.1.2 Isolation of plasmid DNA

Individual bacterial colonies were inoculated into 3ml LB broth containing Ampicillin (100 µg/mL) and incubated in a shaker at 37°C overnight. The bacterial cultures were then used to extract DNA using the QIAprep® Miniprep Plasmid kit (Qiagen) according to the manufacturer's instructions. Briefly, the bacterial culture was resuspended in 250µl of Buffer P1 and transferred to a micro- centrifuge tube in order to lyse the bacterial cells. 250µl of Buffer P2 were added and mixed thoroughly by inverting the tube 4–6 times. Subsequently 350µl of buffer N3 were added and mixed immediately and thoroughly by inverting the tube 4–6 times. The

mixture was centrifuged for 10 min at 13,000 rpm in a table-top microcentrifuge. The supernatant was transferred by pipetting to a QIAprep spin column and centrifuged at maximum speed for 60 seconds; the flow-through was discarded. The column was washed first by adding 0.5 ml Buffer PB (endotoxin removal buffer) and centrifuging for 60s and then by adding 0.75 ml Buffer PE (column wash solution containing ethanol) and centrifuging for 60s. The flow-through was discarded at each step, and the column was finally centrifuged at full speed for an additional 1 min to remove residual wash buffer. The QIAprep column was placed in a clean 1.5 ml microcentrifuge tube and 50 µl Buffer EB (10 mM Tris·Cl, pH 8.5) or water were added to the centre of each QIAprep spin column to elute DNA. The solution was incubated for 1 min, followed by a 1 min max speed centrifugation of the tube. The final DNA concentration was measured using a spectrophotometer (NanoDrop.ND-1000, Lebtech International).

In order to obtain larger quantities of plasmid DNA from individual bacterial colonies bigger culture volumes were set up, and HiSpeed Plasmid Midi Kit (Qiagen) and HiSpeed or EndoFree Plasmid Maxi Kits (Qiagen) were alternatively used according to manufacturer's instructions.

2.1.3 Restriction enzyme digests

Restriction enzyme digests were performed according to manufacturer's instructions. Typically, 0.3µl-0.5µl of DNA were digested in a mix prepared with 10U/µl of restriction enzyme per µg of DNA, 10x restriction buffer and 100x BSA 10µg/µl to a final volume of 50-1-00µl adjusted with H_20. DNA was digested for 1-4 hours or overnight (ON) at 37C° or 65C°, depending on the characteristics and efficiency of the restriction enzyme adopted. According the size of the generated

fragment/s, the digested products were subjected to electrophoresis on 0.7-2% w/v agarose gels [agarose (Invitrogen), 1x TAE buffer (National diagnostic), 0.5% ethidium bromide (Sigma-Aldrich)] in order to be visualised and validated.

2.1.4 Gel extraction

Isolated digested DNA products were purified from the agarose gel using GFX PCR DNA and Gel Band Purification Kit (GE Healthcare) according to the manufacturer's guidelines. The DNA fragment was excised from the agarose gel and weighed. 10µl of Capture buffer type 3 were added to the excised gel band for each 10 mg of gel slice and incubated at 60C° for 15–30 minutes until the agarose was completely dissolved. The Capture buffer type 3- sample mix was then transferred onto an assembled GFX MicroSpin column and collection tube, incubated at room temperature for 1 minute and spun at 16000g for 30 seconds. The flow through was discarded by emptying the collection tube and the GFX MicroSpin column washed with 500µl of Wash buffer type 1 to remove any salt contamination. DNA was then eluted by centrifugation in 30-50µl of DNase/RNase free distilled water (Life Technologies) or TE buffer (Qiagen).

2.1.5 Ligation

DNA fragment and vector were ligated to generate plasmid DNA. Depending on the performed cloning, the molar ratio of choice between the fragment and the vector varied from 1:1 to 5:1. Typically, 50ng of vector were ligated with the required amount of DNA fragment in presence of 1X T4 DNA Ligase Reaction Buffer [50 mM Tris-HCl□10 mM $MgCl_2$□1 mM ATP□10 mM DTT□pH 7.5 at 25°C]

(NewEngland BioLabs), and 1 µl of T4 DNA Ligase (NewEngland BioLabs), in a total reaction volume of 20µl, made up with H_2O. The mixture was incubated at room temperature for at least 1h prior to transformation (see section 2.1).

2.1.6 DNA constructs

A schematic diagram of the lentiviral overexpression vector *pHR-SIN-CSGW-IRES-emGFP*(CSI) backbone is shown in Figure 2-1.

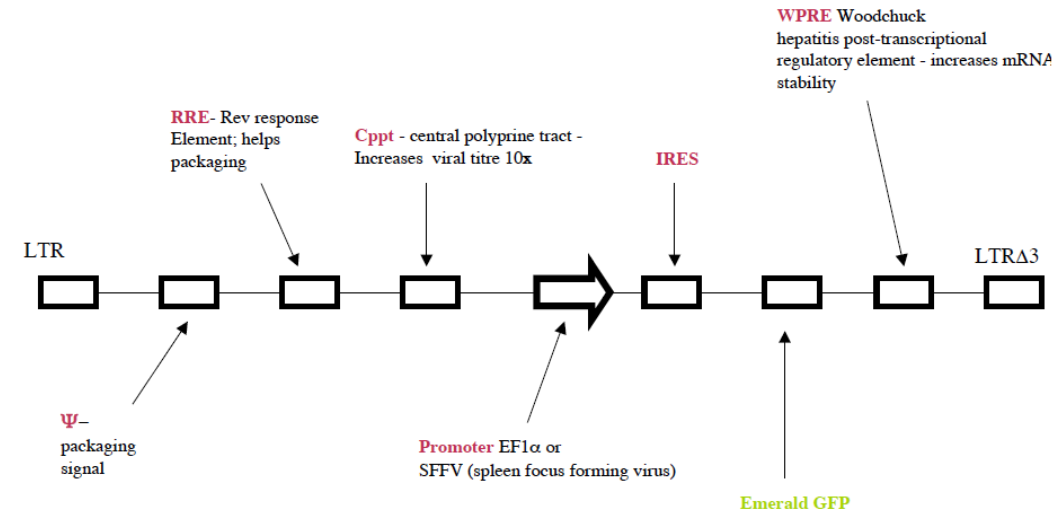

Figure 2-1: Basic structure of the CSI overexpression vectors. A variant of the backbone in which eGFP was replaced by ΔLNGFR as reporter was also adopted.

2.1.6.1 TEL overexpression vectors

Full length human TEL (hTEL) was amplified from an hTEL cDNA fully sequenced I.M.A.G.E clone (6014394) purchased from Source Bioscience. Primers were

designed (Table 2-1) according to the sequence of hTEL mRNA (NCBI: ENST00000396373) to generate the N-terminal tagged, C-terminal tagged or untagged TEL product. PCR products were first subcloned into pGEM T-easy vector (Promega) according to manufacturer instruction. The ligated vector was then digested with BglII (BglII unique restriction sites were included within the sequence of the amplification primers) to lift out TEL constructs and reclone it into a lentiviral expression construct *pHR-SIN-CSGW-IRES-LNGFR*(CSI). CSI vector, part of the Enver lab general plasmids stock, was before head digested with BamHI at 37°C overnight (Figure 2-2). Both digestion products were then gel purified, and the vector backbone was dephosphorylated (calf intestine alkaline phosphatase – CIAP, NEB or Fermentas) to minimize self-ligation during the subsequent ligation reaction.

2.1.6.1 PAX5 overexpression vectors

Full length human PAX5 (hPAX5) was amplified from a previously cloned plasmid containing the gene. Primers were designed based on the sequence of h*PAX5* mRNA (NCBI: ENST00000358127), and an HA (hemagglutinin) tag was added either at the N- or C-terminus (Table 2-1). Following the same strategy previously used to clone *TEL,* amplification products were first sub-cloned into T-vector and then transferred into CSIemerald lentiviral vector (Figure 2-2).

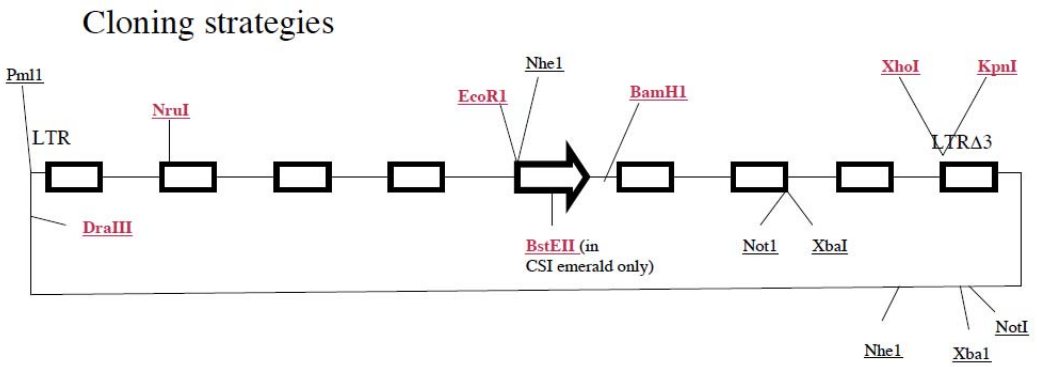

Figure 2-2: Basic strategy for cloning into CSI overexpression vectors.

PRIMER	SEQUENCE
PAX5_Forw	ACGTAGATCTGCCACCATGGATTTAGAGAAAAATTAT
PAX5_Rev	ACGTAGATCTTCATCAGCGTCGGTGCTGAGTAGC
PAX5_HAtag_Forw	ACGTAGATCTGCCACCATGTACCCATACGATGTTCCAGATTACGCTATGGATTTAGAGAAAAATTAT
PAX5_HAtag_Rev	ACGTAGATCTTCATCAAGCGTAATCTGGAACATCGTATGGGTATCAGTGACGGTCATAGGCAGT
TEL_Forw	TACGTAGATCTCCACCATGTCTGAGACTCCTGCTCAG
TEL_Rev	TACGTAGATCTCAGCATTCATCTTCTTGGTATATTTG
TEL_FLAGtag_Forw	TACGTAGATCTCCACCATGGACTACAAGGACGACGATGACAAGATGTCTGAGACTCCTGCTCAG
TEL_FLAGtag_Rev	TACGTAGATCTCACTTGTCATCGTCGTCCTTGTAGTCGCATTCATCTTCTTGGTATATTTG
Bsm-Nde-v5-Bgl-Spe	GAATGCTCTCATATGGGCAAGCCCATCCCCAACCCCCTGCTGGGCCTGGACTCCACCTGAAGATCTACTAGT
Bsm-Nde-v5-Bgl-Spe_lower	CTAGTAGATCTTCAGGTGGAGTCCAGGCCCAGCAGGGGGTTGGGGATGGGCTTGCCCATATGAGAG
Bsm-Nde-v5-Bgl-Spe_upper	CTCATATGGGCAAGCCCATCCCCAACCCCCTGCTGGGCCTGGACTCCACCTGAAGATCTA
Bsm-v5-Bgl-Spe	GAATGCTCTGGCAAGCCCATCCCCAACCCCCTGCTGGGCCTGGACTCCACCTGAAGATCTACTAGT
Bsm-v5-Bgl-Spe_lower	CTAGTAGATCTTCAGGTGGAGTCCAGGCCCAGCAGGGGGTTGGGGATGGGCTTGCCAGAG
Bsm-v5-Bgl-Spe_upper	CTGGCAAGCCCATCCCCAACCCCCTGCTGGGCCTGGACTCCACCTGAAGATCTA

Table 2-1: Amplification Primers.

2.1.6.1 Sequencing

Ahead of packaging of the lentiviral vectors for viral transduction, the newly generated constructs were sequenced both following their insertion into pGEM T-easy vector and once cloned into CSIemerald vector. The sequencing service was provided by Source Bioscience Cambridge UK.

2.1.7 Preparation of total protein lysate for western blot analysis

Cells were harvested and washed in PBS prior to a final centrifugation step at 350g for 5 minutes at 4ºC. Cell pellets were lysed in 50µL of 1x RIPA buffer every 10^6 cells (Radio-Immunoprecipitation Assay) [150 mM NaCl, 1.0% Triton X-100, 0.5% Na Deoxycholate, 0.1% SDS, 50 mM Tris HCl, pH 8.0] to which 25X PIC (Protease Inhibitor Cocktail) (Roche). Lysates were incubated on ice for 30 minutes, vortexed for 10 seconds, and centrifuged at 16,000g for 20 minutes at 4°C. Clear supernatants were removed to a fresh tube and, if required, stored at -80°C. All samples were mixed 1:4 with 4× NuPAGE loading buffer (Invitrogen) and denatured by heating at 95°C for 2-4 minutes before loading. When required protein concentration was measured by mean of BCA protein quantitation kit (Thermo Scientific Pierce) reading absorbance at a wavelength of 562nm on a Ultrospec 2100 pro (Amersham Pharmacia Biotech) spectrophotometer. Alternatively lanes were loaded with approximate cell equivalents. A NuPAGE SDS gel system from Invitrogen was used for the purpose of protein polyacrylamide gel electrophoresis. Bis-Tris 4-12% NuPAGE gels were run in MES running buffer 45 minutes at 200 Volts. Following electrophoresis, samples were transferred onto a polyvinylidenefluoride (PVDF) membrane (Millipore) for 1 hour at 30 Volts at room temperature in a Tris-glycine-methanol transfer buffer [Glycine 28.8g, Tris 6.06g, metOH 400mL, SDS 20% 1.87mL brought up to 2L in water].

2.1.8 Western blot analysis

Membranes were blocked in Phosphate buffered saline (PBS) with 5% non-fat milk and 0.05% Tween-20, and hybridized with the relevant primary (Table 2-2) and

secondary horseradish peroxidise-conjugated antibodies (Table 2-3). For Proteins detection a chemiluminescence (ECL) Western Blotting System (GE Healthcare) was adopted according to the manufacturer's instructions. For stripping purposes membranes were incubated in a home-made stripping solution [tris HCl pH 6.8 100mM 2.26mL, β-mercaptoethanol (2-ME) 100mM 280 µL, SDS 20% 2 mL, milli-Q water 33.16 mL] 30 minutes at 55°C. Following a wash in Tris-buffered saline-Tween (TBST) the membrane was re-probed with different primary and secondary antibodies. The exposed film was developed using the Xograph CompactX4 (BioRad) developer.

Antibody	Supplier	Cat no	Diln.
Pax5 (N19)	Santa Cruz	sc-1975	1/500
Anti-HA High Affinity	Roche	11867423001	1/250
Anti-ETV6	Sigma	HPA000264	1/500
Anti-ETV6	O. Bernard		1/500
Anti-FLAG	Santa Cruz	D8SC807	1/500
Anti -tubulin	Santa Cruz	SC-9161	1/500

Table 2-2: List of primary antibodies used for western blot analyses in this study. The anti–N-terminal ETV6 antibody was kindly provided by O. Bernard (U434 INSERM, Paris, France).

Antibody	Supplier	Cat no	Diln.
Rabbit anti-Rat IgG (H+L) Secondary Antibody	Pierce	31218	1/500
Donkey anti-goat IgG-HRP	Santa Cruz	sc-2020	1/1000
IP/WB Optima A anti-goat	Santa Cruz	sc-45038	1/5000
Anti-rabbit IgG HPR-linked whole antibody	GE HealthCare	NA934	1/5000

Table 2-3: Secondary antibodies used for western blot analyses in this study.

2.1.9 Total RNA isolation

Cell pellets were resuspended and homogenized in Trizol reagent (Invitrogen), and total RNA was isolated according manufacturer's instruction. Briefly, addition

of chloroform to sample lysates, followed by centrifugation, allowed for separation of the solution into an upper aqueous phase containing RNA, and a lower phenol-containing organic phase. The upper aqueous phase was transferred to a new tube and the RNA precipitated by the addition of isopropanol followed by centrifugation. After a wash with 75% ethanol, RNA pellets were dissolved in 30µl of diethylpyrocarbonate (DEPC) treated water and concentrations were determined with NanoDrop 1000 Spectrophotometer (Thermo Scientific).

2.1.10 cDNA preparation and quantitative Real-Time PCR

Equivalent amounts of total RNA from test and control samples were DNase treated (RNase-free DNase, Promega), and reverse transcribed using Superscript II and random primers (250ng/reaction) according to manufacturers' protocols. The cDNA samples were analysed using inventoried Taqman gene expression assays (Table 2-4) (Applied Biosystems) and ABI Prism Sequence Detector Systems 7000 (Applied Biosystems).

Gene	Species	Probe	Supplier	Cat no	Amplicon Length	Dye	Exon Boundary
PAX5	Hu	Hs00172001_m1	Life Technologies	4331182	116	FAM-MGB	7-8
ETV6	Hu	Hs01045746_m1	Life Technologies	4331182	70	FAM-MGB	6-7

Table 2-4: Taqman probes used for western Real-Time PCR in this study.

2.1.11 FISH

2.1.11.1 Cytocell Aquarius probes

Locus specific FISH probes designed to hybridize to chromosomes 9, 12 and 21, were purchased from Cytocell, through "my Probes", a probes customized design

and manufacture service. A mix of consisted of: one probe labelled in blue fluorophore mapping to the specific region of chromosome 9p13.2 between nucleotides 36,819,407 and 37,208,44 (PAX5 probe), one probe labelled in gold fluorophore mapping on chromosome 9p21.3 on between nucleotides 21,862,429 and 22,055,767 (P16 probe), two probes labelled in green fluorophore mapping to chromosome 12p13.2 to the regions between nucleotides 11,728,311 and 11,908,365 (TEL-A probe) and 12,055,716 and 12,223,559 (TEL-B probe), and two probes labelled in red fluorophore mapping to chromosome 21q22.12 to the regions between nucleotides 35,995,366 and 36,143,772 (AML-1A probe) and 36,305,204 and 36,305,204 (AML-B probe). The red fluorophore emitted in the Texas Red spectrum, the green in the FITC spectrum, the Gold in the gold spectrum and the blue in the Aqua spectrum. To segregate mixed fluorescent signals and more clearly resolve the spatial contribution of each fluorophore (emission fingerprinting), the following probes, MYB Gold, CCND1 FITC, RREB1 Texas Red, 6c Aqua were used.

PAX5

Chromosome 9: 36,819,407-37,020,844

Region in detail

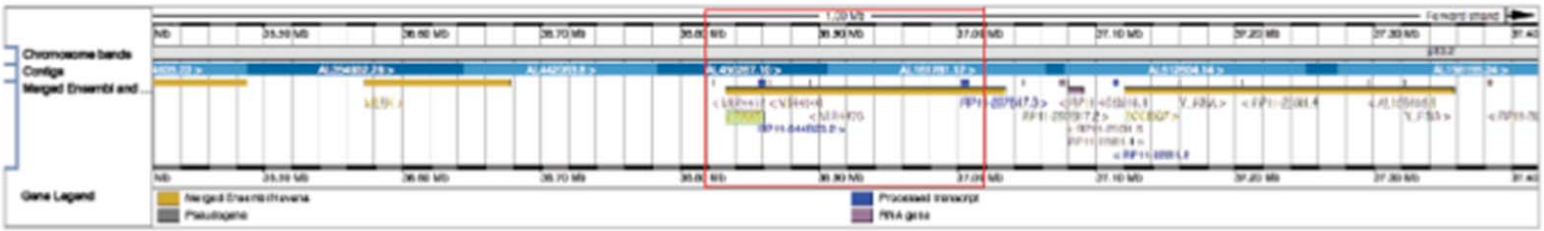

P16

Chromosome 9: 21,862,429-22,055,767

Region in detail

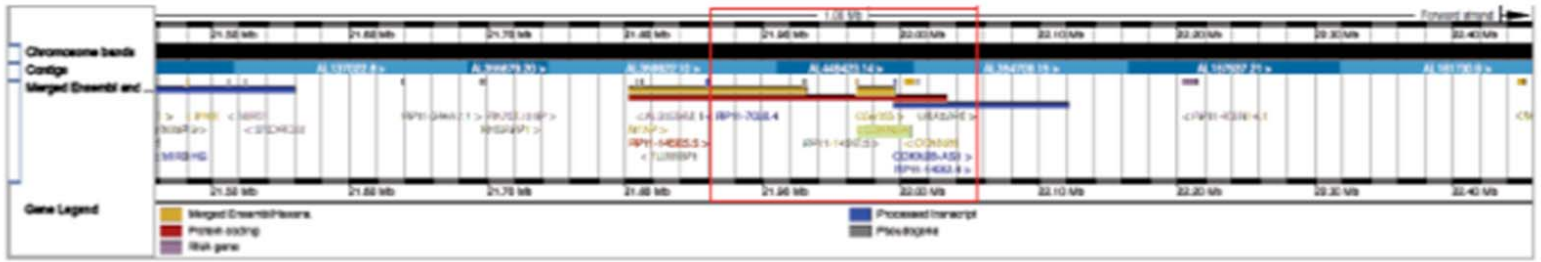

TEL-A

Chromosome 12: 11,728,311-11,908,365

Region in detail

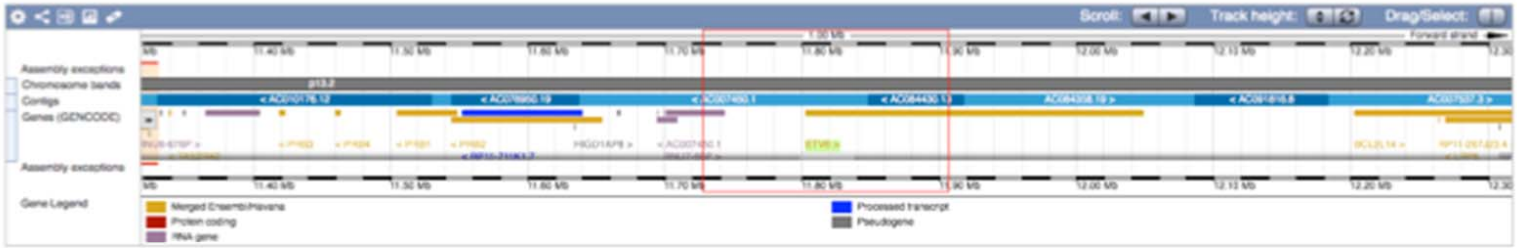

TEL-B

Chromosome 12: 12,055,716-12,223,559

Region in detail

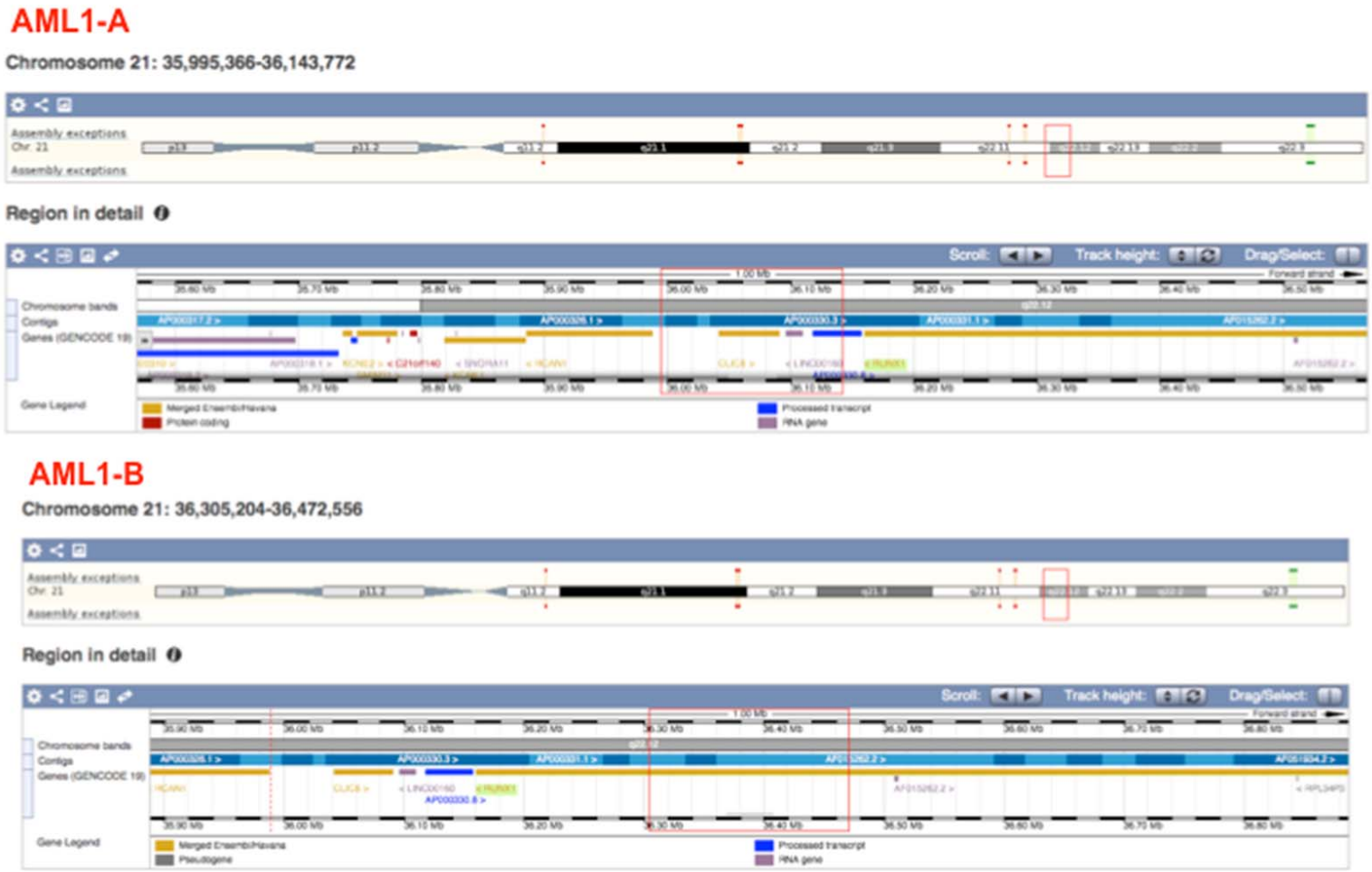

Figure 2-3: genome mapping of Cytocell mFISH probes.

2.1.11.2 Karyotype preparation

Cells were harvested for FISH purposes as for karyotype preparation protocol. Cells isolated from primary samples or from the bones or spleen of transplanted mice were collected in a screwcap tube (106 cells maximum) and centrifuged 10min at 1500rpm. After the supernatant was removed, cells were resuspended in 700µl of warm KCl (5.6g in 1L of purified water) and incubated at 37°C for 20 minutes. Cells were then prefixed by adding 200µl of fresh ice-cold fixing solution mix (3 parts methanol and 1 part glacial acetic acid). Tubes were mixed by inversion and centrifuged 10min at 1500rpm. Subsequently, a final cells fixing step was performed adding 800ul of ice-cold fixing solution dropwise on a vortex (high speed). Tubes were then stored at 4C for short-term storage and -20C for long-term storage.

2.1.11.3 FISH protocol

Superfrost glass microscope slides (VWR) were immersed in 8ml of concentrated acid (HCl) + 500 ml milli-Q water for 1h while shaking, then washed 6x in milli-Q (still shaking) and finally stored in 100% ethanol until usage. Alternatively superfrost plus microscopy slides (VWR) were used as purchased. Cells were spotted on the slide, allowed to air dry, and aged at RT for 24h (long term storage at -20 in a sealed box with silica gel). Slides were then immersed in 2X SSC for 2-10 minutes, incubated in Pepsin Working Solution (Sigma-Aldrich) [Stock solution 250mg: 2,500-3,500 units/mg protein lyophilized powder dissolved to a concentration of 100 mg/ml; Working solution: 0.05 mg/ml] at 37ºC for 3 min, and washed in PBS for 3-5 min at ambient temperature. Subsequently, slides were fixed in 4% paraformaldehyde for 10-15 min, followed by 3x washes in PBS.

Dehydration of the slides was performed by immersion in ethanol series (70%, 85%, 100%) 2 minutes at room temperature (RT) each. Slides were allowed to air dry. Pre-denaturation of the test probe (5µl/slide) and slides was achieved by pre-warming at 37°C for 5 minutes followed by spotting of the probe on the slide, while this was maintained at 37°C. A 22x22 coverslip (VWR) was then applied over the spotted area and sealed to the slide with rubber glue (fixogum). Probe and slides were then co-denatured 2 minutes at 75°C on a hybridizer (Dako) and hybridized at 37°C on the same for a period of 12-72 hours. Post-hybridization the fixogum seal was removed and slides soaked in 2x SSC until the coverslip would come off. A series of washes followed; first 2 minutes in 0.4xSSC at 72^0C for, then 30 seconds in 2xSSC/0.1% IGEPAL at RT. Slides were drained and 20ul of Cytocell DAPI/antifade counterstaining diluted 1:4 in Vectashield (Vectorlabs) were applied under a 22x50 coverslip sealed with nail polish. The fluorescence was allowed to develop in the dark for at least 10 minutes, after which the slides could be visualised under the microscope.

2.1.11.3 Microscopes and probe visualization

The simultaneous use of 4 probes labelled with different fluorochromes introduces technical challenges as to their successful detection and imaging. When first testing the probes numerous obstacles to the identification of a microscope suitable for the purpose were encountered. Among the many microscopes unsuccessfully tested were a Zeiss Axioplan 2 fluorescence microscope (based in the UCL Royal Free Hospital Campus, London), a Leica SP-2 confocal microscope (based in the UCL Wolfson Institute for Biomedical Research, London), a Leica SP-5 confocal microscope (based in the MRC Laboratory for

Molecular Cell Biology, London) and a Leica SP-8vis (based in the UCL Department of Cell and Developmental Biology). Multiple confocal microscopes (Leica SP2, Leica P5 and Leica-SP8vis) were tested. Three of these microscopes were equipped with high sensitivity phototomulipliers (PMTs) for light photodetection, and four lasers, allowing for sample excitation with seven tuneable excitation wavelengths [405 nm, Argon (for excitation of 458, 488, 496, 514), 561 nm DPSS, 594 nm HeNe, 633 nm HeNe], However, only 4 detectors were mounted on the microscopes requiring the imaging of the 5 dyes (4 probes + DAPI nucleus staining) to be carried out either fully sequentially or as a combination of the simultaneous acquisition into some channels and sequentially into others. The microscopes were set up with the laser beam sharply focusing on a particular focal plane in the specimen (multiple focal planes subsequently scanned) and suitable excitation laser lines were selected according to the fluorochromes used (see emission and excitation information below in table 2-5). Unfortunately, the slides scanning with the confocal microscopes revealed a strong spectral overlap between some of the dyes. The worst overlap was detected between Green and Gold spectra. The excitation of either of the Green or Gold resulted equal excitation the other fluorochrome, and an overlap in emission spectra (phenomenon known as cross-talk or bleed-through) (Figure 2-4). Additionally, a less worrying bleed-through of DAPI into the AQUA channel was also detected.

	Dye	Excitation$_{max}$ [nm]	Emission$_{max}$ [nm]
■	Aqua	418	467
■	Green	495	521
■	Gold	539	561
□	Orange	551	572
■	Red	595	610

Table 2-5: Emission and Excitation wavelengths of the 4 fluorochromes used for mFISH. Slides were additionally labeled with DAPI.

To address the issue and correct the cross-talk between the different channels, singularly labelled control slides were prepared for each fluorochrome and their excitation and emission spectra were imaged. The hope was that of making use of a spectral unmixing algorithm to resolve the spatial contribution of each fluorophome/probe (often referred to as emission fingerprinting) to the multi-probe fluorescence images. However, the overlap between emission spectra of green, gold and aqua fluorophores was so extensive (Figure 2-5) that this strategy could not fully solve the problem.

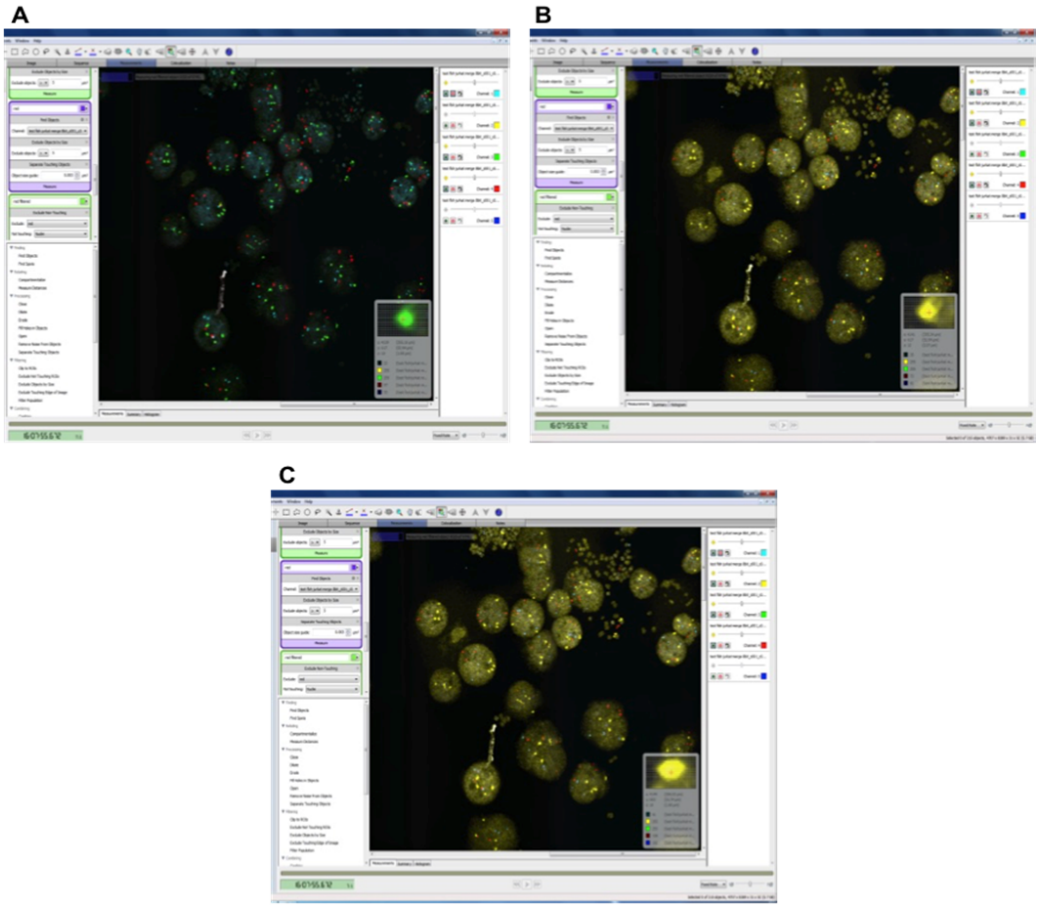

Figure 2-4: Bleed-through of Gold and Green fluorochromes when imaged by confocal microscopy. The top images were collected with the laser line for Gold (A) or FITC (B) deactivated, in turn. In these images the same signal pattern was detected by both laser lines (C) indicative of an overlap between the two fluorochromes' excitation and emission spectra.

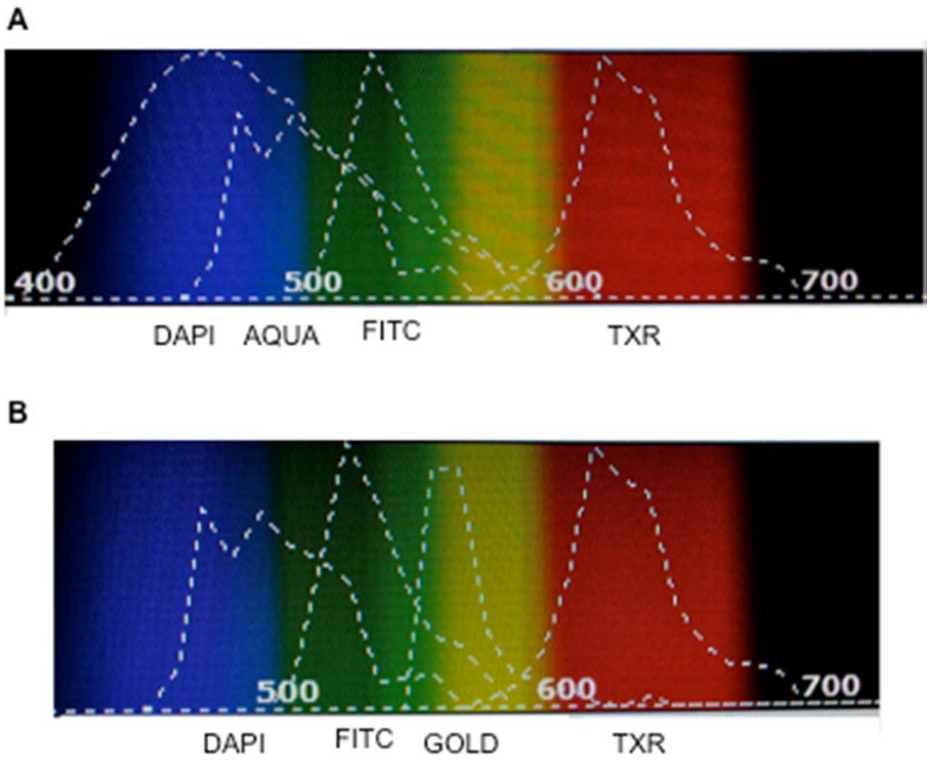

Figure 2-5 Characterization of DAPI, AQUA, FITC, GOLD and TEXAS RED emission spectra. A strong emission spectra overlap is detected between Gold and FITC (B), as well as between AQUA and DAPI (A). The latter, however, is only used for the purpose of nuclei staining in the background.

Consequently, after a few additional fluorescence microscopes were tested, a Zeiss Axio Observer z1 Apotome fluorescence microscope (available at UCL) was set up with selected filters commercialized and customised by Chroma {DEAC 49302, Texas Red 49008, GOLD 49034, FITC/TXR 59022}.

2.1.11.4 Establishing cut-off levels

In each case, at least 200 nuclei were scored for the presence of the TEL-AML1 fusion gene in combination with hemizygous or homozygous deletion of TEL, AML1, PAX5 and P16, as well as gain of AML1 and TEL-AML1 fusion gene. Cut-

off levels for each probe were calculated performing four-colour (+DAPI) FISH on normal control bone marrow and peripheral blood PBMC (total or $CD19^+$ enriched) slides. Combinatorial cut-off levels were established in a similar way by scoring slides for the coexistence of any two lesions (except for the fusion, the presence of which marked all cells) as well as by probabilistic evaluation of the event likelihood.

2.2 Cell biology

2.2.1 Cell culture and cell lines

293FT (Human Embryonic Kidney 293 cells that contain the SV40 Large T-antigen) (Invitrogen) packaging cell lines were cultured in Dulbecco's Modified Eagle's medium (DMEM, Invitrogen Paisley) supplemented with 10% foetal calf serum (FCS, Sigma-Aldrich), 100U/ml penicillin (Invitrogen), 100µg/ml streptomycin (Invitrogen) and 2mM L-glutamine (Invitrogen) (complete DMEM). Human lymphoblastoid leukaemia cell lines REH and UOCB6 (kind gift of Dr. Owen Williams), and the human acute lymphocytic T leukaemia cell line JURKAT were cultured in Roswell Park Memorial Institute (RPMI) medium (Invitrogen) supplemented with 10% heat-inactivated FCS, 100U/ml penicillin (Invitrogen), 100µg/ml streptomycin (Invitrogen) and 2mM L-glutamine (complete RPMI). Each cell line was cultured at between 0.2-0.8x10^6/ml and sub-cultured every three to four days according to the supplier's instructions (DSMZ).

Primary cells were cultured in StemSpan™ Serum-Free Expansion Medium (SFEM) (STEMCELL Technologies) supplemented with 20% FCS, 100ng/ml

hSCF, 50ng/ml IL-7, 20ng/ml IL-3, 50ng/ml FLT-3), standard concentrations of PSA and Glu, for the purpose of lentiviral transduction.

2.2.3 Cord blood CD34 cell enrichment

Prior to transduction and xenotransplantation, cord blood cells were enriched for CD34 sing MACS® Cell Separation magnetic column and human CD34 MicroBead Kit (Miltenyi Biotec) following manufacturer instruction. The buffer used for the enrichment procedure was made of PBS/0.5%FBS (Fetal bovine serum).

2.2.4 Primary patient samples

Diagnostic and follow-up ALL bone marrow (BM) samples were obtained upon informed consent and approval of relevant research ethics committees from patients at John Radcliffe Hospital, Oxford, UK; Centro Ricerca Tettamanti, Clinica Pediatrica Universitaria Milano Bicocca; Great Ormond Street Hospital for Children (GOSH) NHS Foundation Trust, London, UK; and other UK hospitals.

2.2.5 Cell Purification

Mononuclear cells were isolated from leukemic and normal bone marrow and peripheral blood samples by Ficoll gradient centrifugation, and collected for further processing (Table 2-6).

PATIENT N°	PHENOTYPE	SEX	AGE (yrs)	CYTOGENETICS/KARYOTYPE	MOLECULAR DIAGNOSTICS	% BLASTS	RELAPSE (Y/N)	RELAPSE (mths)
1	B-ALL	M	4	46XY TEL-AML1+, No TEL deletion			N	
11	B-ALL	F	4	46XX TEL-AML1+, TEL deletion			N	
72	B-ALL	F	4	46XX TEL-AML1+, TEL deletion			N	
76	B-ALL	F	3	46XX TEL-AML+			N	
107	B-ALL	M	2	46 XY 76/100 cells TEL-AML1+, 62/76 TEL deletion			N	
111	B-ALL	F	7	46 XX 94/100 cells TEL-AML1+, 72/94 2 copies AML1, 4/94 cells 3 copies AML1			N	
B	B-ALL			N/A	TEL-AML1+, No TEL deletion	90%	N	
C	B-ALL			N/A	TEL-AML1+, No TEL deletion	98%	N	
D	B-ALL			N/A	TEL-AML1+, No TEL deletion	high	N	
3	B-ALL	M	3	46XY TEL-AML+	TEL-AML+	99%	N	
7	B-ALL	F	4	47, XX, +21[1]/46,XX[4] TEL-AML+	TEL-AML1+	90%	N	
1988 D	B-ALL	F	3	N/A	TEL-AML1+	92%	Y	10
1988 R				46 XX	TEL-AML1+	N/A		
2278 D	B-ALL	F	3	N/A	TEL-AML1+	98%	Y	17.5
2278 d8 MRD	B-ALL			N/A	TEL-AML1+	18%		
2278 R	B-ALL			N/A	TEL-AML1+	N/A		

Table 2-6: Detailed demographic, cytogenetic, and clinical information of patients from whom BM biopsies were obtained.

2.2.8 Lentiviral packaging cell line transfection

Lentiviruses pseudotyped with the vesicular stomatitis virus G (VSVG) protein were packaged by transient transfection of 293T cells with FuGene6 (Roche). Briefly, 80-90% confluent 293T cells seeded in T75 flask were fed with 8ml fresh medium. A DNA mix of 1µg each of the required packaging plasmids, pMDLg/pRRE (expresses HIV-1 GAG/POL), pSVrv (expresses HIV-1 REV),

pMD2-G(VSV-G) (expresses VSV glycoprotein), and 2 µg of the vector of interest was prepared and brought to a volume of 19.3µl per flask to be transfected with TE buffer. The mix was then incubated 15 minutes at room temperature in presence of 23.1µl of Fugene reagent (Promega) and 260µl Optimem (GIBCO). A final volume of 302.4µl of reagent/DNA mix was then slowly added to each flask. 24h after the transfection the medium was then replaced with 12ml of fresh complete DMEM.

Alternatively, $9x10^6$ 293T cells were plated in 15 cm^2 dishes in complete DMEM. 16 hours later cells were starved in 15ml DMEM (no FBS) for 4 hours after which 3 ml FBS were added to each dish. An additional 4 hours later cell were transfected as follows. A mix of 7.5ug VSV-g, 11.5ug gag pol, 17.5ug transfer vector was prepared in a conical 50 ml tube for each dish to be transfected. 150ul 2M CaCl2 were added to the tube and the volume brought to 1,5 ml with sterile water. Following, 1,5 ml of 2x HEPES-Buffered Saline (HBS) was added dropwise, while vortexing the solution (1-2 drops per second). The transfection mix was then let sit for 15 minutes and added to the plate dropwise. 12-14 hours after transfection, the medium was replaced by 12ml complete DMEM auditioned with Sodium butyrate 0.3 mM (1:1000). Sodium butyrate treatment following transfection has been reported to result in higher levels of transient expression. This effect is thought to be mediated by a more “active” chromatin structure of newly transfected genes.

Independently from the transfection protocol used, ultracentrifugation was performed to concentrate the virus 72 post-transfection. Briefly, the supernatant from the transfected 293T cell cultures was collected, centrifuged 5 minutes at 350g and filtered with Minisart 0.45µm filters (Sartorius Stedim Biotech) into Nalgene™ Oak Ridge High-Speed PPCO Centrifuge Tubes. Up to 36ml of

supernatant from cells transfected with the same vector were collected in an Oak Ridge tube. A 5 ml sucrose cushion was added and the virus concentrated by ultracentrifugation at 22000g for 2.5 hours at 4℃ in an Avanti J series centrifuge system (Beckman Coulter). The supernatant was then discarded and the pellet was resuspended in 30µl Optimem medium per culture flask.

2.2.4 Virus titration

Virus titration was performed on 293T cells followed by FACS analysis. Briefly, 10^5/well 293T cells were plated in a 24-well plate, and left for 24 hour to adhere. 0.001 - 0.01 - 0.1 and 1µl of virus stock were then added to the relevant well. 48 hours later, cells were trypsinised in order to detach them from the bottom of the wells, and washed 3 times with PBS to remove live viral particles. The percentage of (GFP+) infected cells was then evaluated by FACS. The viral titer was calculated according to the formula ‘’viral particles/ml=(% GFP positive cells x10^5) / volume virus added (µl) x 1000’’, based on the viral dose that produced 5-15%GFP+ cells.

2.2.5 Lentiviral transduction of leukaemic cell lines and of human primary leukaemic cells

Reh, UOCB6 and Jurkat, cell lines, cells were maintained in usual RPMI complete medium and transduced by addition of the concentrated virus (volume dependent on the required MOI) to the culture. The following day cells were washed 3 times with PBS, and put back into culture.

Primary leukemic BM mononuclear cells were seeded at $5x10^5$ cells per well in 500µl of StemSpan™ Serum-Free Expansion Medium (SFEM) (STEMCELL Technologies) supplemented with 20% FCS, 100ng/ml hSCF, 50ng/ml IL-7, 20ng/ml IL-3, 50ng/ml FLT-3), PSA, Glu and 4µg/ml polybrene (Sigma-Aldrich). Cells were transduced in 48-well plates (Thermo Fisher Scientific) by spinoculation (centrifugation at 2000rpm, for 90 minutes at 25 ºC). 24 hours after transduction, the medium was replaced with complete DMEM supplemented with growth factors: 100ng/ml hSCF, 50ng/ml IL-7, 20ng/ml IL-3, 50ng/ml FLT-3). 48 hours later transduction efficiency was checked by flow cytometry or microscopy with the EVOS® FL life Technologies Cell Imaging System (GFP expressing constructs only).

2.2.6 Flow cytometry

Peripheral blood cells were obtained by mice tail bleeding. Cells were collected in heparinized or EDTA treated tubes. Bone marrow cells were obtained either from bone marrow aspirates collected from the tibias of mice into an insulin syringe and transferred into eppendorf tubes containing PBS 0.5% FBS, or from crushed mice bones (tibia, femur and pelvis of both sides) at the end of each experiment.

Cells were washed with wash buffer (PBS supplemented with 10% FBS). Primary cells were treated with ACK buffer (0.15M NH4Cl, 1.0mM KHCO3, 0.1mM EDTA) to lyse red blood cells before staining. Peripheral blood cells were lysed a second time with 2% Dextran. Cells were washed and pre-incubated with anti-mouse FcγIII/II Receptor antibody (2.4G2; BD Biosciences) and human FcR-binding inhibitor (Milteny Biotec) for 15 minutes on ice to block non-specific binding.

Blocking reagents were diluted in PBS 1:200 the first and 1:10 the latter. Cells were then stained with the appropriate fluorochrome-conjugated antibodies in PBS 10% FBS 15 minutes in ice, and washed with wash buffer prior to analysis. Anti-mouse or human antibodies used in this study are listed in Table 2-7. Fluorochrome-conjugated streptavidin (Ebioscience) was used to detect biotin-conjugated antibodies (Ebioscience) (Table 2-8). Antibodies were pre-tested for optimal working dilution and staining time. The appropriate unstained, single colour and FMO controls were used for compensation set-up gate and definition.

For intracellular staining, REH cells were washed in PBS/EDTA (2mM)/1% FBS (PEF), resuspended in 0.5 ml of (PEF) and 31.25µl 16% paraformaldehyde (PFA) (1% final) and let sit in ice for at least 30 minutes to fix. 0.5ml of 0.2% Triton was added to permeabilize membranes 15 minutes on ice. Cells were then blocked and stained with the appropriate primary and secondary fluorochrome-conjugated antibody, according to manufacturer's instructions.

Antigen		Conjugate	Diln.	Host/ Isotype	Clone	Supplier	Cat no
Hu	CD10	APC	1/50	Ms IgG1,k	eBioCB-CALLA	eBioscience	17-0106-42
Hu	CD15	FITC	1/50	Ms IgM	MMA	BD	332778
Hu	CD19	PE	1/50	Ms IgG1, k	HIB19	BD	555413
Hu	CD19	Pacific Blue	1/40	Ms IgG1, k	HIB19	BioLegend	302223
Hu	CD19	PE	1/80	Ms IgG1	SJ25C1	BD	345789
Hu	CD19	APC-Cy7	1/50	Ms IgG1,k	SJ25C1	BD	561743
Hu	CD33	FITC	1/20	Ms IgG1	P67.6	BD	345798
Hu	CD38	Biotin	1/100	Ms IgG1, k	HIT2	eBioscience	13-0389-80
Hu	CD38	PE	1/40	Ms IgG1	HIT2	BD	347687
Hu	CD38	PE-TxR	1/40	Ms IgG1	HIT2	Caltag	MHCD3817
Hu	CD45	AF700	1/160	Ms IgG1	HI30	BioLegend	304023
Hu	CD66b	FITC	1/50	Ms IgM	G10F5	BD	555724
Hu	CD34	APC	1/160	Ms IgG1	8G12	BD	345804
Hu	CD34	PC7	1/40	Ms IgG1	581	Beckman Coulter	A51077
Hu	CD271/NGFR	PE	1/50	Ms IgG1, k	C40-1457	BD	557196
Hu	CD271/NGFR	AF647	1/50	Ms IgG1, k	C40-1457	BD	560326
Ms	CD45	FITC	1/100	Rat IgG2b, κ	30-F11	BioLegend	103108
Ms	CD45	PE	1/100	Rat IgG2b, κ	30-F11	eBioscience	12-0451-83
Ms	CD45	PO	1/100	Rat IgG2b, κ	30-F11	Life Technologies	MCD4530

Table 2-7: Flow cytometry antibodies used in this study.

Dye	Conjugate	Supplier	Cat no	Diln.
Strepavidin	PB	Life Technologies	S-11222	1/100
Hoechst 33258, pentahydrate(bis-benzimide)		Invitrogen	H3569	1mg/ml stock, 1/100

Table 2-8: Other dyes used in this study.

Appropriate secondary antibody single staining or IgG isotype control antibodies were included.

Flow cytometry experiments were performed on LRSII (BD Biosciences), Gallios (Beckman Coulter) or Cyan ADP (Beckman Coulter) analysers. An Aria III cell sorter (BD Biosciences) was used for sorting experiments (self run). Data was analysed with FlowJo v8.6 (Tree Star) or Kaluza (Beckman Coulter) software.

2.2.7 Proliferation assays

REH cells transduced with TEL overexpression vectors or the overexpression empty vector were plated at equal density (500-1000-1500cells/well in 100µl medium) in flat-bottomed 96-well plates and cultured in RPMI 10%FBS plus antibiotics. After 1 week in culture cell proliferation rate was determined with ATPlite kit (Perkin Elmer) by measuring the production of light caused by the reaction of ATP with added luciferase and D-luciferin, proportional to ATP concentration in each cell suspension, on a plate reader.

2.3 Animals

2.3.1 Animals welfare and maintenance

NSG mice were purchased from and kept at the BioMedical Service of John Radcliffe Hospital (BMS) or Cancer Research UK London Research Institute (Lincoln Inn field). Animal care was strictly in accordance with the Guidelines of

University of Oxford and London Research Institute (Lincoln Inn field) and experiments were performed according to United Kingdom Home Office regulations. Animals were handled under sterile conditions. Lethal irradiation of mice prior to bone marrow transplantation was performed according to regulation of the relevant Project License. Starting from a week prior to their irradiation, mice were given antibiotic water in order to minimize possible adverse effects and infections caused by the irradiation procedure. In case of severe morbidity, e.g. acute considerable body weight loss, mice were humanely sacrificed by an approved schedule 1 method.

2.3.2 Bone marrow reconstitution assay

Xenotransplantation was performed by intratibial injection of 5-10 week old NOD/SCID IL2Rγ^{hull} (NSG) mice. These mice lack mature T cells, B cells, and natural killer (NK) cells. They are also deficient in multiple cytokine signalling pathways, and carry defects in innate immunity. Mice were sub-lethally irradiated either with 250 cGy of total body irradiation, split into two equal doses administered within an interval of at least 4 hours before cell injection, or with a single dose of 375 cGy. Mice were maintained on Baytril in the drinking water at 25.5 mg/kg for 2 weeks after injection. For most experiments 2 x 10^5 primary leukaemia cells, resuspended in 40µl PBS 0.5% FBS, where injected per mouse. Alternatively, an equal number of leukemic cells transduced with empty or TEL overexpression vectors, or 1.6×10^5 CD34 enriched cord blood cells were injected per mouse. Briefly, mice were anesthetized by isofluorane inhalation, the knee was flexed, and 40 µL of cells suspension were injected through the knee joint into the right tibia through a 28.5-gauge needle. At the time of injection mice were also

ear notched for identification purposes. 12 weeks after transplant the injected bone was then sampled by bone marrow aspiration and analysed for human engraftment by flow cytometry. (hCD45+ and/or $hCD19^{+}$). Cord blood transplants were also tested for multilineage reconstitution. Typically, mice displaying at least 30% human engraftment were assigned to either control or treatment groups and treated consequently (see below). Five to 20 weeks after injection, mice were culled and their tibias, femurs, pelvises, and spleen were removed. Bones were crushed to isolate the marrow while spleens were homogenized. At the time of cells harvesting, total BM and spleen cellularity were assessed through the Sysmex XP-300™ Automated Haematology Analyzer. Cells were then stained for FACS sorting.

2.3.3 Mice Treatment

Mice were treated with Vincristine and Dexamethasone. Both adopted compounds are of pharmaceutical-Grade**:** Vincristine Sulphate 1 mg/ml Injection (Hospira) and Dexamethasone 2mg tablets (Auden Mckenzie). Dosages were first optimised on mice engrafted with cord blood cells by evaluating their cytotoxic effect on human cells populations in the bone marrow and peripheral blood. The following regimens were evaluated in a 4 weeks treatment trial. First week: 0,15 mg/Kg Vincristine IP (intraperitoneal) and 3 mg/L Dexamethasone dissolved in water. Second and third weeks: 0,30 mg/Kg Vincristine IP and 6 mg/L Dexamethasone dissolved in water. Fourth week: 0,50 mg/Kg Vincristine IP and 6 mg/L Dexamethasone dissolved in water. Consequently four weeks of treatment with 0,50 mg/Kg Vincristine IP and 6 mg/L Dexamethasone dissolved in water were shown to have stronger effects than desired on primary cells (but not on cord blood cells). A final regimen of 7 days

treatment 0,50 mg/Kg Vincristine IP and 6 mg/L Dexamethasone in water was therefore established. Variants of the regimen tested for additional experiments included a shorter treatment of 3 days or an increased dosage of dexamethasone, 9mg/L. The latter was associated with increased morbidity and mortality and therefore excluded from further study.

2.4 Statistical analysis

Significance of pre- and post-treatment engraftment differences was determined using a two-tailed paired t-test, and is reported in the scattered graphs as:

ns	$P > 0.05$ (not shown)
*	$P \leq 0.05$
**	$P \leq 0.01$
***	$P \leq 0.001$
****	$P \leq 0.0001$

CHAPTER 3

ESTABLISHMENT OF THE TOOLS REQUIRED FOR TRACKING OF CLONAL DYNAMICS OVER TREATMENT

3.1 Introduction

In the past ten years xenograft mouse models of human leukaemia have represented a unique tool to study diverse aspects of the disease, from basic biology to more clinically relevant perspectives (e.g. the evaluation of novel therapeutic drugs). Additionally, the injection and engraftment of leukemic cells into mice has offered the possibility of *in vivo* amplification of patient samples, the precious and scarce, but crucial material for leukaemia research (Meyer and Debatin, 2011). These tumour graft models (also called patient-derived xenografts or PDX) rely on the transfer, through different methodologies, of primary cancer cells into, often preconditioned, immunodeficient recipients that do not reject xenografts and support cell and tissue differentiation and growth (Siolas and Hannon, 2013). The first mouse model ever developed for the purpose was a strain carrying a mutation responsible for severe combined immunodeficiency (SCID). Residual immunity in these mice does however result in low engraftment efficiency. SCID mice were therefore backcrossed with non-obese diabetic mice (NOD/Lt) to generate the so-called non-obese diabetic/severe combined immunodeficiency (NOD/SCID) strain. These mice lack functional mature B and T cells, carry defects in the natural killer cell population and are impaired in their complement and macrophage functionality. They are therefore more permissive to engraftment of both normal and malignant human hematopoietic cells, particularly towards more aggressive patient samples. Since the early 2000s the development of mouse strains with defective innate immunity and absent natural killer (NK) activity, due to a defect in the interleukin-2 receptor gamma chain (IL-2Rγ), namely NOD/SCID/γc^{null} (NOG) and $Rag2^{null}\gamma c^{null}$ (NSG) (nearly identical but in NSG mice the γ-chain receptor is completely knocked down, while in NOG mice the

intracytoplasmic tail is truncated), has allowed disease penetrance to reach even higher levels, and also facilitated *in vivo* generation of properly differentiated multilineage human hematopoietic cells upon HSC transplantation (Ito et al., 2012; Meyer and Debatin, 2011). The increased permissiveness of these most recent models had a large impact on the estimated frequency of leukaemia stem cells (LSCs), and therefore on the debate over the veracity of the cancer stem cell (CSC) model (Cobaleda et al., 2000). Similarly, it is possible that the xenograft model adopted could also influence analysis of the evolution of genetic subclones in ALL disease progression. It is however reassuring that NSG mice transplanted with lymphoblastic or myeloid leukaemia samples were previously reported to retain the overall phenotypic and genotypic characteristics of the original tumour (Cox et al., 2004; Sanchez et al., 2009). Additionally, clonal diversity of paediatric B-ALL, as well as of other blood and solid malignancies, was shown to be preserved upon serial transplantation into NSG mice. These reports strongly support the suggestion that an epigenetically uniform population of CSC (or LIC) can be genetically diverse, validating the potential of PDX models for the study of genetic heterogeneity. Prevalence within the bulk population of individual subclones was however suggested not to remain necessarily stable upon engraftment, pointing out that these might differ in their repopulation ability. Such functional heterogeneity might be determined not just by the intrinsic oncogenic potential of most of transplanted clones, but also to the lack of a strong system-specific selective pressure (Anderson et al., 2011; Clappier et al., 2011; Notta et al., 2011b; Piccirillo et al., 2009; Schmitz et al., 2011). The permissive cellular environment provided by these immunodeficient mice is in stark contrast with the selective pressures that the cancer is challenged with during treatment of

leukaemia in patients. Understanding the behaviour of different subclones in response to chemotherapy in an *in vivo* setting is therefore of fundamental importance both from the perspective of seeking insight into the basic biology of the disease and from a clinical standpoint.

This thesis describes the establishment of a mouse model for the *in vivo* treatment of primary TEL-AML1+ leukemic cells. The model allows for the characterization of the role of intratumour genetic heterogeneity and the dynamics of different subclones, which may possess distinct functional features, in sensitivity and resistance to chemotherapy, and ultimately in relapse.

It is unclear whether the rare leukaemic cells that survive chemotherapy in patients are inherently more resistant to treatment-induced cytotoxicity, determined by their specific genetic aberrations, or whether they persist by chance alone. These two models, deterministic versus stochastic survival, are difficult to distinguish through the analysis of primary samples alone. Because a mouse model allows for challenging the same patient samples with chemotherapy multiple times, it serves as a unique tool to test whether the survival of TEL-AML1$^+$ leukaemic cells is deterministic or stochastic. The model also serves as a tool to aid dissection of the mechanistic basis for the possible differential sensitivity of some TEL-AML1$^+$ leukaemic cells to chemotherapy.

Such a study clearly relies on the establishment of a robust model for the *in vivo* development of malignancies genetically resembling the leukaemia of origin, as well as on the establishment of an effective treatment protocol and a reliable single cell approach to track clonal dynamics over time and treatment. An obstacle to the first is the observation that, even when transplanted in highly permissive

mouse strains, not all primary leukaemia samples display equal engraftment properties (Meyer et al., 2011). Given this observation, a preliminary screening of the ability of collected candidate TEL-AML1+ samples to *in vivo* propagate the disease was performed early on to identify samples suitable for the study.

Subsequently, we sought to establish a treatment regimen, analogous to the induction phase of the clinical treatment of childhood ALL, to produce *in vivo* partial remission. The clinical management of childhood ALL, structured in three different phases, induction, consolidation/intensification and maintenance, focuses on control of bone marrow and systemic disease, while preventing leukemic cells from spreading to other sites, particularly the central nervous system (CNS). In total the therapy lasts 2-3 years. The induction phase of the treatment achieves most of the leukemic cell killing. Subsequently, the other phases aim at preventing the regrowth of any remaining tumour. Current regimens for the induction phase use a combination of vincristine (VCR), a glucocorticoid, and L-asparaginase (ASP), with or without anthracycline (Figure 1-5). Two studies were priviously published that adopted a VXL-DEX-Asp (Vincristine/Dexamethasone/L-Asparaginase) regimen for the preclinical evaluation in xenograft models of the efficacy of a new compound (ABT-737 a Bcl-2/Bcl-xL-Bcl-w inhibitor) in comparison or in addition to standard treatment. In these studies, both run by the same reseach group, NOD/SCID mice were inoculated via tail vein with $2.5x10^6$-$5x10^6$ cells from a panel of ALL samples. When the percentage of hCD45+ cells in the peripheral blood reached 1%, those mice assigned to the standard treatment group were administerd a combination of vincristine 0.15mg/Kg in saline once per week, dexamethasone 5mg/Kg in saline Monday-Friday, and L-Asparaginase 1000IU/Kg in saline Monday-Friday, for four weeks via IP administration (Kang et

al., 2007). This treatment was efficient in causing delays in individual disease progeression, and the magnitude of the response correlated with patient outcome. However, higher drug doses (VCR 0.25mg/Kg, DEX 7.5mg/Kg and ASP 2500 U/Kg) resulted in high toxicity to the mice both when the drugs were administered in combination and upon L-asparaginase administration on its own (Szymanska et al., 2012). In contrast to these observations, a previous study had shown that both vincristine at even higher dose, 0.5 mg/Kg, and dexamethasone at an intermidiate dose 5mg/Kg did not cause any unwanted toxicity (Liem et al., 2004). Interestingly, when administered as single agents at the attenuated dosages, L-asparaginase and dexamethasone, but not vincristine, were ineffective (Szymanska et al., 2012). This observation was confirmed in a study, in which L-asparaginase (7500 IU/Kg) not only had no single-agent anti-leukemic effect in treatment of murine Ph+ ALL, but did not further enhance dexamathasone-dependent event free survival (EFS) either. The same work showed dexamethasone to be effective when administered orally at 6mg/L for the first week and at 3mg/L for an additional week (Boulos et al., 2011). In light of the work previosly pubblished we shaped our treatment regimen to include the administration of both vincristine and dexamethasone. L-asparaginase was not added to the treatment backbone due to its reported poor efficacy and high toxicity. Xenograft mice engrafted with $CD34^+$ cord blood cells were used for the establishement of a preliminary chemotherapy regimen, which was subsequently further refined on patient-derived xenograts (PDXs).

Finally, the proposed characterization of intratumour clonal dynamics in TEL-$AML1^+$ ALL requires the scrupulous genetic examination of cancer cells at single cell resolution. For this purpose, we adopted a multiplex fluorescence in situ hybridisation (Martinez et al.) approach. Four probes were custom designed and

produced by Cytocell to simultaneously hybridize to PAX5, P16, AML1 and TEL genes within an individual cell. The probes, described in detail in the materials and methods section of this thesis, were directly labelled with Aqua, Gold, FITC, and TexasRed fluorochromes respectively. The combinatorial use of the four probes (mFISH) allowed for the description of the allelic status of each of the selected genes (mono- or bi-allelic deletion, as well as amplification). Copy number variations of these represent the frequent second hits of the leukaemia. The TEL and AML1 probes in particular enabled the characterization of multiple variants: presence of the fusion and its reciprocal (founder event of the leukaemia), duplication or deletion of the fusion, deletion of TEL and amplification of AML1 and chromosome 21.

3.2 Results

3.2.1 Selection of 6 TEL-AML1$^+$ primary samples with in vivo engraftment potential

27 NSG mice (10-16 weeks old) were sublethally irradiated and intrabone (tibia) injected with $2*10^5$ freshly thawed cells from the diagnostic bone marrow aspirates of 11 patients (duplicate or triplicate mice injected with each cell inoculum) (Table 3-1). As the orthotopic transfer of cells directly into the bone marrow niche was previously shown to lead to higher engraftment frequencies, this methodology was preferred to the also widely exploited IV (intravenous) injection. The poorer engraftment efficiency linked to IV injections is attributed to the challenging homing process that cells injected via this route have to undertake. First they enter the circulation through the blood and extravasate through the

marrow vasculature, following which they must migrate to a supportive bone marrow (BM) niche (Mazurier et al., 2003). Of note, preconditioning the mice by irradiation is believed to improve engraftment as it favourably modulates the murine environment. However, the transplanted mice often undergo a 5-10 day irradiation sickness period, from which they typically recover within 14 days (Duran-Struuck and Dysko, 2009). During the experiment described here, 6 newly transplanted mice did not recover from the irradiation morbidity, and had to be euthanized by day 21. The remaining mice were culled 12 weeks post-transplantation. Their bone marrow was analysed by flow cytometry for the presence of cells positive for the human antigen CD45, a molecule that labels human cells of all hematopoietic lineages with the exception of mature red cells. Additionally, the expression of mouse CD45 (mouse hematopoietic cells) was also analysed. The ratio beetween human and mouse cells in the BM is indicative of the agressiveness of the disease with higher proportion of human cells signalling more advanced leukaemia, and more effective suppression of any residual mouse haematopoiesis.

Of the 9 samples analysed, only five, pt11, ptB ptD, pt1988 and pt 2278, led to manifestation of overt leukaemia in one or multiple recipients. The remaining PDXs did not display any sign of disease within the observation time (Table 3-1). Engraftment failure was defined as **<**2% human cells in the BM at 12 weeks post-transplantation (Figure 3-1a). With the exception of 2 PDX injected with patient C, all engrafted mice showed high levels of engraftment, with >25% human cells (Figure 3-1b). Of the three mice injected with primary cells from pt.C, two displayed low levels of engraftment and a third did not display any engraftment by week 12. It is however possible that with longer observation times (e.g 20 weeks)

and by injecting a higher dose of leukemic cells (at least $1*10^6$), almost all samples would ultimately engraft, and show *in vivo* disease manifestation. In fact, in subsequent experiments low engrafted mice (1-3% at week 12 post-engraftment) did dispay fast progression of the disease when mantained for longer time, up to week 20. Additionally, upon injection of a standard number cells from pt.111, 6 out of 12 (4 mice euthanised early) new recipients developed leukaemia by week 16 (<20% human cells in 4 of 6 mice).

PATIENT N°	N° MICE INJECTED	N° MICE ANALYSED	N° MICE ENGRAFTED
1	2	1	0
11	2	1	1
72	2	1	0
76	2	1	0
107	2	1	0
111	2	1	0
B	3	3	3
C	3	3	2
D	3	2	2
1988 D	3	3	3
2278 D	3	3	3

Table 3-1: Selection of TEL-AML1+ samples for in vivo studies. 27 NSG were sublethally irradiated and intrabone injected with $2*10^5$ thawed cells from 11 different patients (duplicate or triplicate mice for each sample). The number of mice injected for each patient, the number of mice analysed, and the number of those engrafted is reported.

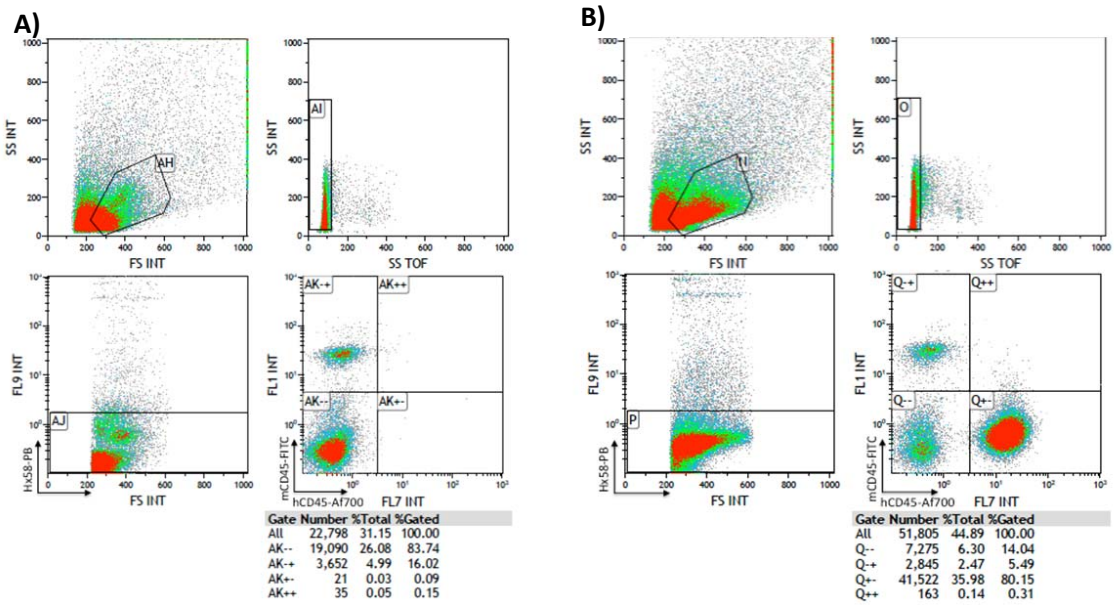

Figure 3-1: Representative FACS plot of the bone marrow of a non-engrafted (A) and an engrafted (B) PDX. Live cells were gated on the basis of DAPI exclusion, and then dissected into human (hCD45 AF-700^{+}) and mouse cells (mCD45 FITC^{+}).

Additionally to samples tested in this experiment, two specimens, whose engraftment ability and heterogeneity were previously characterized, were obtained courtesy of Prof. Mel Greaves. The samples were part of a collaborative study on intratumour heterogeneity of ALL published in 2011 in Nature, and discussed in the introduction to this thesis (Anderson et al., 2011).

3.2.2 Establishment of a chemotherapy regimen for the in vivo treatment of patient-derived xenografts

3.2.2.1 A cord blood trial

A trial experiment was set up to test tolerance of the NSG mice, to 4 weeks of treatment with Vincristine and Dexamethasone, administered either as single agents or in combination, as well as the cytotoxicity of the regimen on engrafted cells. Given the evidence from previous studies suggesting that L-asparaginase if more toxic than efficacacious, this drug was excluded from our regimen. To avoid wasting any precious material, human cord blood cells, rather than leukemic cells, were used for this preliminary experiment.

Twelve NSG mice were sublethally irradiated and transplanted with $1.6x10^5$ CD34-enriched cord blood cells. After 5 weeks, bone marrow aspirates were obtained from each mouse, and assessed for level of human engraftment. In addition to being analysed for viability and hCD45 expression (human hematopoietic cells), cells were also stained with a cocktail of 6 antibodies recognizing lineage-specific and differentiation markers: mCD45 (mouse hematopoietic cells), hCD19 (B-lymphocytes), hCD33/CD15/CD66b (myeloid cells) and hCD34 (early hematopoietic progenitors) (Figure 3-2). All mice showed very high level of total human engraftment (between 68.7 and 98.6%). The majority of human cells in the marrow were CD19+ B cells, with the remaining cells composed of CD33+ myeloid cells. A well defined $CD19^-CD33/CD15/CD66b^-$ $CD34^+$population cells was also detectable.

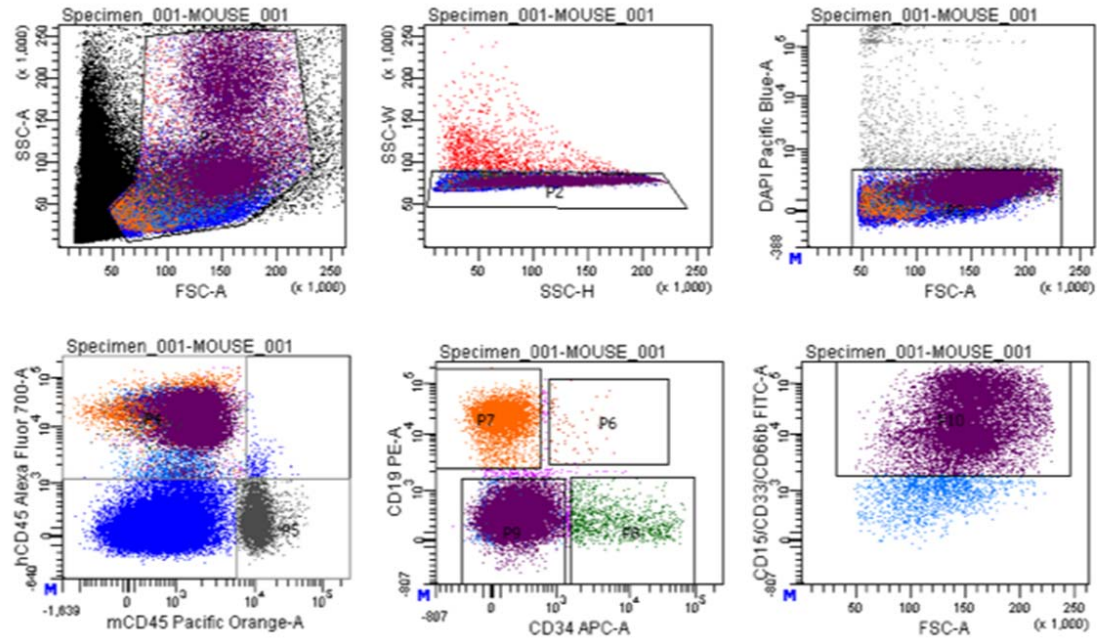

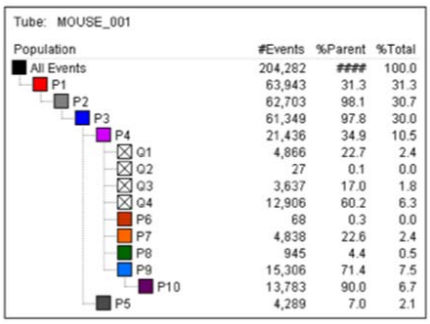

Tube: MOUSE_001			
Population	#Events	%Parent	%Total
All Events	204,282	####	100.0
P1	63,943	31.3	31.3
P2	62,703	98.1	30.7
P3	61,349	97.8	30.0
P4	21,436	34.9	10.5
Q1	4,866	22.7	2.4
Q2	27	0.1	0.0
Q3	3,637	17.0	1.8
Q4	12,906	60.2	6.3
P6	68	0.3	0.0
P7	4,838	22.6	2.4
P8	945	4.4	0.5
P9	15,306	71.4	7.5
P10	13,783	90.0	6.7
P5	4,289	7.0	2.1

Figure 3-2: representative FACS plot of the BM aspiration prior to treatment. Live cells were gated on the basis of DAPI exclusion, and then subdivided between human (hCD45 AF-700$^+$) and mouse cells (mCD45 PO$^+$). Within human cells we looked at B-lineage cells (CD19 PE$^+$), subdivided on the base of differentiation status (CD34 APC expression), and myeloid cells (CD15-CD33-CD66b$^+$).

In accordance with the project license under which the experiments were carried out, treatment administration was only started seventeen days after engraftment was confirmed. This strategy allowed for an additional BM aspirartion to be performed just 5 days after the start of treatment, offering insight into early effects of chemotherapy. A final picture of the overall efficacy of the regimen was exepected from the analysis of total bones engraftment at the of treatment (day 28). Moreover, in an effort to obtain as many “real-time” data points as possible,

mice were bled two days before the administration of the first dose to evaluate peripheral engraftment levels prior to their exposure to the drugs. The same was also performed near the end of the third week of treatment (Figure 3-3).

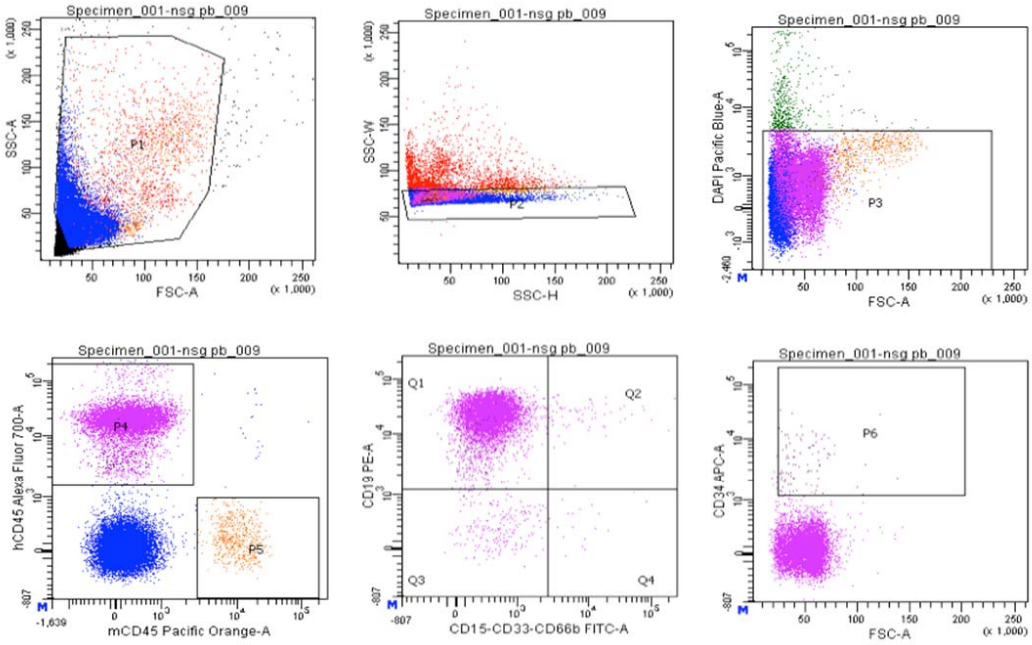

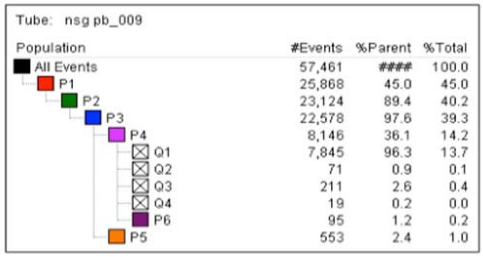

Figure 3-3: representative FACS plot of the peripheral blood analysis prior to treatment. Live cells were gated on the basis of DAPI exclusion, and then subdivided between human (hCD45 AF-700$^+$) and mouse cells (mCD45 PO$^+$). Within human cells we looked at B-lineage cells (CD19 PE$^+$), subdivided on the base of differentiation status (CD34 APC expression), and myeloid cells (CD15-CD33-CD66b$^+$).

As expected, the percentage of human cells in peripheral blood prior to treatment was lower than in bone marrow, with most cells belonging to the B lineage. Myeloid and primitive cells were barely detectable (0.2-13% and 0.7-3.7% of

human cells respectively). A scheme of the treatment and sampling plan is presented in figure 3-4, and bone marrow and blood engraftment levels for each mouse are reported in table 3-2.

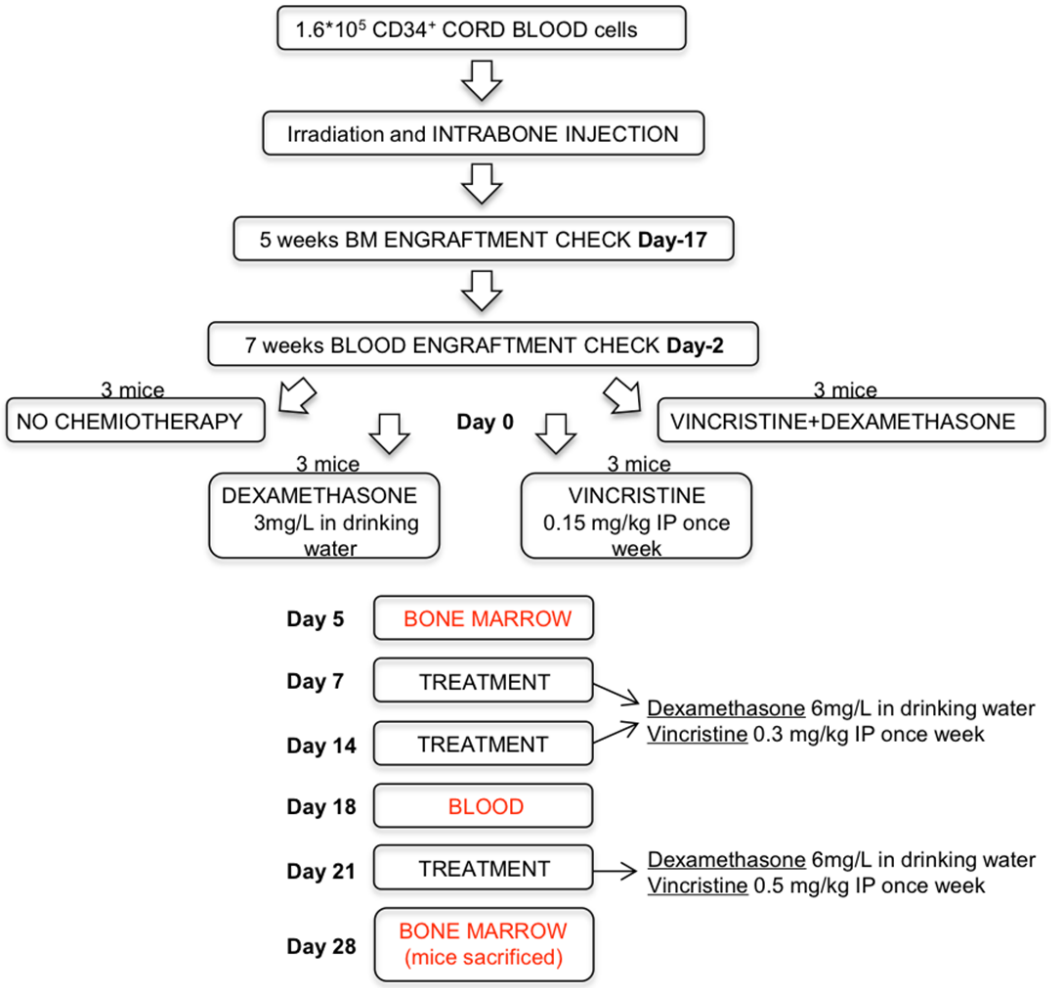

Figure 3-4: Experimental design diagram. The experiment was designed to allow for monitoring of the leukemic burden during and following treatment by estimating the proportion of $hCD45^+$ cells in murine bone marrow and peripheral blood. The frequency at which bone marrow aspirates and blood samples could be taken was dictated by rules stated in the project license. Each specimen collected informed the following adjustments to administered drug doses.

Mice were then randomized to receive drug or control treatment. Three mice each received vincristine (0.15 mg/Kg), or dexamethasone (3 mg/L), three received a combination of the two and another three mice did not receive any compound. Vincristine was administered to the mice via IP injection once per week, while dexamethasone was dissolved in the drinking water. As planned, 5 days later a bone aspiration was performed to evaluate early treatment effects on total human $CD45^+$ and on lineage specific cells in the marrow. Surprisingly, none of the regimens proved effective at this stage, as no significant global cytotoxic effect was detected in any of the mice (Table 3-2).

Given this observation, the same mice were subsequently administered an increased dosage of vincristine, 0.30 mg/Kg IP, and dexamethasone, 6 mg/L dissolved dissolved in water, for an additional two weeks of treatment (IP injections on Day7 and Day14). On day 18 the analyses of human peripheral blood engraftment revealed no significant increase in cytotoxicity (Table 3-2). The proportion of $hCD45^+$ cells in the blood of the mice was stable or even higher than it was prior to drugs exposure. Consequently, on the last week of treatment (IP injection on Day 21) mice were injected with an even higher dose of vincristine, 0.50 mg/Kg IP. The does of dexamethasone was mantained at 6 mg/L dissolved in the water as this dose was in fact previously published as highly effective and to result in plasma concentrations at least as high as those used in human patients (Liem et al., 2004). Two days prior to the end of treatment one of the mice exposed to dexamethasone experienced treatment-unrelated morbidity and was sacrificed. The bones were collected and marrow cells frozen down. On day 28 all mice were sacrificed, their bones harvested and bone marrow cells analysed by FACS.

TREATMENT day 0	BM ENGRAFTMENT % day -14	BLOOD ENGRAFTMENT % day -2	BM ENGRAFTMENT % day 5	BLOOD ENGRAFTMENT % day 18	BM ENGRAFTMENT % day 24
dexa	96.6	45.2	74.7	54.5	34.9
dexa	97.2	54.8	81.4	62	44.5
dexa	97	35.8	94.7	22.4	77.0
vinc	95.7	21.8	76.1	77.3	54.9
vinc	92.3	44	90.9	62.3	54.8
vinc	95.2	30.4	87.9	66.8	60.6
dexa + vinc	96	12.2	87.9	73.4	28.9
dexa + vinc	98.6	24	89.7	41.6	31.3
dexa + vinc	83.9	16.5	86.8	36.4	13.7
ctrl	72.7	36.1	90.8	78.4	72.6
ctrl	84.7	21.2	84.7	69.8	74.7
ctrl	68.7	28	68.7	58.4	82.1

Table 3-2: Bone marrow and blood engraftment percentages of each mouse. Engraftment levels defined through FACS analysis as the percentage of $hCD45^+$ cells within the total population of cells back gated on scatter, singlet and viability. Bone marrow aspirates and peripheral blood samples were obtained twice each (Day-17/Day5 and Day-2/Day18 respectively), once before and once during treatment administration, and informed therapeutic decisions. At the end of the experiment bones were harvested and total bone marrow analysed. One of the dexamethasone treated mice displayed clear signs of morbidity and had to be sacrificed prior to the end of treatment (3^{rd} row mouse). Data from this mouse are reported in the table but were not considered for any of the subsequent analysis, as upon FACS evaluation most cells were found to be dead.

Total bone marrow engraftment was finally decreased compared to pre-treatment levels (Table 3-2). As expected, control mice did not experience any significant variation in engraftment levels during the course of treatment. Dexamethasone displayed higher single agent cytotoxicity than vincristine, proving about 10-fold more effective. When the two drugs were administered in

combination, their effects were additive and provided the greatest anti-leukemic activity. Bone marrow engraftment of mice treated with this combination of drugs was on average 93% on Day 17, 88% on Day 5, and 25% on Day 28, which marked the end of treatment. (Figure 3-5).

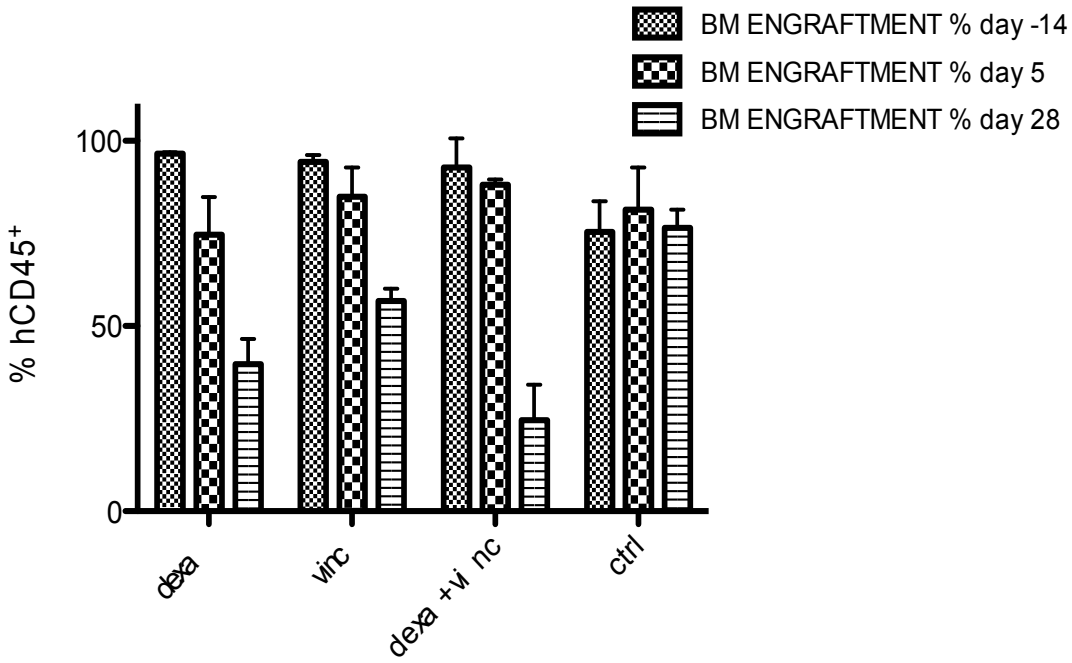

Figure 3-5 Drugs cytotoxic activity as estimated by the reduction in human CD45+ bone marrow engraftment. Bone marrow repopulation data prior to treatment, on treatment day 5, and at the end of the experiment, when mice were sacrificed and bones harvested. Drug dosages were modified along the course of treatment according to their cytotoxic activity on bone marrow or blood populations. Data are the mean (± SD) of 3 mice per group with the exception of dexamethasone single-drug treatment (2 mice only).

The analysis of lineage-specific and differentiation markers allowed for the assessment of the sensitivity of different human cell populations to treatment (Figure 3-6).

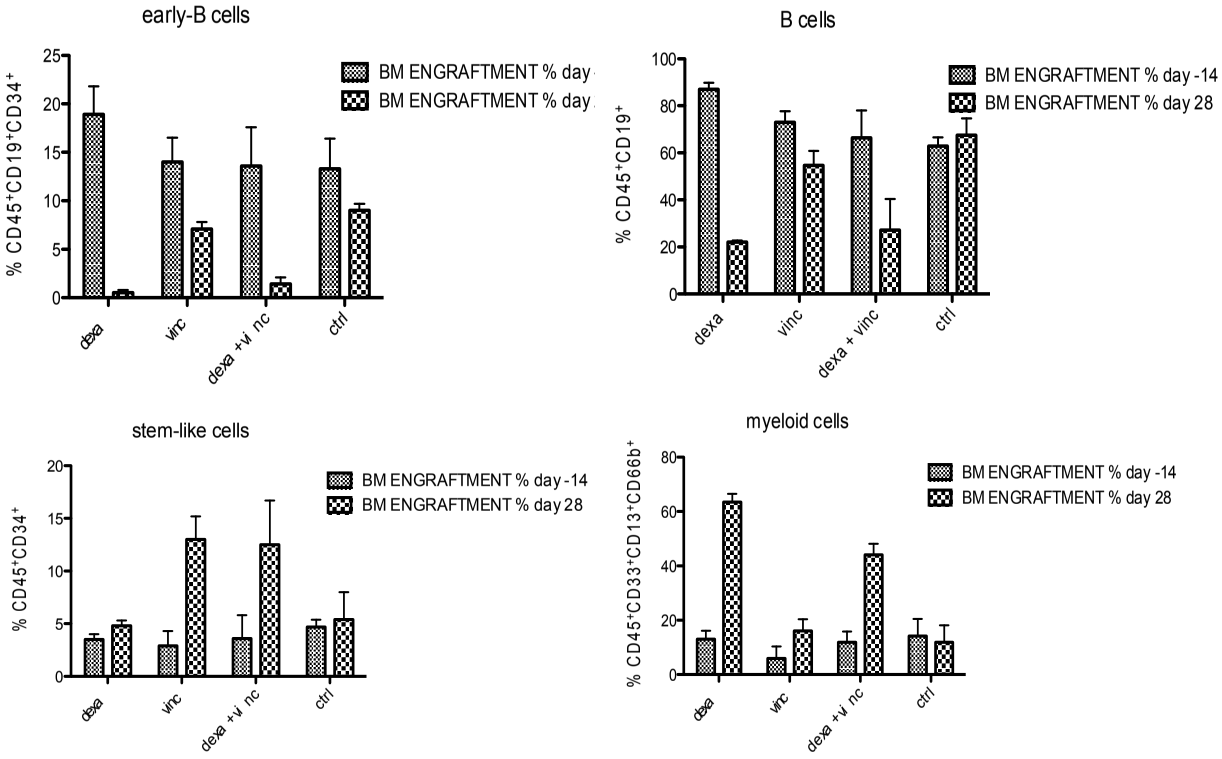

Figure 3-6: Differential resistence of selected leukaemic populations to treatment with dexamethasone and vincristine. Selective cytotoxicity of the drugs towards early-B cells: $CD45^+CD19^+CD34^+$ cells are particularly sensitive to dexamethasone. Selective cytotoxicity of the drugs towards myeloid cells: $CD45^+CD15/CD33/CD66b^+$ are insensitive to both dexamethasone and vincristine. Selective cytotoxicity of the drugs towards hematopoietic stem-like cells: $CD45^+CD34^+$ cells, are resistant to all of the drugs. Selective cytotoxicity of the drugs towards mature B cells: $CD45^+CD19^+CD34^-$ cells, corresponding to early the B progenitors, are particularly sensitive to dexamethasone. Due to the high standard deviation it is difficult to say whether sensitivity to dexamethasone enhanced by vincristine co-treatment. All data are the mean (± SD) of 3 mice per group with the exception of dexamethasone single-drug treatment (2 mice only).

While vincristine, administered as a single drug was not particularly effective against any specific cell lineage, dexamethasone showed preferential activity toward B cells. Stem-like cells, on the other hand, dispayed high resistance to vincristine alone or in combination. This observation is most likely related to the quiescent nature of stem cells, which makes them resistant to chemotherapeutic agents, like vincristine, that act on cycling cells (Lutz et al., 2013).

As shown in the representative FACS plots (Figure 3-7), dexamethasone treatment was particularly cytotoxic to early B cells, 6-fold more effective than on mature B cells. This phenomenon was previously reported, and studies have shown that this drug equally affects pro-, pre-, and immature B cells of the bone marrow (Gruver-Yates et al., 2014). Because differences in GR expression levels represent a major determinant of cell sensitivity to glucocorticoids, the observation that mature lymphocytes cointain 2500-5400 GRs/cell, while GR levels in lymphoblastoid cells range between less than 1000 to greater than 20,000, was suggested to at least partially explain the data (Estlin et al., 2000). In accordance with this data, GR receptor levels in children with early pre-B and pre-B ALL were reported to be on average two-folds higher than in children with T-ALL or B-ALL.

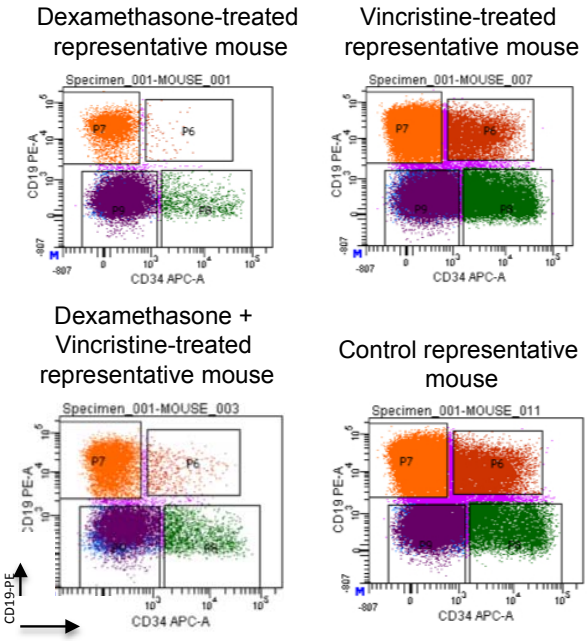

Figure 3-7: Representative FACS plots showing in vivo preferential cytotoxic activity of dexamethasone to proB cells. CD34 staining on the x-axis and CD19 staining is displayed on the y-axis . $CD19^{+}CD34^{+}$ population is drastically reduced upon treatment with dexamethasone.

3.2.2.2 Test of the treatment protocol efficacy on primary cells.

Following the good response of mice to the previously administered treatment, a new test experiment was set up to evaluate the effect of similar regimens on primary leukemic cells. The need for this second experiment was dictated by the differential nature of cord blood and leukemic cells. $CD34^{+}$ cord blood cells do produce multilineage reconstitution upon injection into mice. However, while most cells can be identified as $CD19^{+}$ B cells, their differentiation has, for the most part, progressed beyond the pro-B stage, and they do no longer co-express CD34 antigen. In contrast, expression of TEL-AML1 in human cord blood progenitor cells was previously proven to lead to the expansion of a

preleukaemic cell population with an early B lineage phenotype ($CD34^{+}CD38^{-/low}CD19^{+}$), which bears a differentiation deficit that results in reduced mature B cell production in the marrow (Ford et al., 2009; Tsuzuki et al., 2004). Furthermore, the phenotypic analysis of TEL-AML1^{+} leukemic samples has shown that $CD34^{+}CD38^{+}CD19^{+}$ pro-B-like cells together with an aberrant and rare $CD34^{+}CD38^{-/low}CD19^{+}$ population account for the majority of leukemic cells in the neoplasia (Hong et al., 2008; Kong et al., 2008).

With this data in mind, and given our previous observation of the higher sensitivity of B-cells to dexamethasone, we sought to furter refine our pre-tested two drug regimen on likely differentially sensitive leukemic cell populations. 12 NSG mice were sublethally irradiated and injected with leukemic cells derived from pt.7. The cells used in this experiment were isolated from previously generated primary xenografts. The mice were analysed for human engraftment twelve weeks post-injection. Because only very low levels of human engraftment were detected in the bones of all mice, animals were maintained for an additional four weeks and then sampled again. This time hCD45^{+} cells ranged from 18.50% to 86.50% of all viable cells. Mice were at this point assigned to 4 treatment groups: untreated controls (2 mice), treated with 0.15 mg/Kg vincristine 3 mg/L dexamethasone (2 mice), treated with 0.30 mg/Kg vincristine 6 mg/L dexamethasone (3 mice), treated with 0.50 mg/Kg vincristine 6 mg/L dexamethasone (3 mice) and treated with 0.50 mg/Kg vincristine 9 mg/L dexamethasone (2 mice). The four regimens, with the exception of the 9mg/L dexamethasone dosage, were previously utilized in the cord blood trial. In this new experiment, however, only 2 drug regimens were employed, as this had proven the most effective. Mice were administered treatment for four consecutive weeks, and then sacrificed. Long before treatment

termination one of the mice assigned to the mildest regimen showed signs of distress, most likely related to the leukemic burden, and was sacrificed. Post-treatment analysis of the remaining mice showed surprising results. Independently of how aggressively mice were treated, and of their initial engraftment level, harvested bones of all recipients were cleared of all leukemic cells (Fig 3-8A,B). However control mice, which were poorly engrafted four weeks earlier, display an increase in human repopulation (Fig 3-8A,B). FISH analysis of human cells harvested from control mice, with Vysis LSI TEL/AML1 ES Dual Color Translocation Probe, confirmed the leukemic nature of engrafted cells (Figure 3-9).

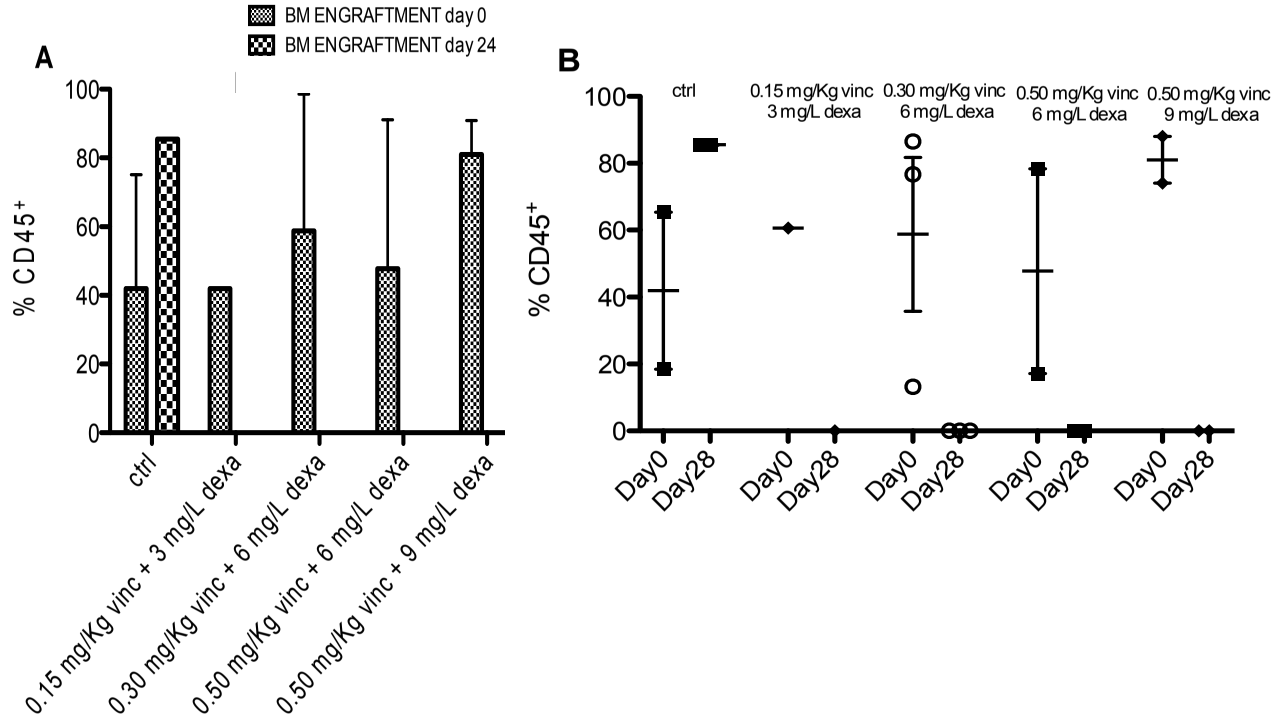

Figure 3-8: Effect of distinct four weeks two-drugs regimens on primary leukaemia cells. The top graph (A) shows the effect of different drug regimens (x-axis) on engrafted primary leukaemia cells from pt7 (y axis). Cells were previously retrieved from primary xenografts. Data are the mean (± SD) of 2-3 mice per group with the exception of the 0.15mg/Kg vincristine and 3mg/L dexamethasone treatment group (1 mouse only). Error bars show the high variability in engraftment levels prior to treatment. B) Data are plotted to show each individual mouse before and post treatment.

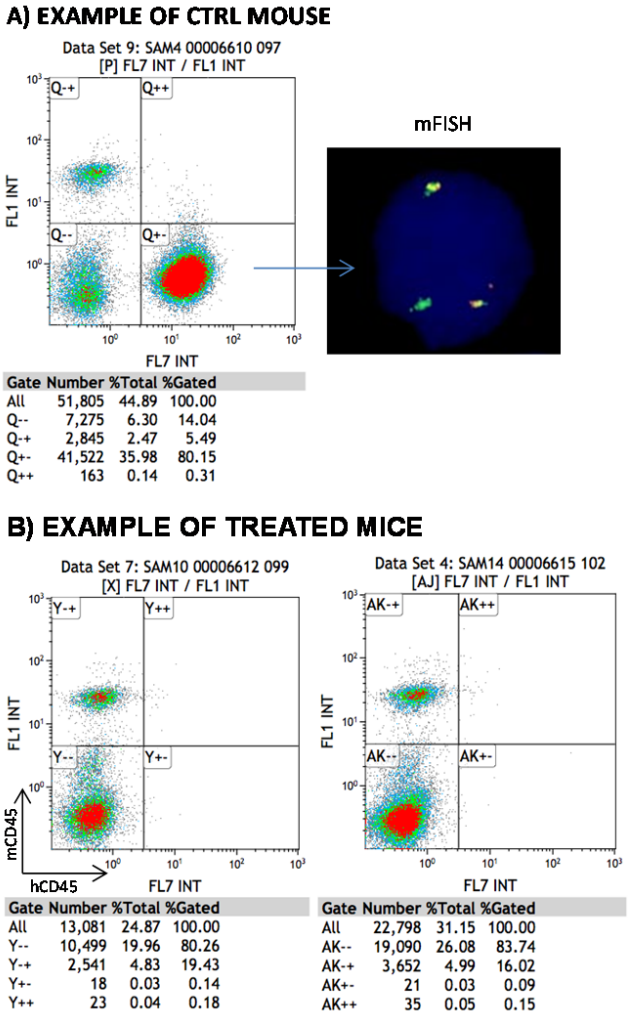

Figure 3-9: Representative FACS plots showing human engraftment in a control and two treated mice at the end of treatment. A and B: dot plots present hCD45 (x-axis) against mCD45 (y-axis) . After four weeks of treatment human cell were completely cleared from the bone marrow of treated mice (B). Over the same period, control mice engraftment remained stable (or increased). FISH with a Vysis probe against ETV6-RUNX1 fusion gene confirmed cells as leukemic. The typical signal pattern displayed by positive cells is: 2 red (1 large not visible as on a different focal plan, 1 small RUNX1 signal), 1 green (ETV6 allele not involved in the translocation), 1 red/green (yellow) fusion signal corresponding to the ETV6-RUNX1 fusion gene. In the represented cell 2 yellow signals are detected but no red signal, indicating the presence of a duplication of the fusion.

In light of the striking effect of four weeks vincristine and dexamethasone administration on PDXs (complete clearance of engrafted leukemic cells from the marrow), we proceeded to test a milder treatment regimen. 9 NSG mice were sublethally irradiated and injected with primary leukemic cells from pt.3. Twelve weeks later, BM engraftment was assessed, and treatment started. Mice assigned to treatment groups were injected with a single dose of vincristine 0.50 mg/Kg and exposed to dexamethasone 6 mg/L for either 3 or 7 days (3 mice each). Mice were subsequently sacrificed at the appropriate time. Control mice (3 mice) were also culled seven days later. FACS analysis of the harvested bones revealed 20% and 70% mean reduction in human engraftment among mice treated for 3 or 7 days respectively, confirming the high chemosensitivity of childhood ALL cells to the selected drugs concentrations. As expected, engraftment of control mice over the treatment time span was stable or increased (Figure 3-10). After 7 of days treatment with 0.50 mg/Kg vincristine and 6 mg/L dexamethasone, which left about 25% residual human leukaemic cells in bone marrow of mice, $5*10^4$, $8.7*10^5$ and $8.7*10^5$ $hCD45^+$ cells could be sorted from each of the PDXs, showing that, while the selected regimen was highly effective in applying selective pressure on the leukaemic population, isolation of survivor cells enough for analysis was still possible.

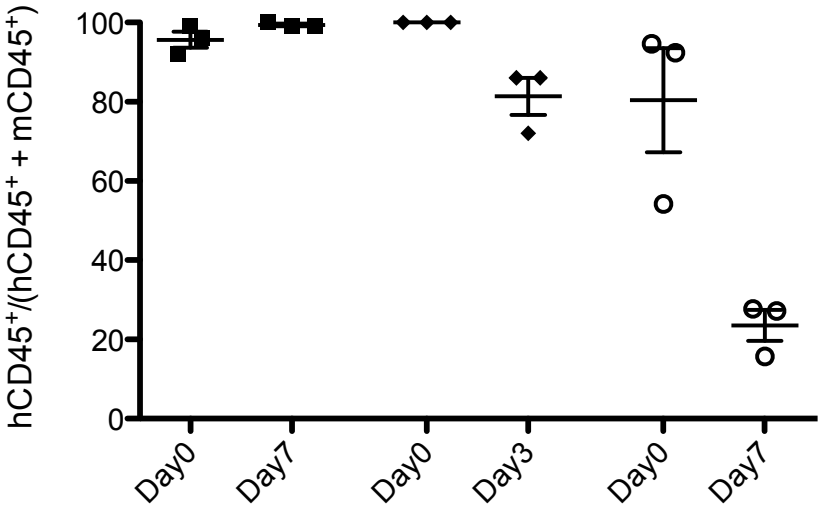

Figure 3-10: Effect of 3 and 7 days chemotherapy regimens on primary pt.3 leukaemia cells. Mice were inoculated with $2*10^5$ cells from pt.3, monitored for engraftment, and treated with 0.50mg/Kg vincristine (single IP injection) and 6mg/L dexamethasone (oral, dissolved in drinking water for either 3 or 7 days) in combination. The graphs show the flow cytometric evaluation of the $\%hCD45^+$ cells of total murine $mCD45^+$ plus human $hCD45^+$ in the BM of recipient mice at the time of engraftment and post-treatment. The values represent means (± SD) of 8 mice per group.

3.3.3 Analysis of interphase nuclei and evaluation of the analytical sensitivity of the FISH assays

Before proceeding to the evaluation of clonal heterogeneity in samples selected through our xenograft models, we tested our probes on a normal karyotype specimen and on REH, a childhood ALL cell line which bears TEL-AML1 translocation (Fig 3-11). The probes, produced by Cytocell as directly labelled with Aqua, Gold, Fitc, and TexasRed fluorochromes, allow the simultaneous evaluation of copy number variations of PAX5, P16, AML1 and TEL genes with single cell resolution. As shown in figure 3-11, in a normal karyotype

individual two signals each can be detected for the four probes in both metaphase and interphase cells. In REH cells however, a fusion signal (yellow signal resulting from the overlap of AML1 in red and TEL in green) can be detected in both interphase and metaphase cells. Additionally, these cells display amplification of the residual allele of AML1 (two additional red signals are detected), as well as homozygous loss of P16 (no orange signals), an observation in line with previous reports (Shah et al., 2001).

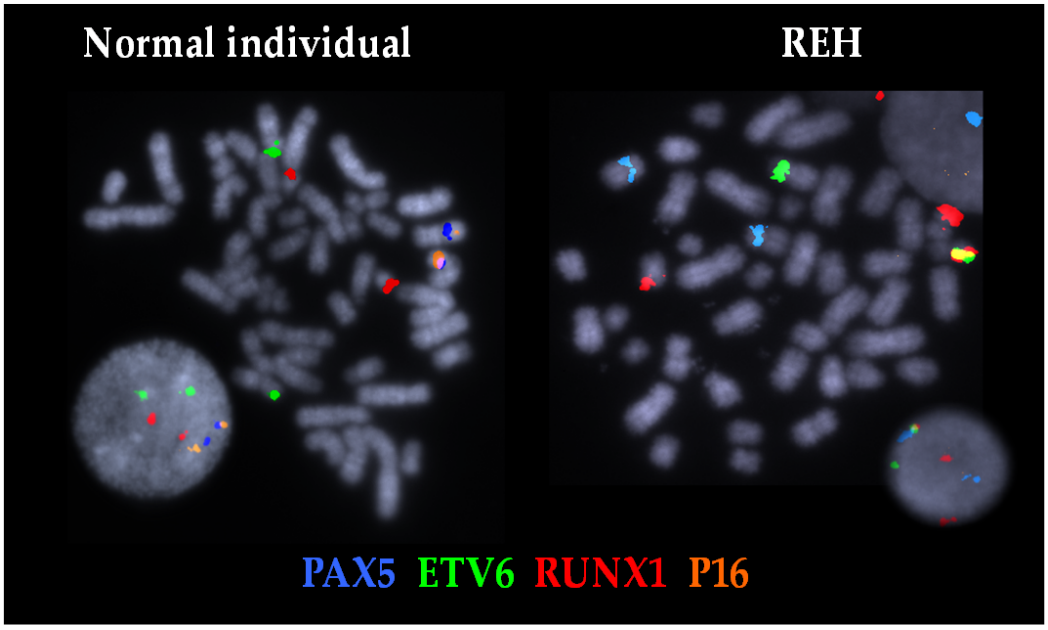

Figure 3-11: Four-colors (+DAPI) mFISH test. Test of the FISH probes on cells from a normal karyotype individual (A) or REH cell line (B) carrying TEL-AML1 translocation. PAX5-Aqua (blue), P16-Gold (orange), RUNX1-Texas Red (Red) and TEL-FITC (Green) probes were hybridised to harvested karyotype preparations. 1 metaphase and one interphase cell are shown for each specimen. REH cells carry a homozygous deletion of p16, therefore no orange signal is detected in the nuclei.

The analysis of metaphase cells, which allows chromosome separation and identification, while potentially more informative, does require overnight culturing of proliferating cells in presence of Colcemid, a mitotic spindle inhibitor. Unfortunately, primary ALL cells, as many other types of primary cells, are extremely difficult to maintain in culture and barely proliferate *in vitro.* Therefore only interphase cells were analysed in subsequent experiments. Scoring was performed following the guidelines presented in figure 3-12.

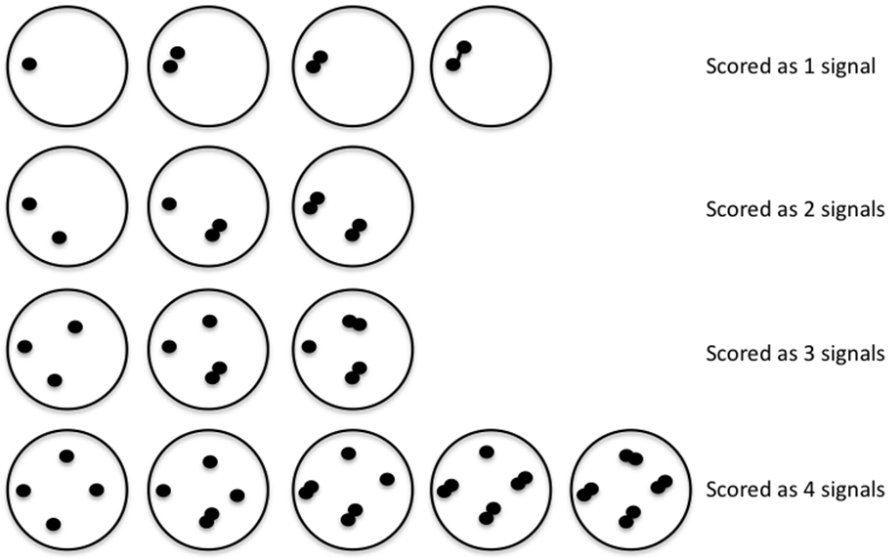

Figure 3-12: Schematic representation of scoring criteria. Shown in the illustration are typical hybridization signal configurations referring to an individual locus-specific probe. Only signals that are more than one signal width apart are evaluated as distinct. Nuclei that have passed through the S phase of the cell cycle may in fact be present as G2-paired signals (i.e., two smaller signals in very close proximity). Signals joined by a string of hybridization are also considered as one signal. Large probes, as the ones used for the study, can sometimes appear as fused signals straddling both chromatids. In interphase nuclei these probes can generate signals that present more diffuse or dispersed hybridization spots in the chromatin of interphase nuclei.

To establish cut-off levels of false positivity of individual and combined copy number variations (CNA), we scored 250 interphase nuclei representing three distinct positive control samples: unenriched PBMCs from normal peripheral blood, as well as CD19-enriched cells from the bone marrow of two normal karyotype individuals. The nuclei were scored and the percentage of nuclei exhibiting the appropriate number of distinct signals was calculated (Figure 3-13). The recommended analytical sensitivity for probes adopted in standard diagnostic studies using FISH is 90%. However, when probes are intended to detect mosaicism, as well as for detection of minimal residual disease, sensitivities ≥95% are preferred. Reassuringly, all of the tested probes performed accordingly, and no false positive rate exceeded 3% in an individual experiment, and 2% when data from multiple experiments were averaged. Random co-localization of TEL (or ETV6) and AML1 (or RUNX1) probes, while still within the target sensitivity range ≥95%, was however detected in a higher percentage (3.74% on average) of normal cells. False positive rates for the co-occurrence of any two abnormalities were estimated to be 0.45%. Using inference from the single probe copy number variation found through scoring, the combinatorial probability rate for these two probes was estimated to be 0.35%. This data allowed the establishment of a 2% cut-off level for four-colour FISH, which we subsequently adopted in all experiments. Subsequent analysis of leukaemia samples would later highlight the existence, in several cases, of intermediate subclones, below the set threshold of 2% frequency (1-2%, at least three cells), displaying higher frequency in separate recipients.

PBMC from normal peripheral blood

Gene/ region	Hemizygous loss of 1 signal %	Homozygous loss of 2 signals %	Gain of 1 signal %	Gene fusion %	Gain of fusion %	Random colocalization Etv6 and Runx1 %	Any two CNA
ETV6-RUNX1	-	-	-	0.00	0.00	4.50	
RUNX1	1.00	0.00	1.00	-	-	-	
ETV6	1.00	0.00	0.50	-	-	-	
P16	0.00	0.00	0.00	-	-	-	
PAX5	1.00	0.00	0.00	-	-	-	

0.01% as scoring

0% as actual count

CD19+ cells from normal BM

Gene/ region	Hemizygous loss of 1 signal %	Homozygous loss of 2 signals %	Gain of 1 signal %	Gene fusion %	Gain of fusion %	Random colocalization Etv6 and Runx1 %	Any two CNA
ETV6-RUNX1	-	-	-			3.07	
RUNX1	2.63	0.00	2.63	-	-	-	
ETV6	0.88	0.00	0.00	-	-	-	
P16	1.32	0.00	0.00	-	-	-	
PAX5	2.63	0.00	0.00	-	-	-	

0.07% as scoring

0.87% as actual count

AVERAGE

Gene/ region	Hemizygous loss of 1 signal %	Homozygous loss of 2 signals %	Gain of 1 signal %	Gene fusion %	Gain of fusion %	Random colocalization Etv6 and Runx1 %	Any two CNA
ETV6-RUNX1	-	-	-	0.00	0.00	3.74	
RUNX1	1.87	0.00	1.87	-	-	-	
ETV6	0.93	0.00	0.23	-	-	-	
P16	0.70	0.00	0.00	-	-	-	
PAX5	1.87	0.00	0.00	-	-	-	

0.35% probability

0.45% scoring

Figure 3-13: Cut-off levels for CNA variations false positivity. Cut-off levels were established by scoring of 250 nuclei from three normal karyotype individuals. Values are the mean percentage of nuclei exhibiting an aberrant number of distinct signals. Scoring of the slides for the incidence of any combinations of false positive signals, as well as probabilistic calculation of event incidence based on single CNA data allowed the evaluation of overall analytical sensitivity of four colour FISH with the relevant probes set.

3.3 Discussion

The aim of this project is to establish a xenotransplantation model of ALL that would serve as a platform for the characterisation of genetically driven mechanisms of chemo-resistance in this disease. By *in vivo* exposure of genetically heterogeneous leukaemia populations to chemotherapy agents routinely used in treatment of the childhood disease, we aimed at bringing to light key and clinically relevant functional properties of leukemic cells. Such a model promises new insight into the relevance and the key aspects of intratumour genetic heterogeneity for standard clinical practice, and would also serve as a platform for additional mechanistic studies aimed at identifying new strategies for eradication of resistant clones. The model relies on the establishment of multiple PDXs, on the optimisation of a reliable induction-like treatment protocol, and on the development of a single cell resolution technique for tracking clonal dynamics.

A preliminary screening of the engraftment ability of 11 TEL-AML1+ ALL samples identified 5 samples with leukaemia initiating properties. Previous studies looking at engraftmernt properties of B cell precursor ALL, AML and T-ALL in mice injected with higher cell numbers of fresh cells (1–10*10^6 blasts per mouse), reported engraftment failure in 4/39 (10.25%) B cell precursor ALL, 1/11 (9.09%) AML and 1/4 (25.0%) T-ALL samples. The median time to engraftment was about 10 weeks for both B cell precursor ALL and AML, and 6.8 weeks for T-ALL blasts. In this setting, engraftment of mice injected with low numbers of blasts, as detected 6–20 weeks post-injection, was poorer, suggesting that when limited number of cells are transplanted engraftemnt efficiency might reflect the original disease aggressiveness and is possibly indicative of clinical outcome (median: B-ALL: 25.4%, AML: 34.6%, T-ALL: 37.5%) (Woiterski et al., 2013). Among samples

selected for further experiments specimens from pt.1988 and 2278 were isolated from leukaemias that had progressed to relapse. Relapse samples, as well as a treatment timepoint (d8) for pt.2278, were also obtained from both patients and were available for further analysis. Unfortunaly, even though PDXs of pt.B dispayed good engraftment, cell numbers for this sample were limiting. However, two additional samples (from pt.3 and pt.7) were obtained courtesy of Prof. Mel Greaves, for a total number of 6 engraftment-competent primary diagnostic leukaemia suitabable for the study.

In order to establish an induction-like treatment regimen, which, while being effective in killing the majority of leukemic cells, would allow to uncover any concomitant genetic bottleneck selection process, we first evaluated the safety and efficacy of vincristine and dexamethasone chemotherapy on cord blood cells. Subsequently, we optimised treatment regimens for leukaemic TEL-AML1^{+} cells, and report on their high sensitivity to treatment compared to cord blood. Four weeks of single- or double-agent treatment was administered to mice with multiliage engraftment, identifying the two drug regimen as highly effective due to the additive activities of dexamethasone and vincristine. Analysis of engraftment in the blood and bone marrow of the mice throughout the course of treatment validated that a dose-escalated regimen of 0.50 mg/Kg of vincristine and 6mg/L of dexamethasone, achieved the required cytotoxicity. Starting from an average total BM engraftment of around 93%, CD45^{+} human cells represented just 25% of all viable hematopoietic cells at the end of the experiment. Reasurringly, no evident signs of elevated treatment morbidity were detected. Upon administration of the same regimen to mice engrafted with primary leukaemia cells, no leukemic cells survived within the bone marrow of any of the mice by the end of the fourth week of chemotherapy. This observation, which is in line with the excellent prognosis

of TEL/AML1-positive ALL (Rubnitz et al., 1999; Zuna et al., 1999), forced us to redesign our treatment protocol to cover a shorter drug administration period. When pt.3 engrafted mice were administered 0.50 mg/Kg of vincristine (single injection) and 6mg/L of dexamethasone for seven days human cell in the BM reduced by 70%, highligting the suitability of the newly modified regimen for future studies.

Analysis of clonal dynamics of TEL-AML1^{+} ALL in our mouse model required establishment and optimization of four colour FISH. Copy number variations in TEL-AML1, *TEL*, *AML1*, *p16* and *PAX5* genes, were selected as markers to dissect clonal heterogeneity and track the fate of individual subclones over treatment. Evaluation of the analytical sensitivity of each probe and that of the overall assay established that any clone detected in the population with a frequency of ≥2% would fall within confidence range. The 2% threshold was in line with cut-off levels previously established by Anderson et al, for three colour FISH with a similar set of probes. In this case, use of a fourth probe increased the cut-off to 6.9%, due to spectral overlap between Texas red (used to detect digoxigenin-labelled probes) and Spectrum orange (used to label *RUNX1* in the commercial *ETV6–RUNX1* ES probe). For this reason, earlier analyses were mostly carried out through three-colour FISH (Anderson et al., 2011). While spectral overlap, particularly between gold and FITC had proven problematic also in our hands, through testing of multiple microscopy systems (described in the materials and methods section) and filter sets, we were able to obtain sufficient dissection of the contribution of individual fluorochromes to fluorescence in each channel, lowering the threshold for four colour FISH to 2%.

CHAPTER 4

IN VIVO TREATMENT OF 6 PATIENT-DERIVED TEL-AML1+ XENOGRAFTED LEUKAEMIAS

4.1. Introduction

Genetic plasticity, or the ability of cancer to adapt as a result of continuous accumulation of somatic mutations that create a substrate for selection, is one of the hallmarks of cancer (Hanahan and Weinberg, 2011). Over the last decades several reports have therefore elucidated the link between genotypic evolution and phenotypic evolution of cancer, as well as the limitations it poses to standard chemotherapy and precision medicine (e.g. emergence of drug resistant clones in treatment of Ph+ patients with imatinib or dasatinib). However, it is only more recently that we have learned that within individual cancers patterns of clonal evolution that follow complex branching trajectories and lead to the co-existence of multiple genetically diverse subpopulations competing for ascendency, are at least as common as the more traditional linear model of sequential clonal expansions (Bozic et al., 2010; Maley et al., 2004). While a natural corollary of these observations is that intratumour genetic heterogeneity likely contributes to the continuous reshaping of the malignancy landscape during disease progression, particularly over treatment, the nature of the interaction between clonal evolution and cancer therapy still remains unknown (Merlo et al., 2006), If preliminary studies have collected evidence that chemotherapy might introduce *de novo* mutations, actively participating in genetic diversification (e.g. in treatment of acute myeloid malignancies), it is also expected that pre-existing sources of genetic heterogeneity (or subclones), will participate in an over-treatment evolutionary shifts (Ding et al., 2012; Parsons et al., 2008). Depending on factors like the tumour type and its kinetics, as well as the nature of the treatment and its cytotoxic efficacy, one might imagine that resistant clones could either be actively selected by chemotherapy or survive treatment as the outgrowth of multiple diverse pre-existing minor, but fit genetic variants. The first scenario of clonal evolution fuelled

by treatment-induced selective pressure, exemplified by BCR_ABL T315I mutation in CML, maybe particularly relevant to precision-based medicine aimed at targeting particular genetic variants that might not be shared by all clones, thus inducing evolutionary convergence at relapse of the clone bearing the resistance-conferring mutation (Shah et al., 2002). The second scenario instead hypothesizes that the emergence of more aggressive genetic subclones might be unlinked from treatment-sensitivity and relate to treatment-induced mass-extinction effect (overall reduction in the bulk tumour size), which, acting as a classic evolutionary bottleneck, might reset clonal dynamic. It is in fact possible that depletion of the dominant clone could shift the evolutionary landscape in favour of a more aggressive variant (Landau et al., 2014). Such a model has found validation in the observation that in CLL a higher preponderance of large subclones (>10% cancer cells) can be observed in samples collected post-treatment compared to pre-treatment specimens (Landau et al., 2013). While both described mechanisms are likely to be at play to generate evolutionary shift in different contexts, the answer to key questions, like which clones survive treatment and why, and whether leukaemic clone survival deterministic or stochastic, are still lacking.

Only better comprehension of the relative fitness of clones in face of the challenge of chemotherapy, and of the prognostic significance of the size of a particular genetic variant will allow us to understand whether clones that survive chemotherapy to emerge during relapse were intrinsically chemotherapy-resistant (or more fit in the face of the challenge than other clones), or rather, have survived by chance. To tackle this question, and contribute to scientific progress in the field of cancer heterogeneity, particularly in the context of TEL-AML+ ALL, we decided to make use of the model system and the single cell analysis method described in the previous chapter of this thesis.

Xenograft models have previously been used to shed light on the hypothesis that the proportion of individual subclones within a patient sample might reflect fitness differences dependent on clonal identity. It is however difficult to obtain an answer to this question through the mere observation of clonal heterogeneity within individual tumours, and even through cross-patient comparison of tumours. Transplantation of samples from individual patients into multiple mice was therefore adopted as the experimental approach to this problem. The method has the potential to test whether leukaemia-initiating ability is restricted to only one or a few subclones within a tumour, and whether the proportions of engrafted subclones in the mouse reflected their proportions in the patients. This work led to the observations that leukaemia propagating cells are indeed genetically variegated, reflecting the overall heterogeneity of the tumour bulk, and vary in their *in vivo* generating potential (Anderson et al., 2011; Kreso et al., 2013).

While these studies gave us valuable insight into the relationship between the genetic identities of the subclones and their disease-propagating abilities, the ability to drive cancer growth does not necessarily correlate with sensitivity to treatment. Assessing clonal dynamics in response to treatment is the object of this thesis. To understand whether relapse in childhood ALL is linked to intratumour genetic heterogeneity, either through selection of intrinsically treatment-resistant cancer subclones, or through a process of size- (or probability-) dependent mass-extinction and stochastic outgrowth of pre-existing aggressive minor genetic variants, we have therefore exploited our previously established *in vivo* model. By challenging the same heterogeneous tumour multiple times with the same chemotherapy, we aimed at gaining enough statistical power to distinguish

between deterministic and stochastic clone survival in the face of treatment generated selective pressure.

4.2 Results

4.2.1 Experimental design

Having set up an effective treatment protocol, as well as a single cell-resolution methodology to track clonal dynamics over treatment, we proceeded to generate PDXs of 6 samples previously selected for their engraftment-competency. We then expose them to chemotherapy. In order to obtain enough statistical power, a large cohort of mice was injected with the same patient inoculum. A fundamental characteristic of the experimental design was the collection from each treated mouse, and control mouse, of pre- and post-treatment samples for analysis, by mFISH, of treatment-induced changes to the overall genetic heterogeneity landscape (Figure 4.1).

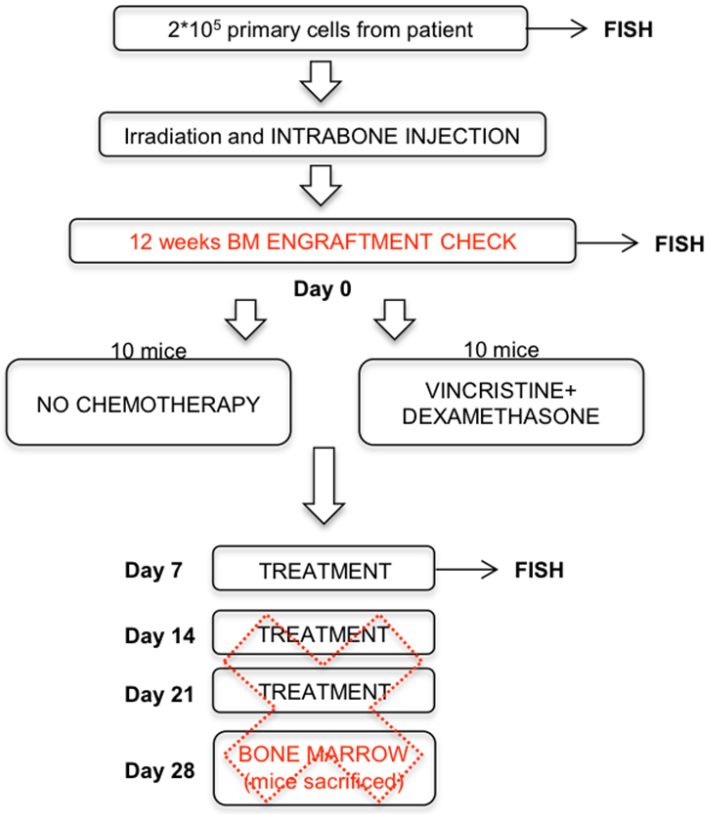

Figure 4-1: Modified experimental design diagram. The original experimental plan was adapted to the high sensitivity of the leukemic cells with administration of a single course of chemotherapy. Mice were sacrificed 7 days post-treatment (3-days in variations to the standard protocol). Human leukaemia burden was evaluated by FACS analysis before and following treatment. At each stage, human cells, defined as $CD45^+$ $CD19^+$, were cell sorted and harvested for mFISH.

Through statistical analysis of data produced by Anderson et al. on diagnostic clonal heterogeneity regeneration across multiple pt.3 and pt.7 ALL xenotransplantation recipients, it was possible to estimate that by including as many as 10 mice in each treatment group all clones present in the diagnostic material with a frequency of 1% or higher would likely be represented (engrafted) and exposed to treatment in at least one or multiple recipients. Independent exposure of most clones to chemotherapy in several PDXs was expected to allow

for the distinction between genetically and stochastically driven mechanisms of chemosensitivity and resistance.

Additionally, comparison of treatment survivor clones with those detected in primary- and PDX-derived samples of patient 2278 day 8 MRD, and patients 2278 and 1988 relapse was hoped to fully reveal the potential of the mouse model. Evidence for a similar genetic or stochastic bottleneck selection process taking place over chemotherapy administration in matching patients and animal models would allow the extrapolation of observation derived from the latter to reconstruct the phylogenetic history of tumour seeding, survival to treatment and regrowth in patients.

4.2.2 Treatment of PDXs of pt.3, pt.7, pt.D, pt.11, pt.1988 and pt.2278

In a multistep process, requiring at least two independent transplantation experiments for each specimen, previously selected diagnostic BM samples were injected into NSG mice, and subsequently exposed to treatment with vincristine and dexamethasone. As in previous experiments, mice were preconditioned through sublethal irradiation and injected with $2*10^5$ cells per recipient. Twelve weeks later engraftment levels were evaluated by BM aspiration and FACS analysis (mCD45-hCD45-hCD19 staining). Successful BM aspirations provided few thousands to few hundred thousands human cells. As downstream mFISH requires the scoring of at least 250 stained nuclei, when less than 2000 cells were retrieved, the procedure was, where possible, repeated a few weeks later. Suboptimally engrafted mice (<40% engraftment) were maintained for an additional 3-5 weeks before bone marrow sampling was performed again. In experiments in which engraftment levels were very different among recipients, downstream experimental procedures were completed at different times. If upon

re-evaluation mice engraftment levels were still <40%, depending on engraftment percentage, mice were either sacrificed (not engrafted) or included in the study anyway (e.g. some recipients of pt.7 and pt.1988 cells). Typically, when engraftment of human $CD45^+$ cells was higher than 40%, mice were assigned to either treatment or control groups (Figure 4-1).

The treatment protocol backbone consisted of 6 days of a single IP injection of 0.50m/Kg vincristine and 7-days oral administration of 6mg/L dexamethasone 6mg/L (Figure 5-1). Depending on the availability of primary cells, variations on this protocol were also adopted in an attempt to establish a short kinetic of leukemic cell killing, and thus obtain information as to dose and time related clonal sensitivity. Additional xenografts of pt.3 and pt.7 were therefore treated with the same regimen for a shorter time (3 days), while additional pt.11 xenografts were administered a higher dosage of the drugs (0.60 mg/Kg vincristine and 12mg/L dexamethasone) over the same duration of time (7 days). While being highly effective on less sensitive leukaemia, this more aggressive regimen resulted in high morbidity to the mice (more than 50% mice had to be humanely sacrificed prior to experiment end point), and was therefore dismissed.

At the time of sacrifice tibias, femurs and pelvic bones were harvested from each mouse, crushed, stained with α-hCD45 (AF700) and α-mCD45(FITC/PE) antibodies, and analysed by FACS. Where hCD45 expression by leukemic cells was evaluated as low, cells were co-stained with hCD19(PE/PE-Cy7) to confirm the B-cell origin of the human $CD45^{low}$ population. Human cells were flow sorted and harvested for FISH. Only mice for which both aspiration and total bone marrow sorting were successful were taken into account for analysis.

Variable numbers of total human cells were retrieved from BM of treated mice, 10^4-10^6 depending on the leukaemia chemosensitivity. In the case of control mice, 10^6 human cells were sorted from each recipient, while additional material was banked for future experiments. In case of xenografts of pt.1988 and 2278, we also harvested the spleen of several recipients. The organ was often enlarged, and highly enriched in leukemic cells in control (untreated) mice, while the splenomegaly was reverted in treated mice. Analysis of leukemic cells from matching BM and spleen of control mice allows for the identification of clone-specific migration and homing properties. In treated mice this also provides information as to whether anatomically separated niches can provide chemo-*protection*.

FACS analysis data presented in this chapter show leukemic burden, as evaluated by estimate of the proportion of human $CD45^+$ in relation to total murine ($mCD45^+$) and human ($hCD45^+$) cells, before and after treatment. Percentages of human and mouse cells refer to values obtained after gating cell populations based on FCS/SSC, doublets exclusion, and negativity for the viability dye Hoechst 33258.

Among xenografts of pt.3 (Figure 4-2), a total of 24 mice injected with the same inoculum were analysed. Recipients were treated with a single IP injection of 0.50mg/Kg vincristine and 6mg/L of dexamethasone by oral route, for either three (8 mice) or six days (8 mice). Treated mice displayed dose-dependent reduction of leukemic burden. In mice sacrificed after three days of exposure to chemotherapy, human leukaemic engraftment in the BM was reduced to ~12% human cells (significant) on average. Among the recipients of seven days of treatment the reduction increased to ~70% human cells (significant). Within the same timescale

(7 days) engraftment of control animals (8 mice) had remained stable or increased to 100% human cells.

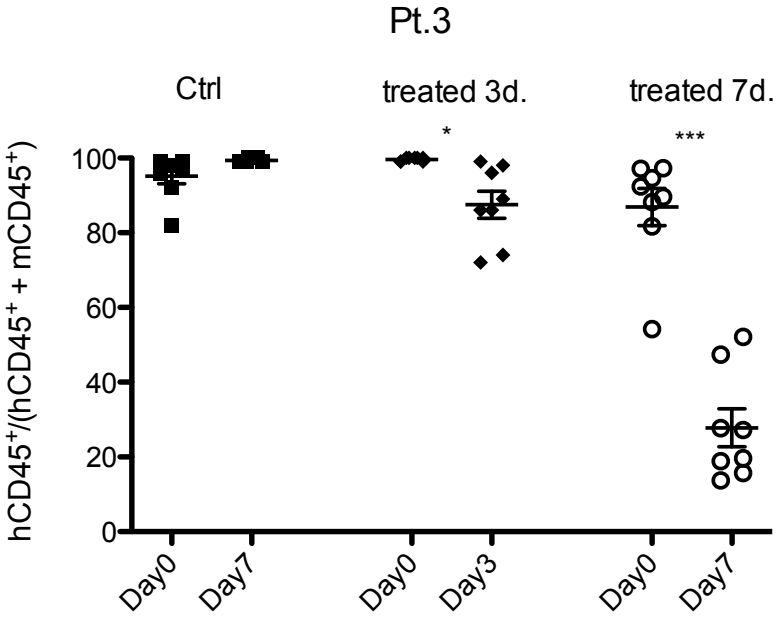

Figure 4-2: In vivo response of pt.3 xenografts to by 3 or 7 days treatment with VCR and DEX. Mice (10-16 weeks old) were inoculated with $2*10^5$ cells from pt.3, monitored for engraftment, and treated with vincristine (0.50mg/Kg, single IP injection) and dexamethasone (6mg/L, oral, dissolved in drinking water) in combination. Each data point on the graph represents the flow cytometric evaluation of the %hCD45$^+$ cells versus total murine mCD45$^+$ and human hCD45$^+$ in the BM of individual recipient mice at the time of engraftment (Day 0) and post-treatment (Day 3 or Day 7). The mean (± SD) of each data set (8 mice per group) is also plotted.

Xenografts of patient 7 (Figure 4-3) were administered the same treatment as PDXs of pt.3. Chemotherapy-induced cytotoxicity in these mice induced 25% (non-significant) reduction in engraftment by day 3, and 45% (significant) by day 7.

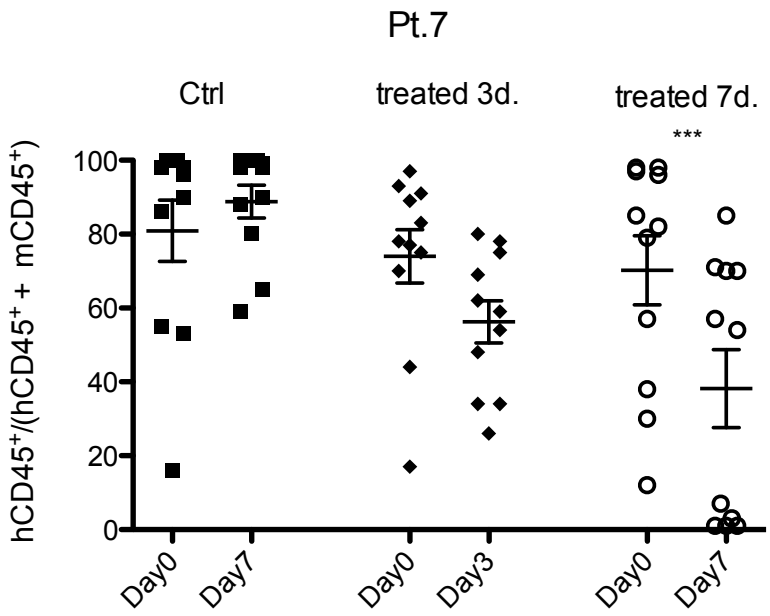

Figure 4-3: In vivo response of pt.7 xenografts to 3 or 7 days treatment with VCR and DEX. Mice (10-16 weeks old) were inoculated with $2*10^5$ cells from pt.7, monitored for engraftment, and treated with vincristine (0.50mg/Kg, single IP injection) and dexamethasone (6mg/L, oral, dissolved in drinking water) in combination. Each data point on the graph represents the flow cytometric evaluation of the %hCD45$^+$ cells versus total murine mCD45$^+$ and human hCD45$^+$ in the BM of individual recipient mice at the time of engraftment (Day 0) and post-treatment (Day 3 or Day 7). The mean (± SD) of each data set (11 mice per group) is also plotted.

Xenografts of patient 11 were administered either the standard regimen of 0.50mg/Kg of vincristine and 6mg/L of dexamethasone or escalated doses of the two drugs, 0.60mg/Kg vincristine and 12mg/L dexamethasone, for the same length of time. Patient 11-derived xenografts were less sensitive to the standard treatment protocol than patient 3 and patient 7 PDXs, as indicated by a significant but mild (12%) mean reduction in human engraftment. The intensified treatment regimen did however prove 6-fold more effective than the standard one, inducing a

mean reduction in human engraftment of about 62% on average (Figure 4-4). Unfortunately, the intensified treatment protocol was associated with high mouse morbidity and was therefore dismissed.

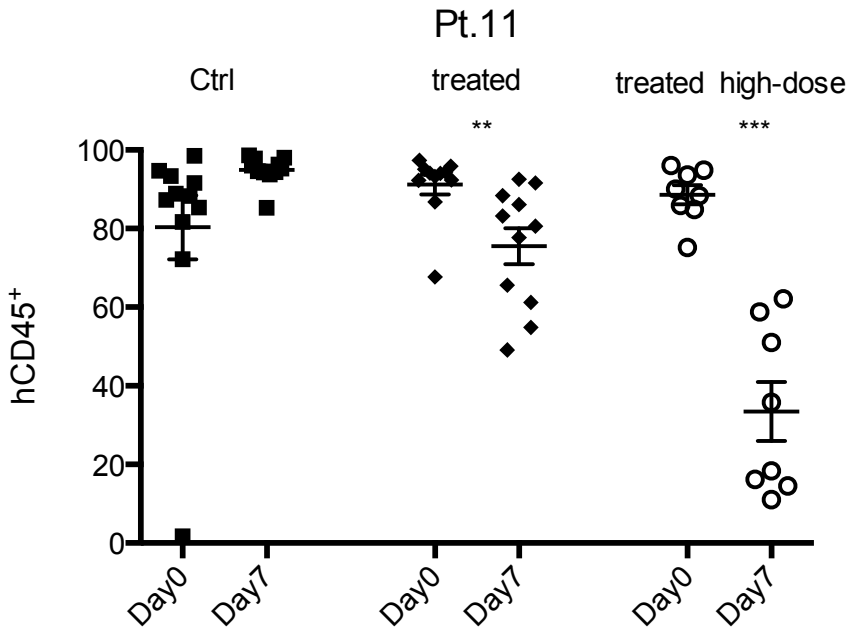

Figure 4-4: In vivo response of pt.11 xenografts to 7 days standard or high dose treatment with VCR and DEX. Mice (10-16 weeks old) were inoculated with $2*10^5$ cells from pt.11, monitored for engraftment, and treated with standard dose (0.50mg/Kg, single ip injection) or high dose (0.60mg/Kg, single IP injection) vincristine, and standard dose (6mg/L) or high dose (12mg/L) dexamethasone (oral, dissolved in drinking water) in combination. Each data point on the graph represents the flow cytometric evaluation of the %$hCD45^+$ cells versus total murine $mCD45^+$ and human $hCD45^+$ in the BM of individual recipient mice at the time of engraftment (Day 0) and post-treatment (Day 7). The mean (± SD) of each data set (8-11 mice per group) is also plotted.

A limited number of cells were available to generate patient D-derived xenografts. Eight mice exposed to standard chemotherapy doses for seven days

showed good response to treatment, with 45% mean reduction in human BM engraftment (Figure 4-5).

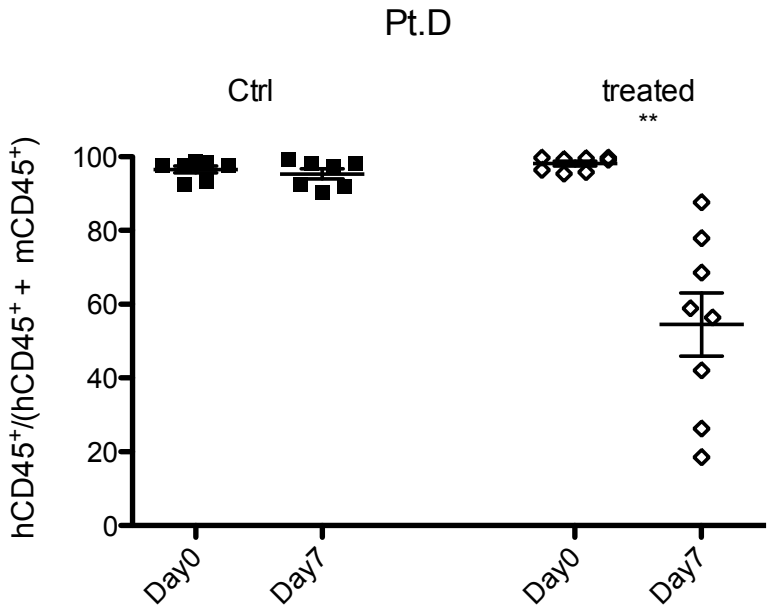

Figure 4-5: In vivo response of pt.D xenografts to 7 days treatment with VCR and DEX. Monitoring of pre and post treatment frequencies of human leukemic cells in murine BM relative to total human and mouse populations. Mice (10-16 weeks old) were inoculated with $2*10^5$ cells from pt.D, monitored for engraftment, and treated with vincristine (0.50mg/Kg, single IP injection) and dexamethasone (6mg/L, oral, dissolved in drinking water) in combination. Each data point on the graph represents the flow cytometric evaluation of the $\%hCD45^+$ cells versus total murine $mCD45^+$ and human $hCD45^+$ in the BM of individual recipient mice at the time of engraftment (Day 0) and post-treatment (Day 7). The mean (± SD) of each data set (7-8 mice per group) is also plotted.

Of note, multi-parametric flow cytometry analysis of this sample revealed the coexistence within the leukaemia, at presentation and upon its *in vivo* regeneration, of three distinct $CD45^+CD10^+$ (haematopoietic cells of B-lineage) phenotypic compartments (Figure 4-6), $CD19^+34^+38^+$(P5) $CD19^+34^-38^+$ (P7) and

$CD19^{+}34^{+}38^{-/low}$ (P6). Cells with the immunophenotype $CD34^{+}CD38^{-/low}CD19^{+}$ appear, so far, to be unique to ALL. All three tumour populations were FACS sorted in order to confirm by mFISH the existence within each of the genetic complexity that characterizes the bulk leukaemic population, as previously described by Anderson et. al, (Anderson et al., 2011).

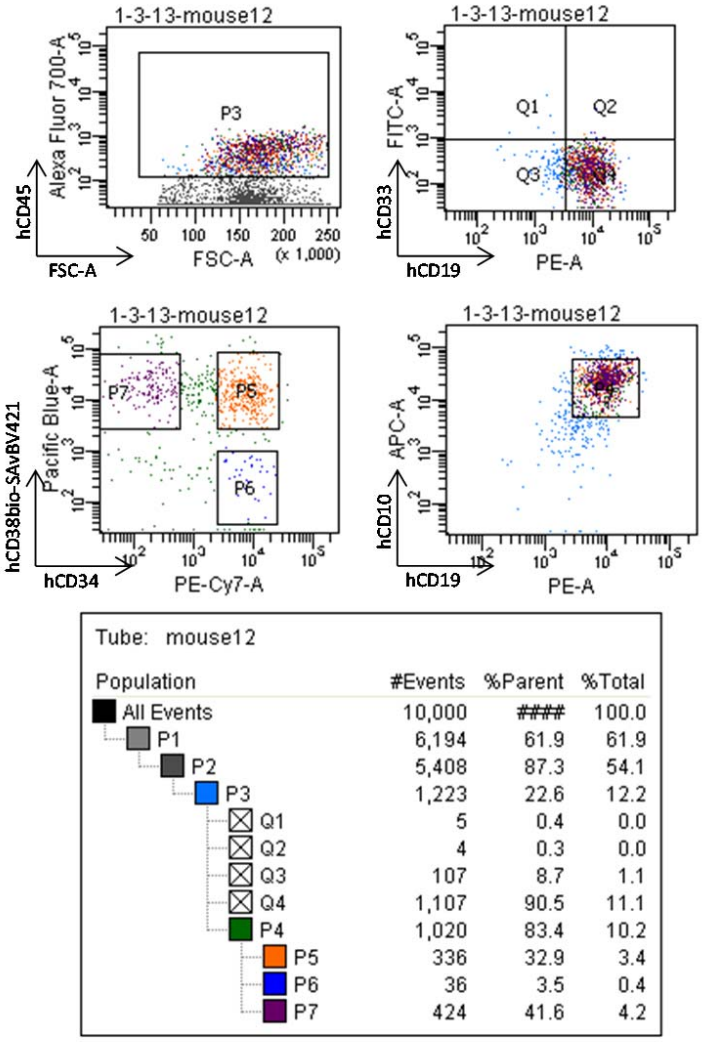

Figure 4-6: Flow sorting of leukemic pt.D BM populations for the evaluation of subclonal diversity by FISH. Human $CD45^{+}$ $CD19^{+}34^{+}38^{+}$(P5), $CD19^{+}34^{-}38^{+}$ (P7), and $CD19^{+}34^{+}38^{-}$ (P6) were flow sorted from the harvested BM of 3 mice and from the diagnostic material. All three populations were $CD10^{+}$. Representative FACS plots in this figure show results obtained for mouse 12.

Xenografts of patient 1988 were particularly difficult to establish. Not only did several mice (4 out of 12) not develop high engraftment (>40%) within the observation period, leukemic burden in these recipients was also associated with unusually high morbidity. Out of 31 total injected mice only 5 control and 7 treated mice developed good engraftment and reached the experimental end point. Additionally, even though significant, sensitivity to treatment of these PDXs was rather low (mean ~24% reduction in human BM engraftment) (Figure 4-7). Unexpectedly, some control mice also showed a drop in engraftment levels (mean ~16% reduction in human BM engraftment, not significant) by day 7 post-aspiration.

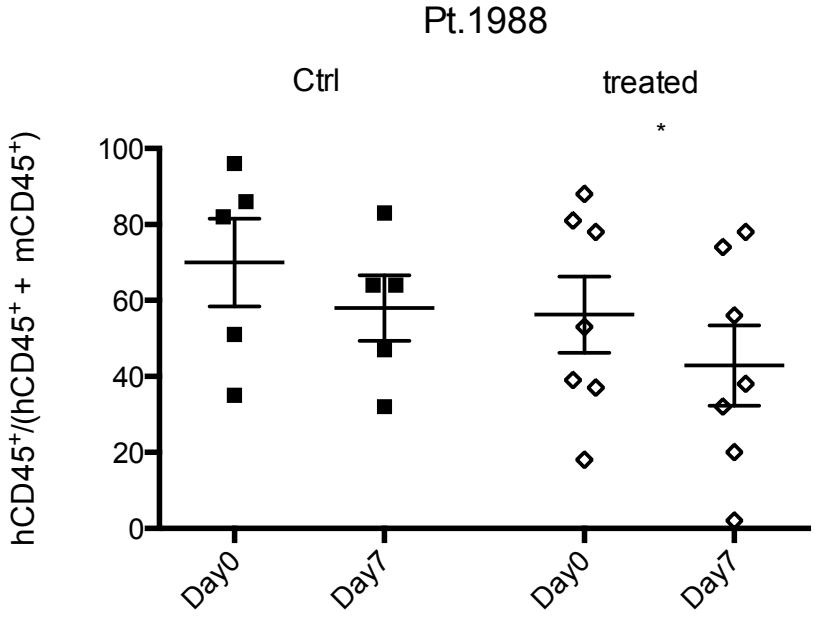

Figure 4-7: In vivo response of pt.1988 xenografts to 7 days of treatment with VCR and DEX. Monitoring of the frequencies of human leukemic cells in murine BM at engraftment and after chemotherapy. Mice (10-16 weeks old) were inoculated with $2*10^5$ cells from pt.1988, monitored for engraftment, and treated with vincristine (0.50mg/Kg, single IP injection), and dexamethasone (6mg/L, oral, dissolved in drinking water) in combination. Each data point on the graph represents the flow cytometric evaluation of the %$hCD45^+$ cells versus total murine $mCD45^+$ and human $hCD45^+$ in the BM of individual recipient mice at the time of engraftment (Day 0) and post-treatment (Day 7). The mean (± SD) of each data set (5-7 mice per group) is also plotted.

FACS evaluation of the spleen of 4 control and 5 treated mice showed higher percentages of leukaemia cells in the spleen (figures 4-7 and 4-8) than in the BM, indicating that the spleen might be a preferential homing site for these cells.

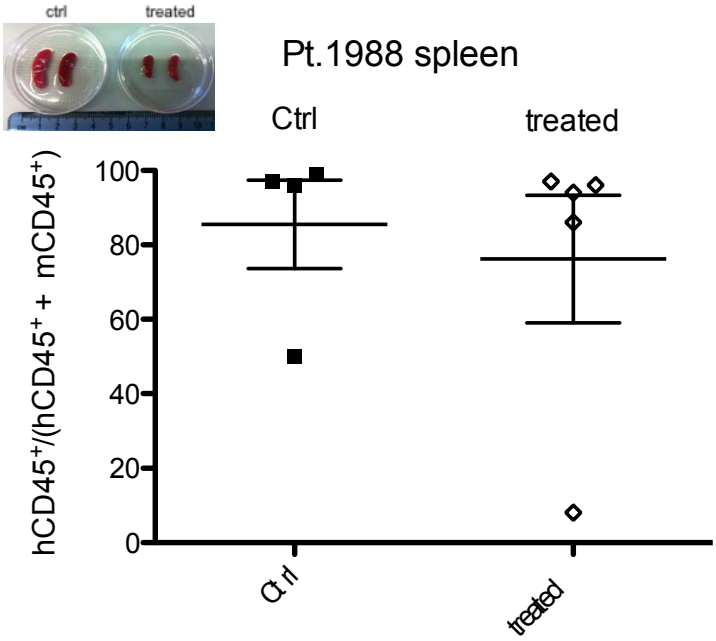

Figure 4-8: Human splenic engraftment analysis in ctrl and treated pt.1988 derived xenografts. Mice (10-16 weeks old) were inoculated with $2*10^5$ cells from pt.2278, monitored for engraftment, and treated with vincristine (0.50mg/Kg, single IP injection), and dexamethasone (6mg/L, oral, dissolved in drinking water). Plotted in scatter chart are flow cytometric engraftment data analysed as the %$hCD45^+$ cells versus total murine $mCD45^+$ plus human $hCD45^+$values for each individual mouse at the time of sacrifice, as well as groups' (4-5 mice) means (± SD).

Even though treated mice showed complete reversion of the leukaemia-associated splenomegaly, not dissimilarly to what was observed for the BM, no significant difference was detected in human splenic engraftment between control

and treated mice. We hypothesize that the physically reduced size of the spleen may therefore relate to chemotherapy-associated reduction in extramedullary haematopoiesis.

Having retrieved the samples from matching bone marrow and spleen of treatment-exposed mice, we began the process of analysis of copy number variations in TEL, AML1, PAX5 and P16 genes by mFISH. Results from a representative mouse are shown in Figure 4-9 and the results discussed here. 250 interphase nuclei of each sample were scored, revealing higher clonal complexity within the site of injection than within the spleen (12 subclones versus 7). Additionally, the complement of identified subclones was significantly different between the two sites, possibly indicating that only some of the clones engrafted in the bone marrow had the competence to also infiltrate the spleen. Consistently with this hypothesis, the two sites only shared the dominant clone (2xTEL-AML1/ 1xAML1/ 1xTEL/ 2xp16/ 2xPAX5), which carried the TEL-AML1 translocation as well the fusion reciprocal and a translocation duplication, but no other copy number variations, and one of its direct descendent subclones (2xTEL-AML1/ 1xAML-1/ 0xTEL/ 2xp16/ 2xPAX5), which additionally harboured a deletion of the second allele of TEL. The dominant clone accounted for 56.6% of leukaemic cells in the marrow and 45% in the spleen, while its evolutionary progeny represented 5.7% and 25% of BM and spleen populations respectively. All of the other subclones were site-specific and evolutionarily related to each other (with the sole exception of a clone present in 5% of the spleen population), suggesting that any possible clonal migration most likely occurred early in the engraftment history. However, it is also worth noting that, according to treatment data, chemotherapy-induced cytotoxicity in patient 1988 xenografts reached higher levels in the spleen than in the BM, possibly encouraging greater clonal complexity at this site. An

alternative interpretation is that both BM and spleen might had had the same clonal structure before treatment, but the spleen, being a more chemosensitive site, potentiated both elimination of some clones and expansion and/or generation of others. Moreover, it is worth pointing out that in these samples clones seen at below the 2% cut-off level tended to be located at the end of a putative subclonal "lineages" rather than intermediates. This may indicate that they are at low frequency either because (i) they are genuinely unique subclones that have arisen relatively late during the evolution of the leukaemia, or (Hashimoto et al.) their apparently unique and complex karyotype is partially a result of false positive signal(s). If the low frequency of these subclones were simply due to their poor engraftment then they could lie anywhere in the hierarchy. Beyond these observations only the analysis of more material from control and treated xenografts of patient1988 and full characterization of the overall complexity of this diagnostic sample will allow for the interpretation of this interesting result.

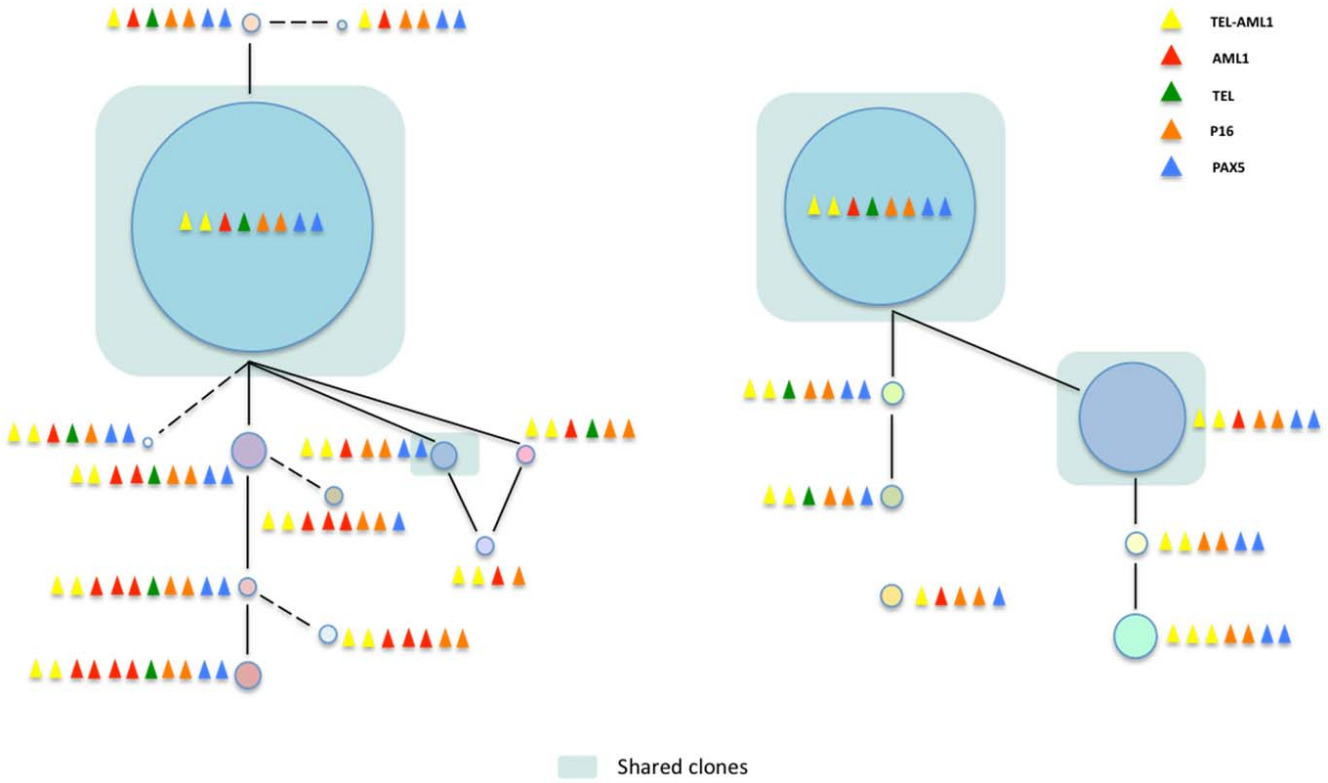

Figure 4-9: Post-treatment multiregional clonal architecture dynamics in a patient 1988–derived xenograft. Scoring for TEL-AML1 fusion and simultaneous copy CNAs involving TEL, AML1, P16 and PAX5, of matching BM (van der Weyden et al.) and spleen (bottom) sample from a mouse injected with patient 1988 diagnostic material and treated with vincristine (0.50mg/Kg, IP, single dose) and dexamethasone (6 mg/L) for 6 days. Clones with the same karyotype (as determined by FISH) are shown in the same colour in the two diagrams. Clones both above and below the cut-off level (2%) are shown. The latter are presented in circles connected with dashed lines. Phylogenetic trees were reconstructed according to the most parsimonious subclonal ancestral relationships. However these do not, in general, represent the only plausible evolutionary pathways.

Xenografts of patient 2278 proved highly resistant to treatment with standard regimen, with the mean reduction in human BM engraftment post-chemotherapy among these PDXs being only of 5% (not significant). Over the same time frame control mice developed a significant 5% increase in BM engraftment (Figure 4-10).

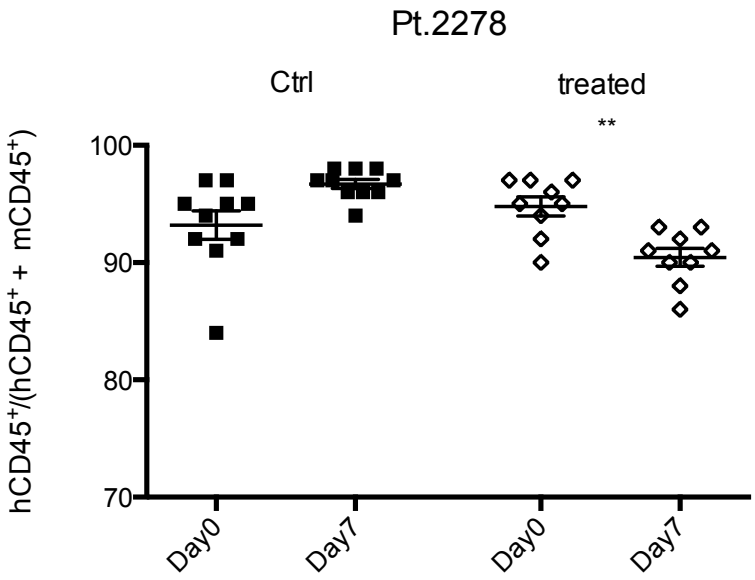

Figure 4-10: In vivo response of pt.2278 xenografts to 7 days treatment with VCR and DEX. Monitoring of pre- and post-treatment frequencies of human leukemic cells in murine BM relative to total human and mouse populations. Mice (10-16 weeks old) were inoculated with $2*10^5$ cells from pt.2278, monitored for engraftment, and treated with vincristine (0.50mg/Kg, single IP injection) and dexamethasone (6mg/L, oral, dissolved in drinking water) in combination. Each data point on the graph represents the flow cytometric evaluation of the %$hCD45^+$ cells versus total murine $mCD45^+$ and human $hCD45^+$ in the BM of individual recipient mice at the time of engraftment (Day 0) and post-treatment (Day 7). The mean (± SD) of each data set (10-9 mice per group) is also plotted.

Flow cytometric analysis of splenic engraftment also showed no significant difference between leukaemic burden in control and treated mice. However, as for

xenografts of pt.1988, visual observation confirmed post-treatment reversion of splenomegaly (Figure 4-11).

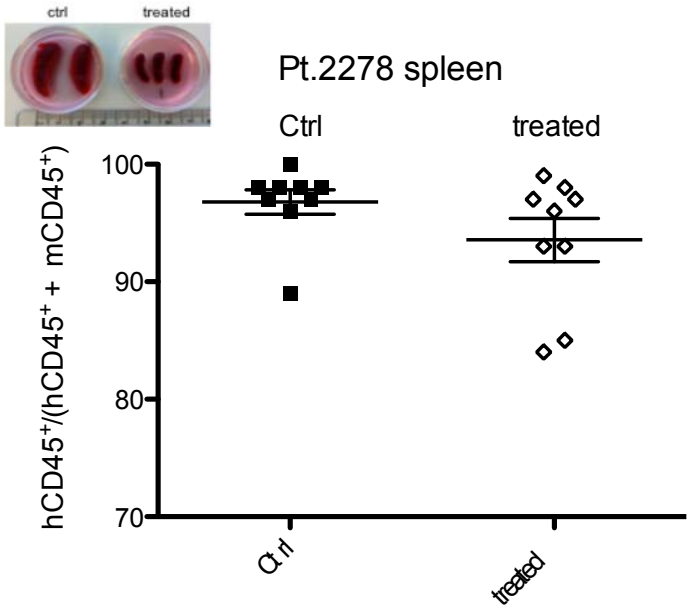

Figure 4-11: Human splenic engraftment analysis in ctrl and treated pt.2278 derived xenografts. Monitoring the leukemic burden in the spleen at engraftment and after chemotherapy. Mice (10-16 weeks old) were inoculated with $2*10^5$ cells from pt.2278, monitored for engraftment, and treated with vincristine (0.50mg/Kg, single IP injection), and dexamethasone (6mg/L, oral, dissolved in drinking water). Plotted in scatter chart are flow cytometric engraftment data analysed as the %$hCD45^+$ cells versus total murine $mCD45^+$ plus human $hCD45^+$values for each individual mouse at the time of sacrifice, as well as groups' (9 mice) means (± SD).

Examination of bone marrow aspirates of two xenografts injected with pt.2278 diagnostic material led to the observation that no fusion signal could be detected in any of the screened cells. The sample was indicated as PCR TEL-AML1 positive by the diagnostic laboratory of the hospital in which the specimen

was collected, possibly suggesting the presence of an unusual breakpoint. We however further validated the absence of the fusion using a different FISH probe (AML1 break apart Cytocell probe) and a breakpoint-specific Taqman qPCR probe (Figure 4-12).

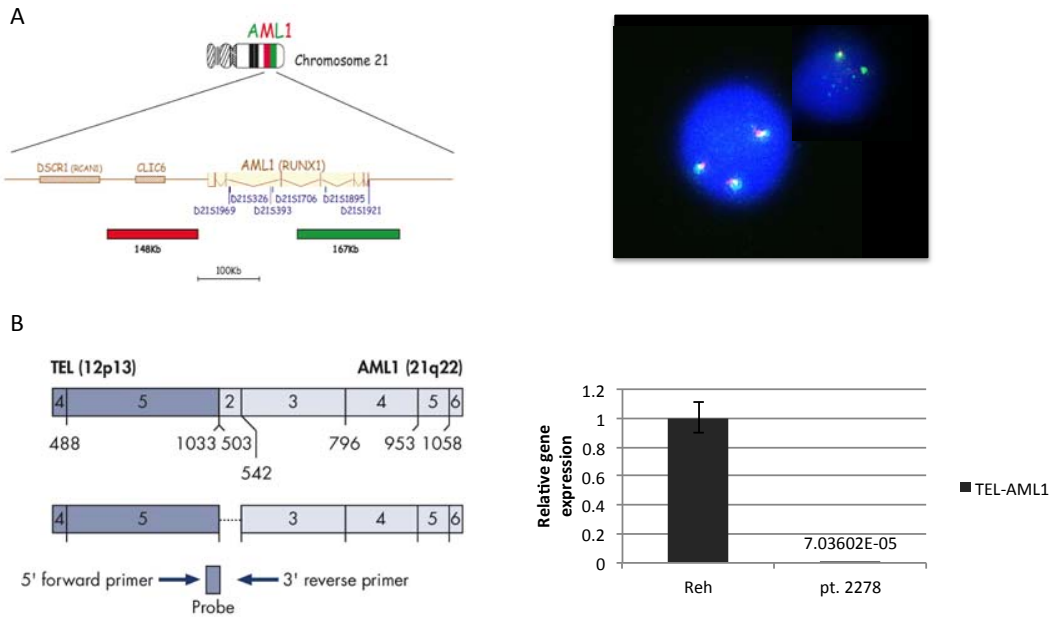

Figure 4-12: Analysis TEL-AML1 translocation status in pt.2278 BM cells. Cells were screened with A) a locus specific AML1 break apart probe, designed with two probes juxtaposed and differently labelled (orange and green) to allow the detection of any rearrangement. Normal Cell: Two green-orange (2GO) fusion signals representing the two normal AML1 loci, as in the image shown. Aberrant Cell (typical results): One green (1G), one orange (1O), and one green-orange (1GO) fusion signals, indicating a chromosome break in the AML1 locus B) Qiagen ipsogen ETV6-RUNX1 Kit designed for detection and quantification of ETV6-RUNX1 (or TEL-AML1) fusion gene transcripts in bone marrow or peripheral blood samples, relative to ABL control gene expression. Both tests proved the absence TEL-AML1 fusion gene in the analysed cell population. Genomic DNA extracted from REH cells was used as a positive control.

Nevertheless, as the fusion represents the only copy number variation shared by all the leukemic cells, we were still able investigate clonal heterogeneity in the two samples. By comparing the phylogenetic trees of the two diagnostic, pre-treatment samples (Figure 4-13), we were able to observe that all clones detected with a frequency higher than 2%, with the exception of the grey subclone in mouse 1 (2x*AML1*, 2x*TEL*, 0xp16, 0x*PAX5*) and the green subclone in mouse 2 (3x*AML1*, 2x*TEL*, 0xp16, 1x*PAX5*), were shared by both xenografts.

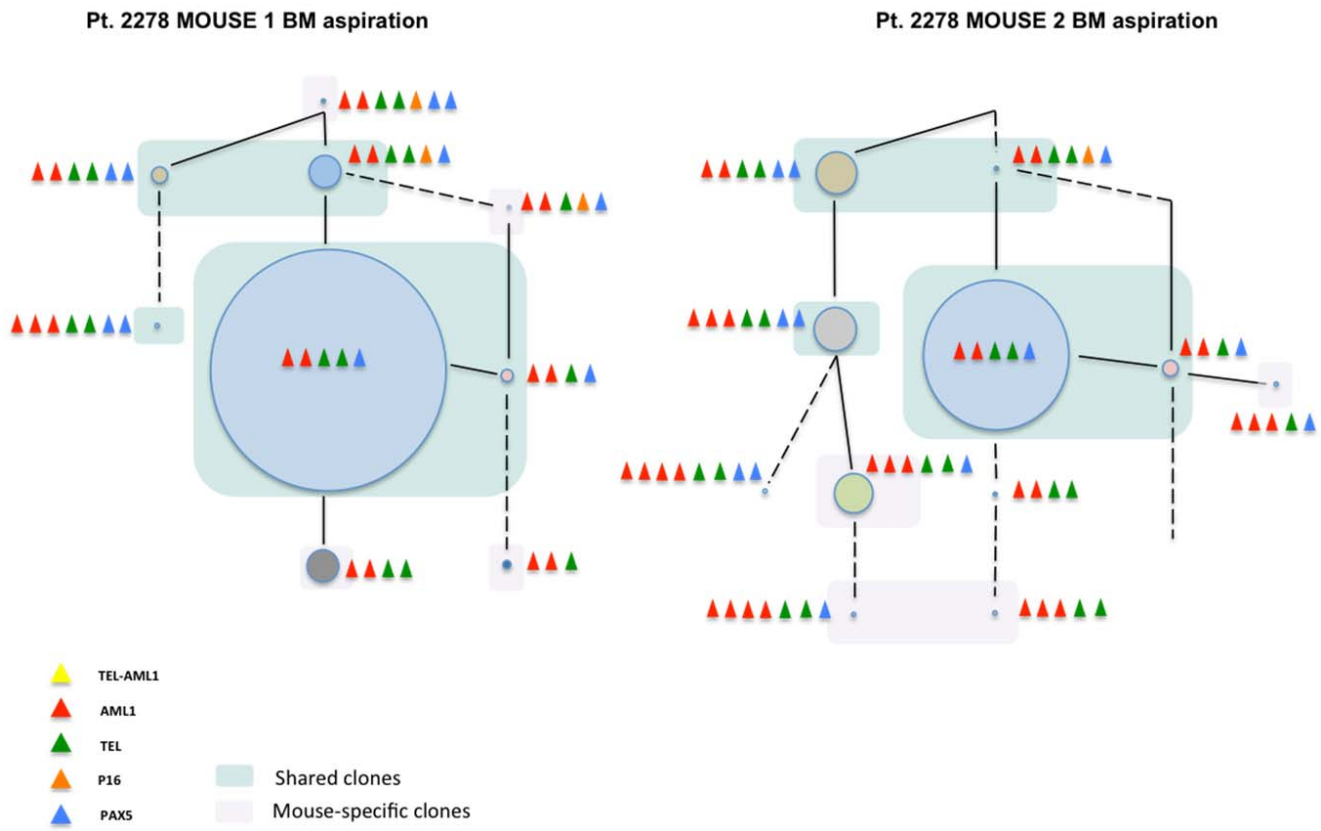

Figure 4-13: Clonal architecture variations in the BM of two mice xenografted with the same patient 2278–derived material. Scoring for TEL-AML1 fusion and simultaneous copy CNAs involving TEL, AML1, P16 and PAX5, of the bone marrow aspirates from 2 mice injected with patient 2278 diagnostic material. Clones both above and below the cut-off level (2%) are shown. Clones with the same karyotype (as determined by FISH) are shown in the same colour in the two diagrams. Presumed ancestor/intermediary clones (not detected) are presented in plain circles connected with dashed line. Phylogenetic trees were reconstructed according to the most parsimonious subclonal ancestral relationships. However these do not, in general, represent the only plausible evolutionary pathways.

This result was encouraging, and suggested that the detection of the same subclones in multiple mice injected with the same inoculum could represent additional useful criteria to determine probe significance thresholds, and thus contribute to accurate “calling” of clones. The analysis of the total bone marrow of one of the two aspirations at the end of the treatment showed signs of treatment-induced changes in clonal composition (Mouse 2; Figure 4-14). Reassuringly, all clones identified in the BM after chemotherapy were also originally detected in the bone marrow aspirates. Clones originally detected at higher frequencies persisted, although their frequencies were altered. One clone (2x*AML1*, 2x*TEL*, 0xp16, 1x*PAX5*) showed a particularly large increase in frequency, from 37.8% to 56.6%. Interestingly, the clone proposed to precede this in the original hierarchy (2x*RUNX1*, 2x*ETV6*, 1xp16, 1x*PAX5*) was not observed post-treatment, raising the possibility that the treatment provoked the loss of the single remaining p16 allele. Overall only five clones were lost, an interesting result in light of the poor drug efficacy on this leukaemia (Figure 5-10, 5-11). The majority of these clones, with the exception of two (light blue and dark purple), were previously present at a frequency lower than 2%, making it more likely that their elimination might have been stochastic. However, the survival of the two clones that originally represented only 0.5% and 1.4% of the leukemic cells, if confirmed in other treated mice, could point towards a different conclusion. A stochastic model of chemotherapy, in which the probability for minor subclones to be cleared from the tumour bulk is expected to be higher than that of more abundant clones, cannot easily be made consistent with the survival of treatment by clones present in the starting population at such low percentages.

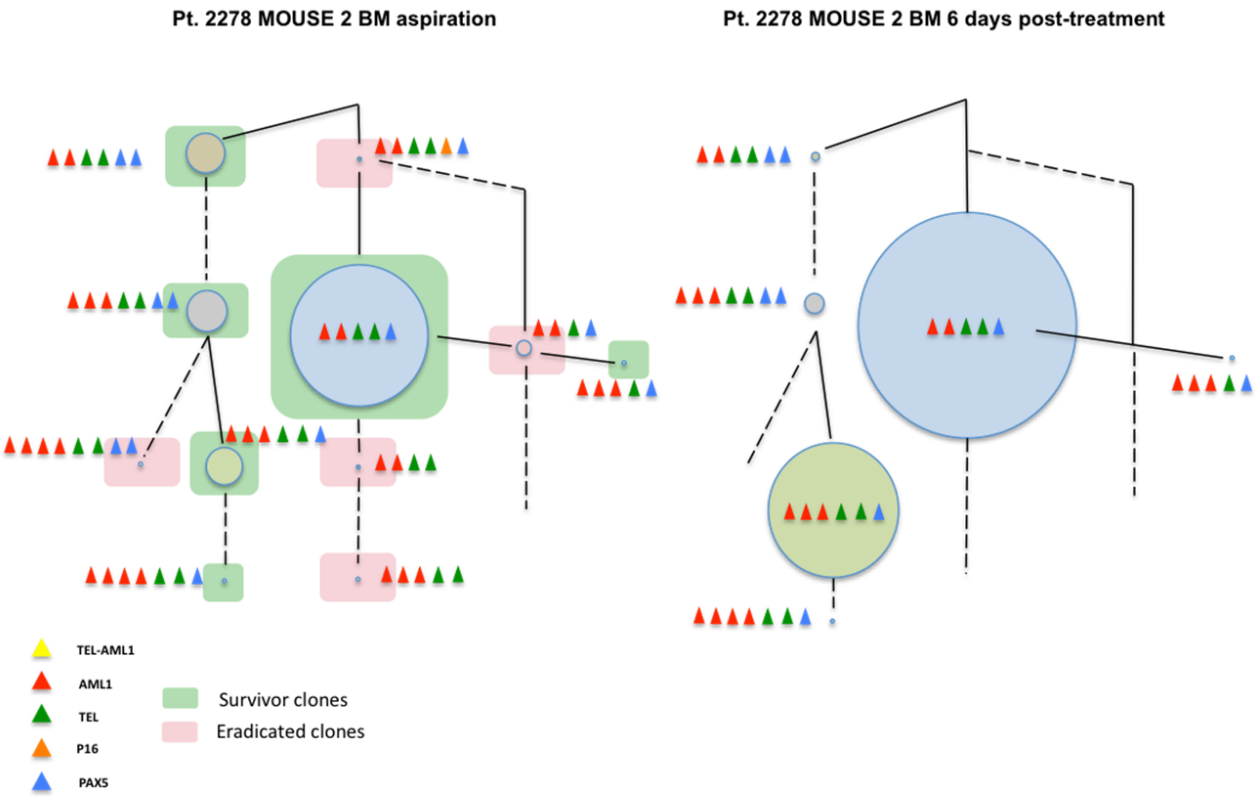

Figure 4-14: Treatment induced clonal architecture changes in a patient 2278-derived xenograft. Scoring for TEL-AML1 fusion and simultaneous copy CNAs involving TEL, AML1, P16 and PAX5, of the bone marrow aspirate (left) and post-treatment total bone marrow (right) of a mouse injected with patient 2278 diagnostic material. Clones both above and below the cut-off level (2%) are shown. Presumed ancestor/intermediary clones (not detected) are presented in plain circles with dashed lines. Phylogenetic trees were reconstructed according to the most parsimonious subclonal ancestral relationships. However these do not, in general, represent the only plausible evolutionary pathways.

4.2.2 Analysis of the leukaemia initiating properties of pt.1988 relapse and pt.2278 d8 MRD and relapse clones

Twenty-one NSG mice were sublethally irradiated and injected with $2*10^5$ cells of one of either relapse or MRD samples (7 mice each). The frequency of leukemic cells in the day 8 MRD sample of patient 2278, was previously estimated to be 1.78% in the work of a former laboratory member (by PCR analysis of the Ig rearrangements) (Lutz et al., 2013). Twelve weeks after injection engraftment levels were evaluated, and after an additional three weeks, leukemic mice were culled. Upon their collection and processing, spleen and bones were analysed by FACS, and flow sorted human cells were harvested for FISH. The engraftment levels for each mouse, as analysed by FACS, are plotted in scatter charts in figures 4-15 and 4-16.

Of the seven mice injected with patient 1988 relapse cells, only two displayed human engraftment. Interestingly, in both of these, but particularly in one, the leukemic burden in the spleen was much higher than in the bone marrow (95% versus 53%), a feature shared also by the diagnostic xenografts for this patient (see Figure 4-7 and 4-8).

All of patient 2278 xenografts were highly engrafted in both organs at the time of sacrifice, confirming the aggressiveness of this sample. At the time of bone marrow aspiration three of the seven mice injected with patient 2278 MRD cells, were highly engrafted. Three weeks later, however, one mouse still displayed high engraftment levels in the spleen only (84% spleen, 2% BM) and one displayed good BM engraftment but no human cells in the spleen (28% BM, 0%). BM engraftment of all other mice was below 10%, while two of these showed 19% and 16% human cells in the spleen respectively. It is possible that the first wave of

high engraftment had been driven by a pool of normal short-term repopulating cells still present in the bone marrow of the child undergoing treatment, underscoring the requirement for the experiment to be repeated with prior cell sorting of the leukemic cells prior to injection. Nevertheless, a limited number of human leukemic cells were sorted from the bones and spleen of injected mice, awaiting to be examined by FISH.

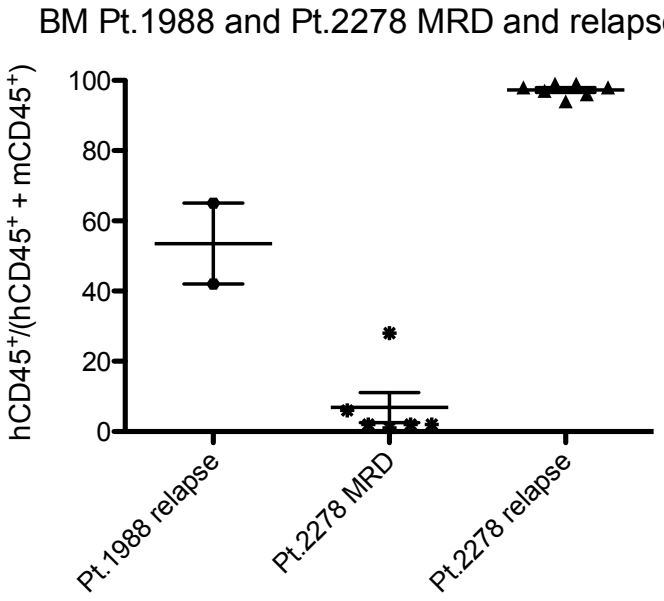

Figure 4-15: Cytometric evaluation of engraftment levels in the BM of pt.1988 relapse xenografts at the time of BM aspiration and harvesting. Mice (10-16 weeks old) were inoculated with $2*10^5$ cells from pt.1988 relapse, monitored for engraftment, and sacrificed. Flow cytometric enumerations for each individual mouse at the time of BM harvesting are shown. Data are plotted as the %$hCD45^+$ cells versus total murine $mCD45^+$ plus human $hCD45^+$.

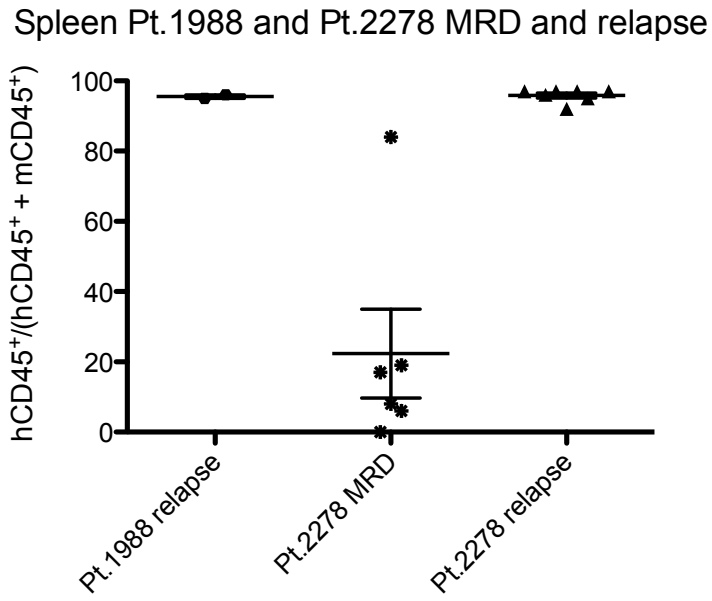

Figure 4-16: Cytometric evaluation of engraftment levels in the spleen of pt.1988 relapse xenografts at the time of BM aspiration and harvesting. Mice (10-16 weeks old) were inoculated with $2*10^5$ cells from pt.1988 relapse, monitored for engraftment, and sacrificed. Flow cytometric enumerations for each individual mouse at the time of spleen harvesting are shown. Data are plotted as the %$hCD45^+$ cells versus total murine $mCD45^+$ plus human $hCD45^+$.

4.3 Discussion

The aim of the here presented work is that of understanding whether genetically distinct subclones are also functionally different, particularly with respect to chemoresistance, thereby shedding light on the deterministic or stochastic nature of treatment survival and disease recurrence in clonally heterogeneous ALL leukaemia.

We established a mouse model that allows for the independent exposure of the same tumour to treatment multiple times and for the tracking of clonal dynamics by mean of a selected pool of genetic markers. While the analysis is still ongoing, this chapter described the successful generation of 6 xenograft models of ALL. To fully understand and characterise clonal heterogeneity and its properties in these samples, compared to the matching diagnostic specimen, multiple NSG mice were injected. Engraftment onset and levels among mice injected with different cell inoculums were highly variable but typically robust among xenografts of the same patient. Relevant to this, differences in overt leukaemia occurrence in SCID mice were previously shown to significantly correlate with patients' prognosis (Lock et al., 2002; Uckun et al., 1995). No clear explanation of this phenomenon has been proposed yet; however, through the correlation of engraftment data with mFISH results, that we will obtain from the analysis of both diagnostic and mouse material, we propose to obtain a better insight into the potential role of clonal heterogeneity. A high degree of clonal diversity correlates with increased risk of progression and therapeutic resistance in breast cancer (Michor and Polyak, 2010), a feature that has not yet been evaluated in ALL.

Upon engraftment, mice were treated with vincristine and dexamethasone. Again, in so doing, we observed large interpatient variations, as to leukemic cells clearance upon the administration of the same regimen. Mice injected with cells derived from patient 3, 7 and D were particularly sensitive to treatment with 0.50mgKg and vincristine 6 mg/L. Xenografts of patient 11 were less susceptible to the cytotoxicity induced by these drugs at these dosages, but proved highly sensitive to an escalated regimen. Finally, patient 1988 and particularly patient 2278 derived leukaemias were mostly resistant to treatment. This observation is

particularly interesting in light of the previously described statistically significant correlation between xenografts in vivo sensitivity to dexamethasone - but not vincristine - and patient outcome (Kang et al., 2007). Both patient 1988 and patient 2278 leukaemias did, in fact, in vivo relapse. In the context of the experiments here descripted, inter-xenograft variations in treatment response provide an additional opportunity for the assessment of a functional role for intratumour genetic heterogeneity in chemosensitivity/resistance. Not just through the observation of clonal disappearance kinetics within an individual heterogeneous tumour, but also, by relating information retrieved from different samples to each other; we will be able to assess the link between clonal diversity and clinically relevant features.

The analysis of clonal diversity in different organs (bone and spleen) infiltrated by the same leukaemia will provide an insight into the migration and homing habits of different clones. At the same time, and with the introduction of treatment, this might unravel the interplay between different sources of tumour heterogeneity, both genetic and microenvironmental, in determining chemoresistance. Interesting, but preliminary, data were collected assessing variations in clonal heterogeneity among geographically separated regions of the same leukaemia, mice engrafted from the same cells inoculum, and pre and post-treatment samples from the same xenograft. While the BM and spleen of the same mouse shared only the dominant clone, two individual animals xenografted with patient 2278-derived material had in common all but one of the clones that were present at a frequency of above 2%. In this scenario, chemotherapy induced cytotoxicity caused the loss of the majority of minor clones, with the only subclone above the detection threshold (3.6%, light pink) to be eliminated, being also the

only one detectable in the other pt.2278 xenograft aspiration analysed. This observation possibly suggests that engraftment potential might not necessarily correlate with chemoresistance, and, that clones with evident propagative potential, might not be equally fit to cope with the treatment generated selective pressure. By fully characterising the relative abundance of specific genetic clones in xenografts, of same or different origin, pre and post treatment, we aim to explore the genetic heterogeneity of leukaemia resistance. Given the encouraging nature of the data collected so far, it is likely that scoring of the rest of the abundant material generated with the treatment of the patient-derived xenografts, will produce the expected new precious data as to the functional relevance of intratumour genetic heterogeneity in ALL, and may ultimately contribute to improved treatment regimens.

With the aim of searching the relapsed leukaemia for the identification of those clones, or their descendants that, being less sensitive to treatment, populate the patient MRD sample and mice bone marrow. Xenografts from the relapse material of patient 2278, and, in limited number, of patient 1988 were established. The material collected from this will be analysed by mFISH, and provide useful information as to clonal dynamics of leukaemia relapse. Without pre-sorting, $2*10^5$ cells leukemic cells from patient 2278 MRD were injected in each of seven mice. Because the percentage of the leukemic cells in this bone marrow sample was previously estimated as 1.78%, each mouse should theoretically have received 3,560 leukemic cells. . The fact that most of the sacrificed mice displayed very low or no bone marrow engraftment past the 12^{th} week post-injection, suggests that the frequency of leukaemia initiating cells within this sample might be lower than 1/3,560. However, it is also possible that a longer observation time would have

produced different results. The FISH analysis of retrieved human cells from these mice will confirm whether any leukemic cell was present in low percentage.

CHAPTER 5

GENERATION OF TEL AND PAX5 LENTIVIRAL VECTORS FOR THE STUDY OF INTRACLONAL INTERACTIONS

5.1 Introduction

Clonally heterogeneous tumours can be seen, from an ecological perspective, as a mixture of distinct “species” (subclonal populations that differ in their heritable traits), sharing the same systemic environment. From this point of view, an expected feature of this coexistence is that clonal populations should inevitably be involved in interactions with the hosting environment and with each other. While the nature of these biological interactions is yet to be experimentally characterized, a range of possibilities exist; the first and most likely of which is *competition*. In an environment in which resources (oxygen, nutrients, growth factors, and space) are limited, competition between cancer subclones probably accompanies and shapes the entire tumour evolutionary process. However, as the majority of cancers never reach fixation (complete outgrowth of a single dominant clone), this process is likely limited by the heterogeneity of the tumour hosting environment itself, causing tumour cells residing in distinct areas to be exposed to different selective pressures. Additionally, *ammensalism*, or the ability of a clone to inhibit other clones while only minimally affecting its own fitness, *commensalism*, a relationship between two clones in which one of the two benefits from the other without affecting it, and *mutualism*, a form of interaction from which both parties benefit, leading to the at least temporary co-existence of clones with no clear fitness superiority, can also be hypothesized to take place within a heterogeneous tumour (Michor and Polyak, 2010). The reality of any speculated relationships between tumour cell populations, and the possible role for genetic heterogeneity in these are still awaiting verification. However, as it becomes clearer that cancer is to be viewed, from an evolutionary perspective, as an ecology of different populations in the context of their environment, preliminary data in support of the

existence of complex co-dependency relationships between subpopulations, other than competition, are also being collected (Bissonnette et al., 1992). The understanding that complex evolutionary trajectories drive cancer has important clinical implications that challenge the traditional design of cancer treatment and force us to re-evaluate the ground rules of precision medicine. As clearly showed by increasingly sophisticated cancer genomics studies, in a disease that is far from being a single entity, rather represents a collection of related disorders (intertumour heterogeneity), information on genetic lesions play an important role in defining patient prognosis and informing molecular subtype-driven targeted treatment. Molecular lesion-specific targeted treatments do in fact have the potential to greatly improve therapeutic response (e.g. in case of FIP1L1-PDGFRA eosinophilia-associated myeloproliferative disorders (Pardanani and Tefferi, 2004)). The existence of an additional dimension of intratumoural clonal heterogeneity, which on its own is likely to play a role in chemoresistance, does however suggest that in most cases it's not just the presence or absence of a mutation that should be assessed in the effort of linking somatic mutations to treatment outcome, but also its prevalence within the population. The value of this concept is clearly exemplified by the observations that in CLL the existence of a strong subclonal-driver mutation that is often likely to go undetected in canonical genomic studies, nevertheless negatively impacts clinical outcome (Landau et al., 2013), and that synthetic lethal approaches are highly effective when all cancer cells contain the targeted variation, as it is for PARP (Poly ADP-ribose polymerase) inhibitors in BRCA germline carriers (Fong et al., 2009). Altogether these observations raise the question of whether it is preferable to target genetic variations found on the "trunk" (present in all cells) or on the "branches" of the evolutionary phylogenetic tree. If intuitively the former approach would be

expected to lead to complete eradication of the disease, it is yet to be clarified whether, with the acquisition of additional “branch”-specific genetic events, cells remain addicted to the selected “trunk” target. It is likely that both strategies would prove valuable in different settings. For example, targeting “branch” mutations with the aim of promoting clonal equilibrium and discouraging the selection of more aggressive genotypes, at the expenses of maximising cell kill, might prove effective in less aggressive malignancies, such as CLL (Landau et al., 2014). However, to fully appreciate the differential effect of targeting “trunk” versus “branch” mutations, and acquire the ability to foresee and manipulate the evolutionary trajectory of an individual over treatment (anticipation-based chemotherapy), a deeper comprehension of the complex epistatic relationship linking different genetic lesions within the same population is required. To contribute to the elucidation of the dynamics of clonal interactions in childhood ALL, as part of this project we designed a functional experiment aimed at preliminarily assessing the impact of individual, variable genetic aberrations on clonal competition and co-dependency. Our approach makes complementary use of the previously established ALL xenotransplantation models and of newly generated lentiviral vectors for the genetic manipulation of selected recurrent ALL second hits.

To evaluate the impact of genetic variation on clonal hierarchies and interactions of primary leukaemia, we aimed at restoring the expression of two frequently deleted genes TEL and PAX5 *in vivo*. Overexpression vectors were generated for this purpose. Our experimental plan is to transduce primary childhood ALL cells using our vectors, followed by injection into recipient NSG mice. We hope to test whether the genetic manipulation affects tumour

engraftment properties of the leukaemia as bulk as well as of the individual clones. FACS or fluorescence microscopy will facilitate rapid identification of transduced cells on the basis of co-expression of LNGFR or GFP reporter molecules. Intratumour clonal composition will be evaluated by performing multiplex FISH on the engrafted cells. By comparing the prevalence of single clones within the leukaemia of mice injected with cells transduced with the empty vector to that of mice injected with cells carrying the gene of interest, we will be able to estimate the importance of a single gene in regulating clonal dynamics.

5.2 Results

5.2.1 Generation and validation of lentiviral vectors for overexpression of human TEL

Full length human *TEL* (*hTEL*) was amplified from hTEL cDNA IMAGE clone with primers designed according to the sequence of hTEL mRNA in three variants, either untagged or with the addition of a FLAG tag at the N- or C-terminus. Amplification products were cloned into the backbone of the lentiviral vector CSI-NGFR following an intermediate subcloning step into T-vector. The bicistronic vector allowed for the co-expression of a truncated version of the low-affinity nerve growth factor receptor (ΔLNGFR), utilized as a marker for the identification of transduced cells (Figure 5-1A). To validate the vector we transduced REH cells, a leukemic cell line derived from the peripheral blood of a patient with TEL-AML1 positive preB-ALL, which also has TEL deleted, and analysed the transduced cells by qPCR and western blot. Figure 5-1B shows mRNA expression levels for TEL, as determined by real-time q-PCR, in cells

transduced with LNGFR TEL, LNGFR FLAG TEL and LNGFR TEL FLAG vectors. Expression was extremely high both compared to the mRNA level detected in REH cells transduced with the control vectors and to those detected in JURKAT cells, a cell line endogenously expressing TEL, which we used as a control. We were able to confirm that transduction of each construct, untagged, N-terminal tagged and C-terminal tagged resulted in production of Tel protein. As figure 5-1C shows, the protein was detectable with both ∝-TEL and ∝-Flag antibodies.

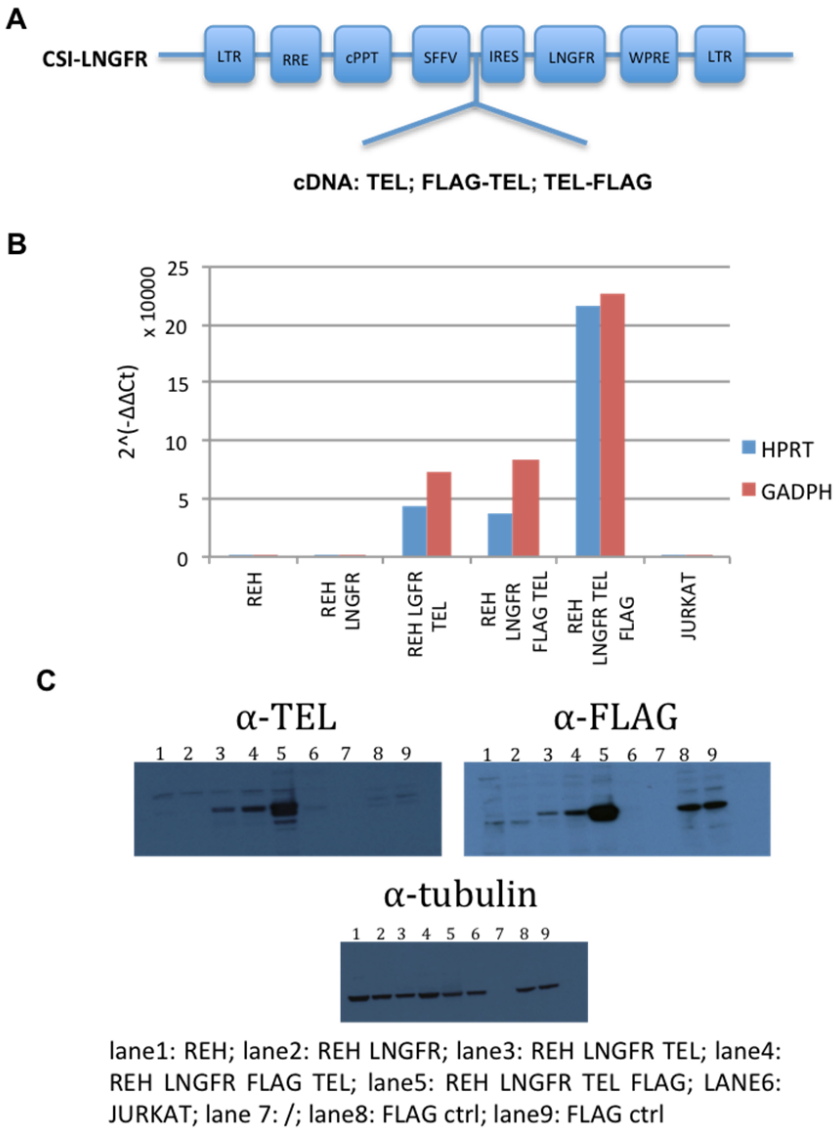

Figure 5-1: TEL overexpression vectors. A) Schematic representation of the CSI-LNGFR vector for overexpressing TEL. TEL overexpression vectors were generated in three versions: targeted with FLAG tag at the N-terminal or C-terminal of TEL sequence or not tagged at all. B) RT-PCR results confirmed TEL overexpression in REH cells transduced with TEL vectors, and showed much lower expression of the gene in REH untransduced cells, in REH cells transduced with the empty vector and in Jurkat cells. Expression relative to HPRT (violet set of data) or GAPH (purple set of data). C) Western blot confirmed TEL overexpression at the protein level in transduced REH cells.

As TEL mRNA and protein expression within the bulk populations of transduced cells was extremely high relative to the Jurkat control, particularly for LNGFR TEL FLAG vector, we tested whether it would be possible to select cells expressing it at more physiological levels. TEL is a nuclear protein, which makes sorting live cells directly on the basis of its expression problematic. However, we took advantage of the surface protein encoded by LNGFR to FACS sort cells expressing it at different levels. Through the analysis of the retrieved populations by qPCR we were able to demonstrate that LNGFR expression correlates with TEL expression at the mRNA level (Fig 5-2A). By optimizing a western blot TEL antibody for intracellular FACS analysis, we were not only able to examine TEL expression at the protein level, but were also granted a picture of its distribution across the population. This analysis showed that higher LNGFR expression corresponds to higher average TEL expression at the protein level, although all populations contained some highly expressing cells (Figure 5-2B).

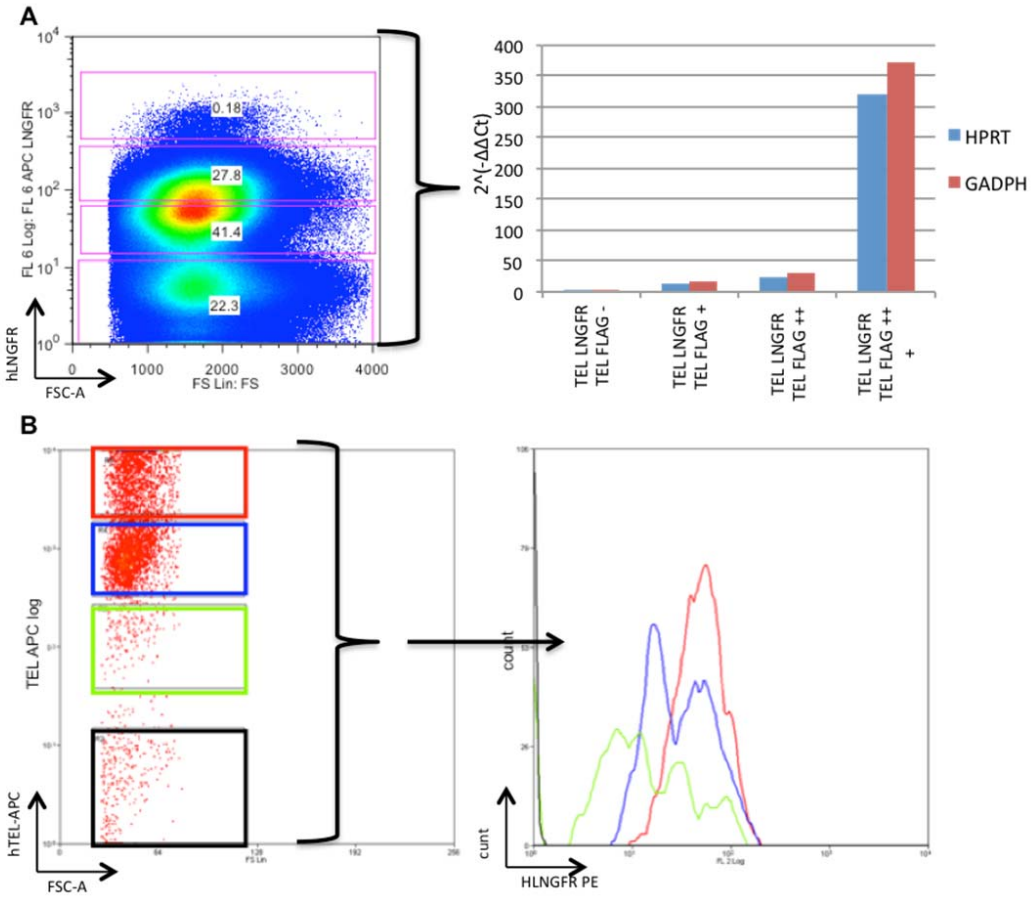

Figure 5-2: Dissection of REH cells transduced with LNGFR TEL FLAG vector. REH cells transduced with LNGFR TEL FLAG vector were sorted in four different populations on the basis of LNGFR expression A). Evaluation of TEL gene expression through qPCR was then shown to correlate with LNGFR expression determined by FACS B). REH cells transduced with LNGFR TEL FLAG vector were fixed and permeabilized in order to prepare them for intracellular staining. Cells were then stained with α-TEL Santa Cruz C-20, normally used for western blot, followed by an α-mouse APC conjugated secondary antibody. Finally cells were surface stained with α-LNGFR PE conjugated antibody. LNGFR expression was shown to correlate with TEL expression also at protein level.

5.2.2 Results: infection of patient 7 leukemic cells with CSI-LNGFR control vector and CSI-LNGFR-TEL and injection into NSG mice.

$2.5*10^6$ cells obtained from one of the previously established patient 7 xenografts were plated in equal amount in two wells of a multiwell plate. Cells of patient seven were specifically selected as the sample was previously shown to contain an almost equal load of clones deleted and non-deleted for the normal *TEL* allele (Anderson et al., 2011). Cells were then infected by spinoculation with one of the newly packaged CSI-lngfr and CSI-LNGFR-TEL-FLAG overexpression vectors (MOI 50). Over the infection period cells were mantained in SFEM medium supplemented with 20% FBS, antibiotics at standard concentrations, and cytokines (IL-7, IL3, Flt3, and SCF) (Figure 5-3). Three days after the spinfection was performed the percentage of lngfr positive cells was evaluated by flow cytometry on a small sample. Both lentiviral construsts had infected cells with high efficiency (94% CSI-lngfr and 95.3% CSI-LNGF-TEL-FLAG) (Figure5-3 A/B), confirming the high efficiency of the spinfection procedure.

Cells were then injected at $1.5*10^5$ cells per mouse into 20 sublethally irradiated NSG mice. Due to a bacterial infection that affected the majority of NSG mice hosted in the animal house during the time frame of this experiment, as many as 12 mice were culled in the early phases of the xenotransplantation procedure. Nineteen weeks post-injection surviving mice were sacrificed, and their bones and spleens were harvested. Cells were then stained and analysed by FACS for total human and $LNGFR^+$ human engraftment. Engraftment levels were highly variable within both groups, resulting in high standard variations, which reduced the statistical power of our observation of the effect of TEL-overexpression on the engraftment properties of the leukemic cells (Figure 5-3 C/D). Of note, a drop in

LNGFR expression levels compared to values recorded at the time of injection was observed for both vectors. A process of selection of the transduced cells over the transduced ones could explain this, suggesting that sorting might be required even in presence of very high transduction efficiency.

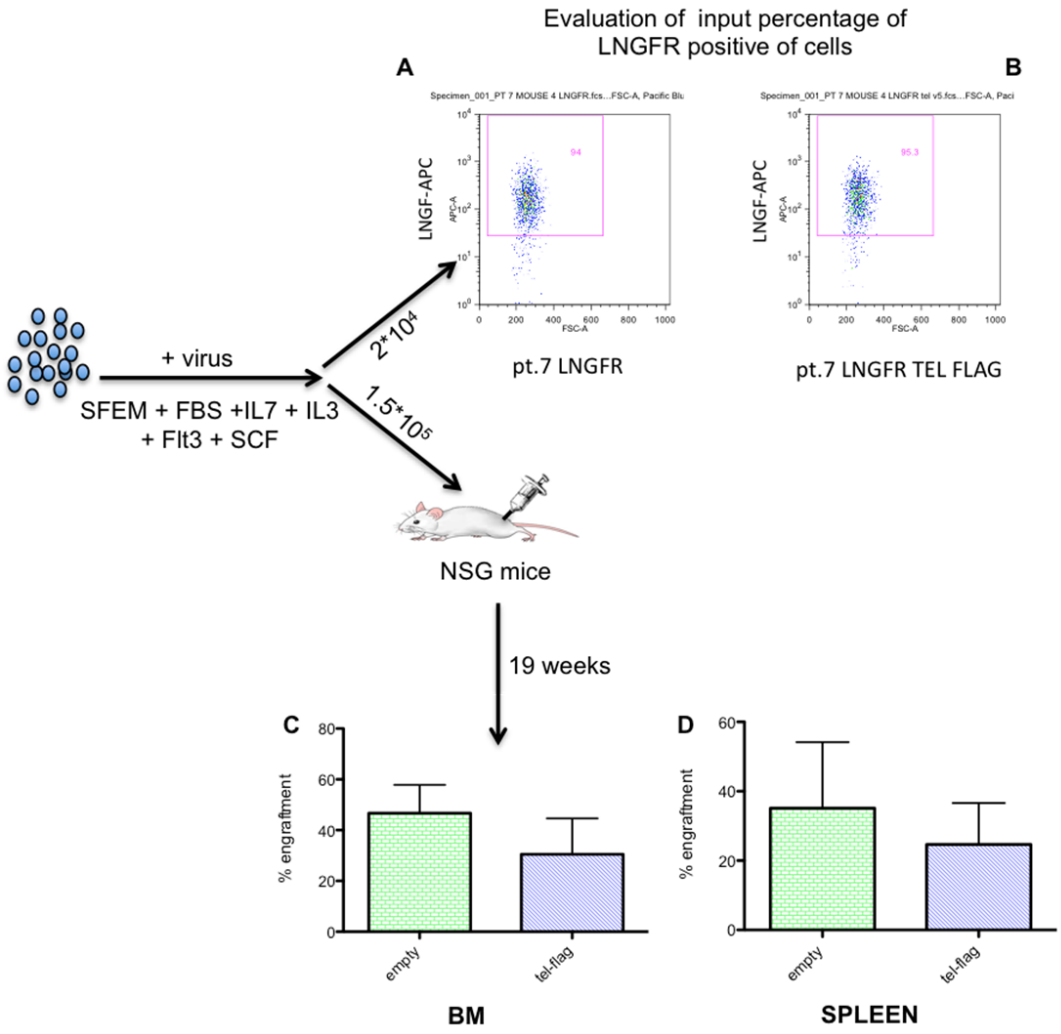

Figure 5-3: TEL overexpression in pt.7 cells and xenografts generation. Schematic representation of the experimental protocol for cells transduction and bone marrow transplantation. Transduction efficiency prior to cell injection for cells infected with (a) csi –lngfr control vector and (b) cells infected with csi-lngfr-tel-flag. (c) BM transduced cell engraftment efficiency presented as percentage of total hcd45^{+l}ngfr^{+} cells. (d) Spleen transduced cell engraftment efficiency presented as percentage of total hcd45^{+l}ngfr^{+} cells.

5.2.3 Generation and verification of lentiviral vectors for overexpression of human PAX5

Full length human *PAX5* (*hPAX5*) was amplified from a previously cloned plasmid containing the gene. Primers were designed based on the sequence of hPAX5 mRNA, and HA (hemagglutinin) tag was added either at the N- or C-terminus. Amplification products were sub-cloned into T-vector and then transferred into the lentiviral vector CSIemerald (Figure 5-4A). In this case eGFP was used as a reporter for *PAX5* expression. The transplantation results may indicate a requirement for simultaneous manipulation of more than one second hit, which will necessitate combinatorial use of the two vectors, and will be facilitated by use of a different reporter in this second construct. A T cell leukaemia cell line, JURKAT, was used to validate the expression upon transduction (Figure 5-4B). As for TEL, mRNA expression of PAX5 was validated and shown. Both constructs, N-terminal tagged and C-terminal tagged, led to the production of PAX5 protein, as detected by western blot upon hybridization with a ∝-PAX5 antibody (Fig 5-4C, upper panel). However, following the staining with a ∝-HA antibody, only the C-terminal tagged version of the protein was detectable on the membrane (Fig 5-4C, lower panel). Most likely, the tag affects the confirmation and stability of PAX5 when positioned at its N-terminus).

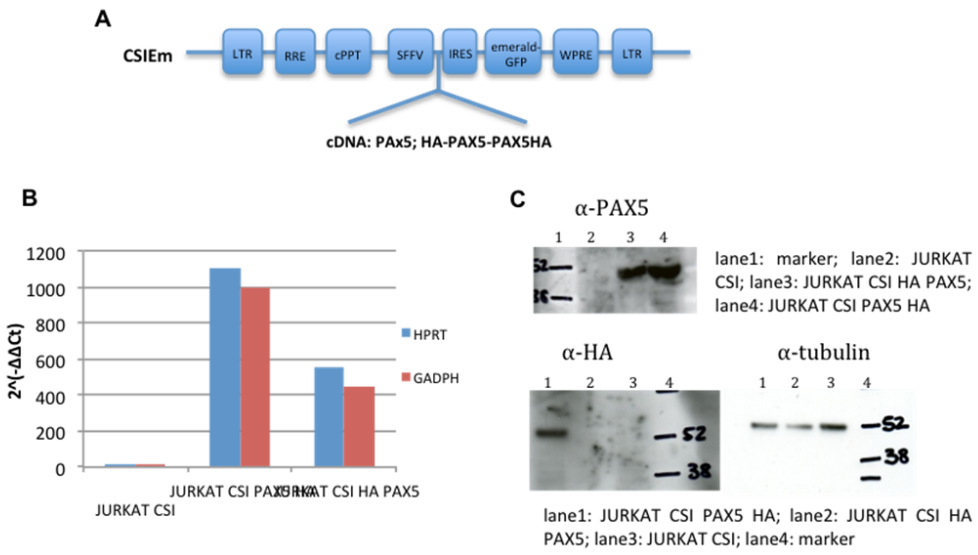

Figure 5-4: PAX5 overexpression vectors. (A) Schematic representation of the CSI-emerald vectors for PAX5 overexpression. PAX5 overexpression vectors were generated in two versions: targeted with HA at the N-terminal or at the C-terminal. (B) RT-PCR results confirmed the change in Pax5 gene expression upon transduction of JURKAT cells with each of the vectors. Expression data are normalized to HPRT (blue set of data) or GAPH (red set of data. (C) Pax5 protein was detectable by western blot upon overexpression of both constructs, however the tag was functional only when positioned at C-terminus (as the α-HA antibody did otherwise not detect it).

5.3 Discussion

We hope to gain understanding of the impact of individual genetic aberrations on clonal dynamics in childhood ALL by restoring expression of common second hit deletions in an *in vivo* model. To this end we have generated and validated a set of TEL and PAX5 overexpression vectors. As well as representing a useful tool for the study of clonal interactions in ALL, the central

interest of this thesis work, the vectors also represent a valuable asset to other investigations carried out in the laboratory.

We transduced primary ALL cells with TEL lentiviral overexpression vector to assess the effect of the restoration of *TEL* expression on the engraftment properties of leukaemic cells. Some unfortunate and unforeseeable events unrelated to the experiment drastically reduced the number of mice available for analysis and negatively impacted its statistical power. The drop in percentage of the LNGFR$^+$ human cell population, both for CSI-LNGFR and CSI-LNGFR-TEL-FLAG transduced cells, further complicated the interpretation of the results. However, the experiment was successful in that a good number of LNGFR, expressing cells were sorted from the bone marrow and spleen of engrafted mice and harvested for mFISH analysis. By comparing clonal architectures, and frequencies, in the LNGFR$^+$ population of cells transduced with either the empty vector or TEL overexpression vector, it should be possible to highlight any direct effect of *TEL* restored expression on functional behaviour (engraftment and/or migratory properties) of individual clones. Moreover we speculated that if tumours do indeed possess properties of complex ecological systems, within which cells may compete and/or cooperate with each other, then selectively hitting highly recurrent genetic lesion could reveal and affect clonal interactions that are responsible for natural leukaemia progression. As a consequence, new clonal relationships might be established that allow for previously disadvantaged clones to expand. Even though it has not yet been demonstrated, genetic diversity is likely to impact the functional properties of cells with tumour propagating properties. Whether this manifests as variations in niche occupancy, quiescence,

or drug resistance, perturbing the seemingly steady state of genetic heterogeneity of a tumour promises insight and clues of the existence of the phenomenon.

.

CHAPTER 6

FINAL REMARKS AND FUTURE PLANS

The aim of the work presented in this thesis was the establishment of an *in vivo* model for the study of functional genetic heterogeneity in TEL-AML1+ childhood ALL. This disease, like many other cancers, has recently been described as characterized by patterns of branching clonal evolution (Anderson et al., 2011). However, although genetic heterogeneity in ALL has been studied, data collected so far are limited to static snapshots of clonal diversity at a given time. Therefore, in an attempt to interrogate ALL clonal dynamics during tumour progression and treatment, and to link these to biologically relevant clonal features, we established an *in vivo* model that includes a chemotherapy induction-like regimen based on the administration of vincristine and dexamethasone. The treatment was optimized to induce good cytotoxicity in newly generated patient-derived xenografts. The treatment was included in order to induce a selective pressure that would challenge the clones' clinically important "survival" skills. Interestingly, in the model, the efficacy of the drugs in killing leukaemia cells inversely correlated with the tumour aggressiveness in the patient. Specifically, of the samples that we tested, the only two leukaemias that relapsed in human we found to be resistant to the chemotherapy in our mouse model.

While in the human a given leukaemia can only be analysed once prior to treatment and once post-treatment, often leaving data difficult to interpret given the lack of statistical power, the xenograft model offers the unique opportunity to in principle expose the same tumour to chemotherapy as many times as required to provide replicates. Enrolment of more transplanted mice into the study easily overcomes the issue that in reality not all clones contribute to tumour propagation on all occasions and in all recipients. To ensure that even clones present in the diagnostic population at a very low percentage would be represented in a number

of mice sufficient to ensure data reproducibility, we injected each sample in at least ten mice per treatment group.

Two to three samples were collected from each mouse. A snapshot of genetic heterogeneity in every xenograft was obtained prior to their assignment to a treatment group. Additionally, karyotype preparations for the examination of clonal heterogeneity were prepared from the bone marrow and the spleen of the mice at the time of sacrifice. Overall, more than 300 samples were harvested for FISH. Data as to treatment efficacy were reported in chapter 4 of this thesis. Once all FISH results are obtained, the analysis of pre- and post-treatment genetic architectures will be combined with treatment efficacy data to obtain an insight into the relationships between intratumour genetic heterogeneity in TEL-AML1 ALL and cancer treatment.

Preliminary observations obtained so far from the FISH analysis of *TEL*, *AML1,* P16 and *PAX5* genomic loci in three pairs of matching samples have already allowed for some interesting speculations. First, the longitudinal sampling of paired BM and spleen of a control mouse revealed a much higher degree of clonal diversity in the primary tumour site. The dominant clone (2xfusion, 1x*RUNX1*, 1x*ETV6*, 2x*PAX5*) (56.6% in the BM, 45% in the spleen) as well as one of its progeny subclones (2xfusion, 1x*RUNX1*, 0x*ETV6*, 2xp16, 2x*PAX5*), an intermediate subclone in the BM, which had become the second most abundant variant in the spleen (25 %), were the only two shared variants. The fact that no other subclone was detected in both sites could be due to (i) the early migration of the aggressive dominant BM clone/s to the spleen, followed by its further genetic differentiation within the new environment, or (Hashimoto et al.) to the weaker treatment protection offered to clones by the splenic microenvironment. It was also

particularly interesting to find in the spleen, but not in the BM, 4 clones (out of 7), with frequency between 5-10%, carrying the deletion of the non-rearranged allele of Aml1. This genetic lesion represents a highly uncommon feature for to this leukaemia.

Analysis of bone marrow aspirates from two mice injected with a sample from patient 2278 showed that 5 clones were shared by both xenografts. Even though these variants repopulated the marrow of both xenografts, their frequencies tended to vary between the two. For example the dominant clone (2x*RUNX1*, 2x*ETV6*, 1xp16, 1x*PAX5*) in the BM marrow of a mouse (61.7%) represented only 33.3% of the total leukemic cells of a second mouse. Moreover, in this second xenograft a novel clone of almost identical frequency was identified (3x*RUNX1*, 2x*ETV6*, 0xp16, 1x*PAX5*). This clone was absent from mouse 2, and appeared to be a direct evolutionary product of the first one (gain of an additional copy of Runx1).

Analysis of the matching pre- and post-treatment material of a xenograft injected with cells from patient 2278 showed that the majority of clones lost over treatment represented variants detected in the population at frequencies below probes' cut-off levels. However, a clone sitting early in the branching evolution tree, and with the estimated 3.6% frequency (2x*RUNX1*, 0x*ETV6*, 0xp16, 1x*PAX5*), was also cleared from the leukaemia. In contrast, a different subclone, positioned at the bottom of the phylogenetic tree, survived treatment, even though it only represented 0.5% of the tumour. Although these data are awaiting validation, they point in the direction of the possibility that the genetic identities of clones partake in determining resistance to treatment. This is particularly likely in light of the fact that pt.1988 and 2278 were previously validated as poor

responders to chemotherapy. We are optimistic that the scoring of multiple xenografts injected with the same cell inoculums and exposed to the same treatment will, in a continuation of the presented project, allow for the identification of reiterative clonal behaviours relevant to critical features of tumour biology (like aggressiveness and tumour resistance).

Additionally, the genetic manipulation of recurrent genetic lesions in TEL-AML1 ALL (second hits) represents an opportunity to perturb clonal interactions that might be responsible for the hierarchical organisation of clones within the tumour. For this purpose TEL and PAX5 overexpression vectors were successfully generated. TEL vectors were then used to restore the expression of the gene in cells of patient 7 retrieved from primary xenografts. *TEL* overexpression did not affect the growth properties of the cells overall, as these were still able to engraft mice. Transduced cells were therefore sorted and harvested for FISH. The evaluation of the effects of the overexpression on clonal hierarchies remains to be completed. As loss of the non-rearranged *TEL* allele represents the most frequent second hit of the leukaemia, often involving a high percentage of cells within the tumour, restoring its expression within the leukemic population might be expected to affect clonal competition.

Overall the thesis work presented here reports the successful establishment of an *in vivo* model for the study of clonal dynamics of TEL-AML1+ ALL in response to chemotherapy-induced selective pressure. Additionally the model has also been adapted to study the effect of genetic manipulation of clonal populations on interclonal relationships.

The feasibility and potential of the study has been demonstrated by the collection of preliminary results obtained from the analysis of paired longitudinal

and treatment spanning samples. We are confident that the tools generated here will contribute to the characterization of the role of genetic heterogeneity in clonal dynamics, providing important insights into their relevance to the treatment of leukaemia.

REFERENCES

Adams, G.B., Chabner, K.T., Alley, I.R., Olson, D.P., Szczepiorkowski, Z.M., Poznansky, M.C., Kos, C.H., Pollak, M.R., Brown, E.M., and Scadden, D.T. (2006). Stem cell engraftment at the endosteal niche is specified by the calcium-sensing receptor. Nature *439*, 599-603.

Adolfsson, J., Mansson, R., Buza-Vidas, N., Hultquist, A., Liuba, K., Jensen, C.T., Bryder, D., Yang, L., Borge, O.J., Thoren, L.A.*, et al.* (2005). Identification of Flt3+ lympho-myeloid stem cells lacking erythro-megakaryocytic potential a revised road map for adult blood lineage commitment. Cell *121*, 295-306.

Aguiar, R.C., Sohal, J., van Rhee, F., Carapeti, M., Franklin, I.M., Goldstone, A.H., Goldman, J.M., and Cross, N.C. (1996). TEL-AML1 fusion in acute lymphoblastic leukaemia of adults. M.R.C. Adult Leukaemia Working Party. British journal of haematology *95*, 673-677.

Al-Shehhi, H., Konn, Z.J., Schwab, C.J., Erhorn, A., Barber, K.E., Wright, S.L., Gabriel, A.S., Harrison, C.J., and Moorman, A.V. (2013). Abnormalities of the der(12)t(12;21) in ETV6-RUNX1 acute lymphoblastic leukemia. Genes, chromosomes & cancer *52*, 202-213.

Almendro, V., Cheng, Y.K., Randles, A., Itzkovitz, S., Marusyk, A., Ametller, E., Gonzalez-Farre, X., Munoz, M., Russnes, H.G., Helland, A.*, et al.* (2014a). Inference of Tumor Evolution during Chemotherapy by Computational Modeling and In Situ Analysis of Genetic and Phenotypic Cellular Diversity. Cell reports *6*, 514-527.

Almendro, V., Kim, H.J., Cheng, Y.K., Gonen, M., Itzkovitz, S., Argani, P., van Oudenaarden, A., Sukumar, S., Michor, F., and Polyak, K. (2014b). Genetic and phenotypic diversity in breast tumor metastases. Cancer research *74*, 1338-1348.

Almendro, V., Marusyk, A., and Polyak, K. (2013). Cellular heterogeneity and molecular evolution in cancer. Annual review of pathology *8*, 277-302.

Amsellem, S., Pflumio, F., Bardinet, D., Izac, B., Charneau, P., Romeo, P.H., Dubart-Kupperschmitt, A., and Fichelson, S. (2003). Ex vivo expansion of human hematopoietic stem cells by direct delivery of the HOXB4 homeoprotein. Nature medicine *9*, 1423-1427.

Anderson, K., Lutz, C., van Delft, F.W., Bateman, C.M., Guo, Y., Colman, S.M., Kempski, H., Moorman, A.V., Titley, I., Swansbury, J.*, et al.* (2011). Genetic variegation of clonal architecture and propagating cells in leukaemia. Nature *469*, 356-361.

Andreasson, P., Schwaller, J., Anastasiadou, E., Aster, J., and Gilliland, D.G. (2001). The expression of ETV6/CBFA2 (TEL/AML1) is not sufficient for the transformation of hematopoietic cell lines in vitro or the induction of hematologic disease in vivo. Cancer genetics and cytogenetics *130*, 93-104.

Anjos-Afonso, F., Currie, E., Palmer, H.G., Foster, K.E., Taussig, D.C., and Bonnet, D. (2013). CD34(-) Cells at the Apex of the Human Hematopoietic Stem Cell Hierarchy Have Distinctive Cellular and Molecular Signatures. Cell stem cell *13*, 161-174.

Antonchuk, J., Sauvageau, G., and Humphries, R.K. (2002). HOXB4-induced expansion of adult hematopoietic stem cells ex vivo. Cell *109*, 39-45.

Ashworth, A., Lord, C.J., and Reis-Filho, J.S. (2011). Genetic interactions in cancer progression and treatment. Cell *145*, 30-38.

Attarbaschi, A., Mann, G., Konig, M., Dworzak, M.N., Trebo, M.M., Muhlegger, N., Gadner, H., Haas, O.A., and Austrian Berlin-Frankfurt-Munster cooperative study, g. (2004). Incidence and relevance of secondary chromosome abnormalities in childhood TEL/AML1+ acute lymphoblastic leukemia: an interphase FISH analysis. Leukemia *18*, 1611-1616.

Bateman, C.M., Colman, S.M., Chaplin, T., Young, B.D., Eden, T.O., Bhakta, M., Gratias, E.J., van Wering, E.R., Cazzaniga, G., Harrison, C.J*., et al.* (2010). Acquisition of genome-wide copy number alterations in monozygotic twins with acute lymphoblastic leukemia. Blood *115*, 3553-3558.

Baum, C.M., Weissman, I.L., Tsukamoto, A.S., Buckle, A.M., and Peault, B. (1992). Isolation of a candidate human hematopoietic stem-cell population. Proceedings of the National Academy of Sciences of the United States of America *89*, 2804-2808.

Bernardin, F., Yang, Y., Cleaves, R., Zahurak, M., Cheng, L., Civin, C.I., and Friedman, A.D. (2002). TEL-AML1, expressed from t(12;21) in human acute lymphocytic leukemia, induces acute leukemia in mice. Cancer research *62*, 3904-3908.

Bissonnette, R.P., Echeverri, F., Mahboubi, A., and Green, D.R. (1992). Apoptotic cell death induced by c-myc is inhibited by bcl-2. Nature *359*, 552-554.

Boily, G., Larose, J., Langlois, S., and Sinnett, D. (2007). Identification of transcripts modulated by ETV6 expression. Br J Haematol *136*, 48-62.

Borkhardt, A., Cazzaniga, G., Viehmann, S., Valsecchi, M.G., Ludwig, W.D., Burci, L., Mangioni, S., Schrappe, M., Riehm, H., Lampert, F*., et al.* (1997). Incidence and clinical relevance of TEL/AML1 fusion genes in children with acute lymphoblastic leukemia enrolled in the German and Italian multicenter therapy trials. Associazione Italiana Ematologia Oncologia Pediatrica and the Berlin-Frankfurt-Munster Study Group. Blood *90*, 571-577.

Boulos, N., Mulder, H.L., Calabrese, C.R., Morrison, J.B., Rehg, J.E., Relling, M.V., Sherr, C.J., and Williams, R.T. (2011). Chemotherapeutic agents circumvent emergence of dasatinib-resistant BCR-ABL kinase mutations in a precise mouse model of Philadelphia chromosome-positive acute lymphoblastic leukemia. Blood *117*, 3585-3595.

Bozic, I., Antal, T., Ohtsuki, H., Carter, H., Kim, D., Chen, S., Karchin, R., Kinzler, K.W., Vogelstein, B., and Nowak, M.A. (2010). Accumulation of driver and passenger mutations during tumor progression. Proceedings of the National Academy of Sciences of the United States of America *107*, 18545-18550.

Buffler, P.A., Kwan, M.L., Reynolds, P., and Urayama, K.Y. (2005). Environmental and genetic risk factors for childhood leukemia: appraising the evidence. Cancer investigation *23*, 60-75.
Burns, C.E., Traver, D., Mayhall, E., Shepard, J.L., and Zon, L.I. (2005). Hematopoietic stem cell fate is established by the Notch-Runx pathway. Genes & development *19*, 2331-2342.

Burrell, R.A., McGranahan, N., Bartek, J., and Swanton, C. (2013). The causes and consequences of genetic heterogeneity in cancer evolution. Nature *501*, 338-345.

Buske, C., Feuring-Buske, M., Abramovich, C., Spiekermann, K., Eaves, C.J., Coulombel, L., Sauvageau, G., Hogge, D.E., and Humphries, R.K. (2002). Deregulated expression of HOXB4 enhances the primitive growth activity of human hematopoietic cells. Blood *100*, 862-868.

Busslinger, M. (2004). Transcriptional control of early B cell development. Annual review of immunology *22*, 55-79.

Buza-Vidas, N., Woll, P., Hultquist, A., Duarte, S., Lutteropp, M., Bouriez-Jones, T., Ferry, H., Luc, S., and Jacobsen, S.E. (2011). FLT3 expression initiates in fully multipotent mouse hematopoietic progenitor cells. Blood *118*, 1544-1548.

Calvi, L.M., Adams, G.B., Weibrecht, K.W., Weber, J.M., Olson, D.P., Knight, M.C., Martin, R.P., Schipani, E., Divieti, P., Bringhurst, F.R.*, et al.* (2003). Osteoblastic cells regulate the haematopoietic stem cell niche. Nature *425*, 841-846.

Campbell, P.J., Yachida, S., Mudie, L.J., Stephens, P.J., Pleasance, E.D., Stebbings, L.A., Morsberger, L.A., Latimer, C., McLaren, S., Lin, M.L.*, et al.* (2010). The patterns and dynamics of genomic instability in metastatic pancreatic cancer. Nature *467*, 1109-1113.

Cantor, A.B., and Orkin, S.H. (2001). Hematopoietic development: a balancing act. Current opinion in genetics & development *11*, 513-519.

Cao, X., Littlejohn, J., Rodarte, C., Zhang, L., Martino, B., Rascoe, P., Hamid, K., Jupiter, D., and Smythe, W.R. (2009). Up-regulation of Bcl-xl by hepatocyte growth factor in human mesothelioma cells involves ETS transcription factors. Am J Pathol *175*, 2207-2216.

Chaffer, C.L., Brueckmann, I., Scheel, C., Kaestli, A.J., Wiggins, P.A., Rodrigues, L.O., Brooks, M., Reinhardt, F., Su, Y., Polyak, K.*, et al.* (2011). Normal and neoplastic nonstem cells can spontaneously convert to a stem-like state. Proceedings of the National Academy of Sciences of the United States of America *108*, 7950-7955.

Chakrabarti, S.R., and Nucifora, G. (1999). The leukemia-associated gene TEL encodes a transcription repressor which associates with SMRT and mSin3A. Biochemical and biophysical research communications *264*, 871-877.

Chakrabarti, S.R., Sood, R., Nandi, S., and Nucifora, G. (2000). Posttranslational modification of TEL and TEL/AML1 by SUMO-1 and cell-cycle-dependent assembly into nuclear bodies. Proceedings of the National Academy of Sciences of the United States of America *97*, 13281-13285.

Chen, C., Liu, Y., Liu, Y., and Zheng, P. (2009). mTOR regulation and therapeutic rejuvenation of aging hematopoietic stem cells. Science signaling *2*, ra75.
Chen, J., Odenike, O., and Rowley, J.D. (2010). Leukaemogenesis: more than mutant genes. Nature reviews Cancer *10*, 23-36.

Cicalese, A., Bonizzi, G., Pasi, C.E., Faretta, M., Ronzoni, S., Giulini, B., Brisken, C., Minucci, S., Di Fiore, P.P., and Pelicci, P.G. (2009). The tumor suppressor p53 regulates polarity of self-renewing divisions in mammary stem cells. Cell *138*, 1083-1095.

Clappier, E., Gerby, B., Sigaux, F., Delord, M., Touzri, F., Hernandez, L., Ballerini, P., Baruchel, A., Pflumio, F., and Soulier, J. (2011). Clonal selection in xenografted human T cell acute lymphoblastic leukemia recapitulates gain of malignancy at relapse. The Journal of experimental medicine *208*, 653-661.

Cobaleda, C., Gutierrez-Cianca, N., Perez-Losada, J., Flores, T., Garcia-Sanz, R., Gonzalez, M., and Sanchez-Garcia, I. (2000). A primitive hematopoietic cell is the target for the leukemic transformation in human philadelphia-positive acute lymphoblastic leukemia. Blood *95*, 1007-1013.

Cobaleda, C., Schebesta, A., Delogu, A., and Busslinger, M. (2007). Pax5: the guardian of B cell identity and function. Nat Immunol *8*, 463-470.

Corsetti, M.T., and Calabi, F. (1997). Lineage- and stage-specific expression of runt box polypeptides in primitive and definitive hematopoiesis. Blood *89*, 2359-2368.

Cox, C.V., Evely, R.S., Oakhill, A., Pamphilon, D.H., Goulden, N.J., and Blair, A. (2004). Characterization of acute lymphoblastic leukemia progenitor cells. Blood *104*, 2919-2925.

DeKoter, R.P., Lee, H.J., and Singh, H. (2002). PU.1 regulates expression of the interleukin-7 receptor in lymphoid progenitors. Immunity *16*, 297-309.

DeKoter, R.P., and Singh, H. (2000). Regulation of B lymphocyte and macrophage development by graded expression of PU.1. Science *288*, 1439-1441.

Dias, S., Mansson, R., Gurbuxani, S., Sigvardsson, M., and Kee, B.L. (2008). E2A proteins promote development of lymphoid-primed multipotent progenitors. Immunity *29*, 217-227.

Dieterlen-Lievre, F., and Martin, C. (1981). Diffuse intraembryonic hemopoiesis in normal and chimeric avian development. Developmental biology *88*, 180-191.

Ding, L., Ley, T.J., Larson, D.E., Miller, C.A., Koboldt, D.C., Welch, J.S., Ritchey, J.K., Young, M.A., Lamprecht, T., McLellan, M.D.*, et al.* (2012). Clonal evolution in relapsed acute myeloid leukaemia revealed by whole-genome sequencing. Nature *481*, 506-510.

Ding, Y., de Wet, J.R., Cavalcoli, J., Li, S., Greshock, T.J., Miller, K.A., Finefield, J.M., Sunderhaus, J.D., McAfoos, T.J., Tsukamoto, S.*, et al.* (2010). Genome-based characterization of two prenylation steps in the assembly of the stephacidin and notoamide anticancer agents in a marine-derived Aspergillus sp. Journal of the American Chemical Society *132*, 12733-12740.

Doulatov, S., Notta, F., Laurenti, E., and Dick, J.E. (2012). Hematopoiesis: a human perspective. Cell stem cell *10*, 120-136.

Duran-Struuck, R., and Dysko, R.C. (2009). Principles of bone marrow transplantation (BMT): providing optimal veterinary and husbandry care to irradiated mice in BMT studies. Journal of the American Association for Laboratory Animal Science : JAALAS *48*, 11-22.

Dzierzak, E., and Medvinsky, A. (1995). Mouse embryonic hematopoiesis. Trends in genetics : TIG *11*, 359-366.

Estlin, E.J., Ronghe, M., Burke, G.A., and Yule, S.M. (2000). The clinical and cellular pharmacology of vincristine, corticosteroids, L-asparaginase, anthracyclines and cyclophosphamide in relation to childhood acute lymphoblastic leukaemia. British journal of haematology *110*, 780-790.

Fears, S., Gavin, M., Zhang, D.E., Hetherington, C., Ben-David, Y., Rowley, J.D., and Nucifora, G. (1997). Functional characterization of ETV6 and ETV6/CBFA2 in the regulation of the MCSFR

proximal promoter. Proceedings of the National Academy of Sciences of the United States of America *94*, 1949-1954.

Fenrick, R., Wang, L., Nip, J., Amann, J.M., Rooney, R.J., Walker-Daniels, J., Crawford, H.C., Hulboy, D.L., Kinch, M.S., Matrisian, L.M*., et al.* (2000). TEL, a putative tumor suppressor, modulates cell growth and cell morphology of ras-transformed cells while repressing the transcription of stromelysin-1. Mol Cell Biol *20*, 5828-5839.

Firat, H., Favier, R., Adam, M., Leverger, G., Landman-Parker, J., Cayre, Y., and Douay, L. (2001). Determination of myeloid antigen expression on childhood acute lymphoblastic leukaemia cells: discrepancies using different monoclonal antibody clones. Leukemia & lymphoma *42*, 75-82.

Fischer, M., Schwieger, M., Horn, S., Niebuhr, B., Ford, A., Roscher, S., Bergholz, U., Greaves, M., Lohler, J., and Stocking, C. (2005). Defining the oncogenic function of the TEL/AML1 (ETV6/RUNX1) fusion protein in a mouse model. Oncogene *24*, 7579-7591.

Fong, P.C., Boss, D.S., Yap, T.A., Tutt, A., Wu, P., Mergui-Roelvink, M., Mortimer, P., Swaisland, H., Lau, A., O'Connor, M.J*., et al.* (2009). Inhibition of poly(ADP-ribose) polymerase in tumors from BRCA mutation carriers. N Engl J Med *361*, 123-134.

Ford, A.M., Bennett, C.A., Price, C.M., Bruin, M.C., Van Wering, E.R., and Greaves, M. (1998). Fetal origins of the TEL-AML1 fusion gene in identical twins with leukemia. Proceedings of the National Academy of Sciences of the United States of America *95*, 4584-4588.

Ford, A.M., Palmi, C., Bueno, C., Hong, D., Cardus, P., Knight, D., Cazzaniga, G., Enver, T., and Greaves, M. (2009). The TEL-AML1 leukemia fusion gene dysregulates the TGF-beta pathway in early B lineage progenitor cells. The Journal of clinical investigation *119*, 826-836.

Fuka, G., Kantner, H.P., Grausenburger, R., Inthal, A., Bauer, E., Krapf, G., Kaindl, U., Kauer, M., Dworzak, M.N., Stoiber, D*., et al.* (2012). Silencing of ETV6/RUNX1 abrogates PI3K/AKT/mTOR signaling and impairs reconstitution of leukemia in xenografts. Leukemia *26*, 927-933.
Fuka, G., Kauer, M., Kofler, R., Haas, O.A., and Panzer-Grumayer, R. (2011). The leukemia-specific fusion gene ETV6/RUNX1 perturbs distinct key biological functions primarily by gene repression. PloS one *6*, e26348.

Fuxa, M., and Busslinger, M. (2007). Reporter gene insertions reveal a strictly B lymphoid-specific expression pattern of Pax5 in support of its B cell identity function. J Immunol *178*, 8222-8228.

Georgopoulos, K., Bigby, M., Wang, J.H., Molnar, A., Wu, P., Winandy, S., and Sharpe, A. (1994). The Ikaros gene is required for the development of all lymphoid lineages. Cell *79*, 143-156.

Gerlinger, M., Rowan, A.J., Horswell, S., Larkin, J., Endesfelder, D., Gronroos, E., Martinez, P., Matthews, N., Stewart, A., Tarpey, P*., et al.* (2012). Intratumor heterogeneity and branched evolution revealed by multiregion sequencing. N Engl J Med *366*, 883-892.

Greaves, M. (2006a). The causation of childhood leukemia: a paradox of progress? Discovery medicine *6*, 24-28.

Greaves, M. (2006b). Infection, immune responses and the aetiology of childhood leukaemia. Nature reviews Cancer *6*, 193-203.

Greaves, M. (2010). Cancer stem cells: back to Darwin? Seminars in cancer biology *20*, 65-70.

Greaves, M., and Maley, C.C. (2012). Clonal evolution in cancer. Nature *481*, 306-313.

Greaves, M.F., Maia, A.T., Wiemels, J.L., and Ford, A.M. (2003). Leukemia in twins: lessons in natural history. Blood *102*, 2321-2333.

Gruver-Yates, A.L., Quinn, M.A., and Cidlowski, J.A. (2014). Analysis of glucocorticoid receptors and their apoptotic response to dexamethasone in male murine B cells during development. Endocrinology *155*, 463-474.

Hanahan, D., and Weinberg, R.A. (2011). Hallmarks of cancer: the next generation. Cell *144*, 646-674.

Harris, N.L., Jaffe, E.S., Diebold, J., Flandrin, G., Muller-Hermelink, H.K., Vardiman, J., Lister, T.A., and Bloomfield, C.D. (1999). World Health Organization classification of neoplastic diseases of the hematopoietic and lymphoid tissues: report of the Clinical Advisory Committee meeting-Airlie House, Virginia, November 1997. Journal of clinical oncology : official journal of the American Society of Clinical Oncology *17*, 3835-3849.

Hashimoto, M., Shahdat, M.H., Shimada, T., Yamasaki, H., Fujii, Y., Ishibashi, Y., and Shido, O. (2001). Relationship between age-related increases in rat liver lipid peroxidation and bile canalicular plasma membrane fluidity. Experimental gerontology *37*, 89-97.

Heerema, N.A., Sather, H.N., Sensel, M.G., Liu-Mares, W., Lange, B.J., Bostrom, B.C., Nachman, J.B., Steinherz, P.G., Hutchinson, R., Gaynon, P.S*., et al.* (1999). Association of chromosome arm 9p abnormalities with adverse risk in childhood acute lymphoblastic leukemia: A report from the Children's Cancer Group. Blood *94*, 1537-1544.
Hiebert, S.W., Sun, W., Davis, J.N., Golub, T., Shurtleff, S., Buijs, A., Downing, J.R., Grosveld, G., Roussell, M.F., Gilliland, D.G*., et al.* (1996). The t(12;21) translocation converts AML-1B from an activator to a repressor of transcription. Molecular and cellular biology *16*, 1349-1355.

Hill, R.P. (2006). Identifying cancer stem cells in solid tumors: case not proven. Cancer research *66*, 1891-1895; discussion 1890.

Hock, H., Meade, E., Medeiros, S., Schindler, J.W., Valk, P.J., Fujiwara, Y., and Orkin, S.H. (2004). Tel/Etv6 is an essential and selective regulator of adult hematopoietic stem cell survival. Genes Dev *18*, 2336-2341.

Hong, D., Gupta, R., Ancliff, P., Atzberger, A., Brown, J., Soneji, S., Green, J., Colman, S., Piacibello, W., Buckle, V*., et al.* (2008). Initiating and cancer-propagating cells in TEL-AML1-associated childhood leukemia. Science *319*, 336-339.

Huang, G., Shigesada, K., Ito, K., Wee, H.J., Yokomizo, T., and Ito, Y. (2001). Dimerization with PEBP2beta protects RUNX1/AML1 from ubiquitin-proteasome-mediated degradation. The EMBO journal *20*, 723-733.

Huntly, B.J., Shigematsu, H., Deguchi, K., Lee, B.H., Mizuno, S., Duclos, N., Rowan, R., Amaral, S., Curley, D., Williams, I.R*., et al.* (2004). MOZ-TIF2, but not BCR-ABL, confers properties of leukemic stem cells to committed murine hematopoietic progenitors. Cancer Cell *6*, 587-596.

Ichikawa, M., Asai, T., Saito, T., Seo, S., Yamazaki, I., Yamagata, T., Mitani, K., Chiba, S., Ogawa, S., Kurokawa, M*., et al.* (2004). AML-1 is required for megakaryocytic maturation and lymphocytic

differentiation, but not for maintenance of hematopoietic stem cells in adult hematopoiesis. Nat Med *10*, 299-304.

Imai, Y., Kurokawa, M., Tanaka, K., Friedman, A.D., Ogawa, S., Mitani, K., Yazaki, Y., and Hirai, H. (1998). TLE, the human homolog of groucho, interacts with AML1 and acts as a repressor of AML1-induced transactivation. Biochemical and biophysical research communications *252*, 582-589.

Inaba, H., Greaves, M., and Mullighan, C.G. (2013). Acute lymphoblastic leukaemia. Lancet *381*, 1943-1955.

Irvin, B.J., Wood, L.D., Wang, L., Fenrick, R., Sansam, C.G., Packham, G., Kinch, M., Yang, E., and Hiebert, S.W. (2003a). TEL, a putative tumor suppressor, induces apoptosis and represses transcription of Bcl-XL. J Biol Chem *278*, 46378-46386.

Irvin, B.J., Wood, L.D., Wang, L., Fenrick, R., Sansam, C.G., Packham, G., Kinch, M., Yang, E., and Hiebert, S.W. (2003b). TEL, a putative tumor suppressor, induces apoptosis and represses transcription of Bcl-XL. The Journal of biological chemistry *278*, 46378-46386.

Ito, R., Takahashi, T., Katano, I., and Ito, M. (2012). Current advances in humanized mouse models. Cellular & molecular immunology *9*, 208-214.

Ivanovs, A., Rybtsov, S., Anderson, R.A., Turner, M.L., and Medvinsky, A. (2014). Identification of the niche and phenotype of the first human hematopoietic stem cells. Stem cell reports *2*, 449-456.

Kang, M.H., Kang, Y.H., Szymanska, B., Wilczynska-Kalak, U., Sheard, M.A., Harned, T.M., Lock, R.B., and Reynolds, C.P. (2007). Activity of vincristine, L-ASP, and dexamethasone against acute lymphoblastic leukemia is enhanced by the BH3-mimetic ABT-737 in vitro and in vivo. Blood *110*, 2057-2066.

Kebriaei, P., and Larson, R.A. (2003). Progress and challenges in the therapy of adult acute lymphoblastic leukemia. Curr Opin Hematol *10*, 284-289.

Kempski, H.M., and Sturt, N.T. (2000). The TEL-AML1 fusion accompanied by loss of the untranslocated TEL allele in B-precursor acute lymphoblastic leukaemia of childhood. Leukemia & lymphoma *40*, 39-47.

Kheifets, L., Ahlbom, A., Crespi, C.M., Draper, G., Hagihara, J., Lowenthal, R.M., Mezei, G., Oksuzyan, S., Schuz, J., Swanson, J*., et al.* (2010). Pooled analysis of recent studies on magnetic fields and childhood leukaemia. British journal of cancer *103*, 1128-1135.

Kiel, M.J., Yilmaz, O.H., Iwashita, T., Yilmaz, O.H., Terhorst, C., and Morrison, S.J. (2005). SLAM family receptors distinguish hematopoietic stem and progenitor cells and reveal endothelial niches for stem cells. Cell *121*, 1109-1121.

Kim, J., Sif, S., Jones, B., Jackson, A., Koipally, J., Heller, E., Winandy, S., Viel, A., Sawyer, A., Ikeda, T*., et al.* (1999). Ikaros DNA-binding proteins direct formation of chromatin remodeling complexes in lymphocytes. Immunity *10*, 345-355.

Kim, S.I., and Bresnick, E.H. (2007). Transcriptional control of erythropoiesis: emerging mechanisms and principles. Oncogene *26*, 6777-6794.

Kinlen, L. (2004). Infections and immune factors in cancer: the role of epidemiology. Oncogene *23*, 6341-6348.

Kirstetter, P., Thomas, M., Dierich, A., Kastner, P., and Chan, S. (2002). Ikaros is critical for B cell differentiation and function. European journal of immunology *32*, 720-730.

Klein, C.A. (2009). Parallel progression of primary tumours and metastases. Nature reviews Cancer *9*, 302-312.

Ko, D.H., Jeon, Y., Kang, H.J., Park, K.D., Shin, H.Y., Kim, H.K., Cho, H.I., Ahn, H.S., and Lee, D.S. (2011). Native ETV6 deletions accompanied by ETV6-RUNX1 rearrangements are associated with a favourable prognosis in childhood acute lymphoblastic leukaemia: a candidate for prognostic marker. British journal of haematology *155*, 530-533.

Kobayashi, H., Montgomery, K.T., Bohlander, S.K., Adra, C.N., Lim, B.L., Kucherlapati, R.S., Donis-Keller, H., Holt, M.S., Le Beau, M.M., and Rowley, J.D. (1994). Fluorescence in situ hybridization mapping of translocations and deletions involving the short arm of human chromosome 12 in malignant hematologic diseases. Blood *84*, 3473-3482.

Kong, Y., Yoshida, S., Saito, Y., Doi, T., Nagatoshi, Y., Fukata, M., Saito, N., Yang, S.M., Iwamoto, C., Okamura, J.*, et al.* (2008). CD34+CD38+CD19+ as well as CD34+CD38-CD19+ cells are leukemia-initiating cells with self-renewal capacity in human B-precursor ALL. Leukemia *22*, 1207-1213.

Kreso, A., and Dick, J.E. (2014). Evolution of the cancer stem cell model. Cell stem cell *14*, 275-291.
Kreso, A., O'Brien, C.A., van Galen, P., Gan, O.I., Notta, F., Brown, A.M., Ng, K., Ma, J., Wienholds, E., Dunant, C.*, et al.* (2013). Variable clonal repopulation dynamics influence chemotherapy response in colorectal cancer. Science *339*, 543-548.

Krivtsov, A.V., Twomey, D., Feng, Z., Stubbs, M.C., Wang, Y., Faber, J., Levine, J.E., Wang, J., Hahn, W.C., Gilliland, D.G.*, et al.* (2006). Transformation from committed progenitor to leukaemia stem cell initiated by MLL-AF9. Nature *442*, 818-822.

Kuiper, R.P., Schoenmakers, E.F., van Reijmersdal, S.V., Hehir-Kwa, J.Y., van Kessel, A.G., van Leeuwen, F.N., and Hoogerbrugge, P.M. (2007). High-resolution genomic profiling of childhood ALL reveals novel recurrent genetic lesions affecting pathways involved in lymphocyte differentiation and cell cycle progression. Leukemia *21*, 1258-1266.

Kurokawa, M., and Hirai, H. (2003). Role of AML1/Runx1 in the pathogenesis of hematological malignancies. Cancer science *94*, 841-846.

Kwiatkowski, B.A., Bastian, L.S., Bauer, T.R., Jr., Tsai, S., Zielinska-Kwiatkowska, A.G., and Hickstein, D.D. (1998). The ets family member Tel binds to the Fli-1 oncoprotein and inhibits its transcriptional activity. The Journal of biological chemistry *273*, 17525-17530.

Lai, A.Y., and Kondo, M. (2006). Asymmetrical lymphoid and myeloid lineage commitment in multipotent hematopoietic progenitors. The Journal of experimental medicine *203*, 1867-1873.

Lai, A.Y., Lin, S.M., and Kondo, M. (2005). Heterogeneity of Flt3-expressing multipotent progenitors in mouse bone marrow. Journal of immunology *175*, 5016-5023.

Landau, D.A., Carter, S.L., Getz, G., and Wu, C.J. (2014). Clonal evolution in hematological malignancies and therapeutic implications. Leukemia *28*, 34-43.

Landau, D.A., Carter, S.L., Stojanov, P., McKenna, A., Stevenson, K., Lawrence, M.S., Sougnez, C., Stewart, C., Sivachenko, A., Wang, L.*, et al.* (2013). Evolution and impact of subclonal mutations in chronic lymphocytic leukemia. Cell *152*, 714-726.

Lausten-Thomsen, U., Madsen, H.O., Vestergaard, T.R., Hjalgrim, H., Nersting, J., and Schmiegelow, K. (2011). Prevalence of t(12;21)[ETV6-RUNX1]-positive cells in healthy neonates. Blood *117*, 186-189.

Liem, N.L., Papa, R.A., Milross, C.G., Schmid, M.A., Tajbakhsh, M., Choi, S., Ramirez, C.D., Rice, A.M., Haber, M., Norris, M.D.*, et al.* (2004). Characterization of childhood acute lymphoblastic leukemia xenograft models for the preclinical evaluation of new therapies. Blood *103*, 3905-3914.
Lin, H., and Grosschedl, R. (1995). Failure of B-cell differentiation in mice lacking the transcription factor EBF. Nature *376*, 263-267.

Linabery, A.M., and Ross, J.A. (2008). Trends in childhood cancer incidence in the U.S. (1992-2004). Cancer *112*, 416-432.

Lock, R.B., Liem, N., Farnsworth, M.L., Milross, C.G., Xue, C., Tajbakhsh, M., Haber, M., Norris, M.D., Marshall, G.M., and Rice, A.M. (2002). The nonobese diabetic/severe combined immunodeficient (NOD/SCID) mouse model of childhood acute lymphoblastic leukemia reveals intrinsic differences in biologic characteristics at diagnosis and relapse. Blood *99*, 4100-4108.

Loh, M.L., and Rubnitz, J.E. (2002). TEL/AML1-positive pediatric leukemia: prognostic significance and therapeutic approaches. Current opinion in hematology *9*, 345-352.

Loncarevic, I.F., Roitzheim, B., Ritterbach, J., Viehmann, S., Borkhardt, A., Lampert, F., and Harbott, J. (1999). Trisomy 21 is a recurrent secondary aberration in childhood acute lymphoblastic leukemia with TEL/AML1 gene fusion. Genes, chromosomes & cancer *24*, 272-277.

Lutz, C., Woll, P.S., Hall, G., Castor, A., Dreau, H., Cazzaniga, G., Zuna, J., Jensen, C., Clark, S.A., Biondi, A.*, et al.* (2013). Quiescent leukaemic cells account for minimal residual disease in childhood lymphoblastic leukaemia. Leukemia *27*, 1204-1207.

Maley, C.C., Galipeau, P.C., Li, X., Sanchez, C.A., Paulson, T.G., and Reid, B.J. (2004). Selectively advantageous mutations and hitchhikers in neoplasms: p16 lesions are selected in Barrett's esophagus. Cancer research *64*, 3414-3427.

Martinez, P., Birkbak, N.J., Gerlinger, M., McGranahan, N., Burrell, R.A., Rowan, A.J., Joshi, T., Fisher, R., Larkin, J., Szallasi, Z.*, et al.* (2013). Parallel evolution of tumour subclones mimics diversity between tumours. The Journal of pathology *230*, 356-364.

Marusyk, A., and Polyak, K. (2010). Tumor heterogeneity: causes and consequences. Biochimica et biophysica acta *1805*, 105-117.

Marusyk, A., and Polyak, K. (2013). Cancer. Cancer cell phenotypes, in fifty shades of grey. Science *339*, 528-529.

Mazurier, F., Doedens, M., Gan, O.I., and Dick, J.E. (2003). Rapid myeloerythroid repopulation after intrafemoral transplantation of NOD-SCID mice reveals a new class of human stem cells. Nature medicine *9*, 959-963.

Merlo, L.M., Pepper, J.W., Reid, B.J., and Maley, C.C. (2006). Cancer as an evolutionary and ecological process. Nature reviews Cancer *6*, 924-935.

Metcalf, D. (2010). The colony-stimulating factors and cancer. Nature reviews Cancer *10*, 425-434.
Meyer, L.H., and Debatin, K.M. (2011). Diversity of human leukemia xenograft mouse models: implications for disease biology. Cancer research *71*, 7141-7144.

Meyer, L.H., Eckhoff, S.M., Queudeville, M., Kraus, J.M., Giordan, M., Stursberg, J., Zangrando, A., Vendramini, E., Moricke, A., Zimmermann, M.*, et al.* (2011). Early relapse in ALL is identified by time to leukemia in NOD/SCID mice and is characterized by a gene signature involving survival pathways. Cancer cell *19*, 206-217.

Michor, F., and Polyak, K. (2010). The origins and implications of intratumor heterogeneity. Cancer prevention research *3*, 1361-1364.

Moore, M.A., Williams, N., and Metcalf, D. (1973). In vitro colony formation by normal and leukemic human hematopoietic cells: characterization of the colony-forming cells. Journal of the National Cancer Institute *50*, 603-623.

Mori, H., Colman, S.M., Xiao, Z., Ford, A.M., Healy, L.E., Donaldson, C., Hows, J.M., Navarrete, C., and Greaves, M. (2002a). Chromosome translocations and covert leukemic clones are generated during normal fetal development. Proceedings of the National Academy of Sciences of the United States of America *99*, 8242-8247.

Mori, H., Colman, S.M., Xiao, Z., Ford, A.M., Healy, L.E., Donaldson, C., Hows, J.M., Navarrete, C., and Greaves, M. (2002b). Chromosome translocations and covert leukemic clones are generated during normal fetal development. Proc Natl Acad Sci U S A *99*, 8242-8247.

Morrison, S.J., and Weissman, I.L. (1994). The long-term repopulating subset of hematopoietic stem cells is deterministic and isolatable by phenotype. Immunity *1*, 661-673.

Morrow, M., Horton, S., Kioussis, D., Brady, H.J., and Williams, O. (2004). TEL-AML1 promotes development of specific hematopoietic lineages consistent with preleukemic activity. Blood *103*, 3890-3896.

Mullighan, C.G. (2012). The molecular genetic makeup of acute lymphoblastic leukemia. Hematology / the Education Program of the American Society of Hematology American Society of Hematology Education Program *2012*, 389-396.

Mullighan, C.G., Goorha, S., Radtke, I., Miller, C.B., Coustan-Smith, E., Dalton, J.D., Girtman, K., Mathew, S., Ma, J., Pounds, S.B.*, et al.* (2007). Genome-wide analysis of genetic alterations in acute lymphoblastic leukaemia. Nature *446*, 758-764.

Mullighan, C.G., Phillips, L.A., Su, X., Ma, J., Miller, C.B., Shurtleff, S.A., and Downing, J.R. (2008). Genomic analysis of the clonal origins of relapsed acute lymphoblastic leukemia. Science *322*, 1377-1380.

Mullighan, C.G., Su, X., Zhang, J., Radtke, I., Phillips, L.A., Miller, C.B., Ma, J., Liu, W., Cheng, C., Schulman, B.A.*, et al.* (2009). Deletion of IKZF1 and prognosis in acute lymphoblastic leukemia. N Engl J Med *360*, 470-480.

Navin, N., Kendall, J., Troge, J., Andrews, P., Rodgers, L., McIndoo, J., Cook, K., Stepansky, A., Levy, D., Esposito, D.*, et al.* (2011). Tumour evolution inferred by single-cell sequencing. Nature *472*, 90-94.
Navin, N., Krasnitz, A., Rodgers, L., Cook, K., Meth, J., Kendall, J., Riggs, M., Eberling, Y., Troge, J., Grubor, V.*, et al.* (2010). Inferring tumor progression from genomic heterogeneity. Genome research *20*, 68-80.

Navin, N.E., and Hicks, J. (2010). Tracing the tumor lineage. Molecular oncology *4*, 267-283.
Ng, S.Y., Yoshida, T., Zhang, J., and Georgopoulos, K. (2009). Genome-wide lineage-specific transcriptional networks underscore Ikaros-dependent lymphoid priming in hematopoietic stem cells. Immunity *30*, 493-507.

Niebuhr, B., Kriebitzsch, N., Fischer, M., Behrens, K., Gunther, T., Alawi, M., Bergholz, U., Muller, U., Roscher, S., Ziegler, M.*, et al.* (2013). Runx1 is essential at two stages of early murine B-cell development. Blood *122*, 413-423.

Nik-Zainal, S., Van Loo, P., Wedge, D.C., Alexandrov, L.B., Greenman, C.D., Lau, K.W., Raine, K., Jones, D., Marshall, J., Ramakrishna, M.*, et al.* (2012). The life history of 21 breast cancers. Cell *149*, 994-1007.

Notta, F., Doulatov, S., Laurenti, E., Poeppl, A., Jurisica, I., and Dick, J.E. (2011a). Isolation of single human hematopoietic stem cells capable of long-term multilineage engraftment. Science *333*, 218-221.

Notta, F., Mullighan, C.G., Wang, J.C., Poeppl, A., Doulatov, S., Phillips, L.A., Ma, J., Minden, M.D., Downing, J.R., and Dick, J.E. (2011b). Evolution of human BCR-ABL1 lymphoblastic leukaemia-initiating cells. Nature *469*, 362-367.

Nowell, P.C. (1976). The clonal evolution of tumor cell populations. Science *194*, 23-28.
Nutt, S.L., Heavey, B., Rolink, A.G., and Busslinger, M. (1999). Commitment to the B-lymphoid lineage depends on the transcription factor Pax5. Nature *401*, 556-562.

Nutt, S.L., Urbanek, P., Rolink, A., and Busslinger, M. (1997). Essential functions of Pax5 (BSAP) in pro-B cell development: difference between fetal and adult B lymphopoiesis and reduced V-to-DJ recombination at the IgH locus. Genes & development *11*, 476-491.

Oikawa, T., and Yamada, T. (2003). Molecular biology of the Ets family of transcription factors. Gene *303*, 11-34.

Olsen, M., Madsen, H.O., Hjalgrim, H., Gregers, J., Rostgaard, K., and Schmiegelow, K. (2006). Preleukemic TEL-AML1-positive clones at cell level of 10(-3) to 10(-4) do not persist into adulthood. Journal of pediatric hematology/oncology *28*, 734-740.

Orkin, S.H. (1995). Hematopoiesis: how does it happen? Current opinion in cell biology *7*, 870-877.
Orkin, S.H. (2000). Diversification of haematopoietic stem cells to specific lineages. Nature reviews Genetics *1*, 57-64.

Orkin, S.H., and Zon, L.I. (2008). Hematopoiesis: an evolving paradigm for stem cell biology. Cell *132*, 631-644.

Panzer-Grumayer, E.R., Cazzaniga, G., van der Velden, V.H., del Giudice, L., Peham, M., Mann, G., Eckert, C., Schrauder, A., Germano, G., Harbott, J.*, et al.* (2005). Immunogenotype changes prevail in relapses of young children with TEL-AML1-positive acute lymphoblastic leukemia and derive mainly from clonal selection. Clinical cancer research : an official journal of the American Association for Cancer Research *11*, 7720-7727.

Papaemmanuil, E., Rapado, I., Li, Y., Potter, N.E., Wedge, D.C., Tubio, J., Alexandrov, L.B., Van Loo, P., Cooke, S.L., Marshall, J.*, et al.* (2014). RAG-mediated recombination is the predominant driver of oncogenic rearrangement in ETV6-RUNX1 acute lymphoblastic leukemia. Nature genetics *46*, 116-125.

Pardanani, A., and Tefferi, A. (2004). Imatinib therapy for hypereosinophilic syndrome and eosinophilia-associated myeloproliferative disorders. Leukemia research *28 Suppl 1*, S47-52.
Parsons, D.W., Jones, S., Zhang, X., Lin, J.C., Leary, R.J., Angenendt, P., Mankoo, P., Carter, H., Siu, I.M., Gallia, G.L.*, et al.* (2008). An integrated genomic analysis of human glioblastoma multiforme. Science *321*, 1807-1812.

Peschon, J.J., Morrissey, P.J., Grabstein, K.H., Ramsdell, F.J., Maraskovsky, E., Gliniak, B.C., Park, L.S., Ziegler, S.F., Williams, D.E., Ware, C.B.*, et al.* (1994). Early lymphocyte expansion is severely impaired in interleukin 7 receptor-deficient mice. The Journal of experimental medicine *180*, 1955-1960.

Petrie, K., Guidez, F., Howell, L., Healy, L., Waxman, S., Greaves, M., and Zelent, A. (2003). The histone deacetylase 9 gene encodes multiple protein isoforms. The Journal of biological chemistry *278*, 16059-16072.

Piccirillo, S.G., Combi, R., Cajola, L., Patrizi, A., Redaelli, S., Bentivegna, A., Baronchelli, S., Maira, G., Pollo, B., Mangiola, A.*, et al.* (2009). Distinct pools of cancer stem-like cells coexist within human glioblastomas and display different tumorigenicity and independent genomic evolution. Oncogene *28*, 1807-1811.

Pieper, K., Grimbacher, B., and Eibel, H. (2013). B-cell biology and development. The Journal of allergy and clinical immunology *131*, 959-971.

Pixley, F.J., and Stanley, E.R. (2004). CSF-1 regulation of the wandering macrophage: complexity in action. Trends in cell biology *14*, 628-638.

Puel, A., Ziegler, S.F., Buckley, R.H., and Leonard, W.J. (1998). Defective IL7R expression in T(-)B(+)NK(+) severe combined immunodeficiency. Nature genetics *20*, 394-397.

Pui, C.H., Carroll, W.L., Meshinchi, S., and Arceci, R.J. (2011). Biology, risk stratification, and therapy of pediatric acute leukemias: an update. Journal of clinical oncology : official journal of the American Society of Clinical Oncology *29*, 551-565.

Pui, C.H., Relling, M.V., and Downing, J.R. (2004). Acute lymphoblastic leukemia. N Engl J Med *350*, 1535-1548.
Quesnel, B., Preudhomme, C., Philippe, N., Vanrumbeke, M., Dervite, I., Lai, J.L., Bauters, F., Wattel, E., and Fenaux, P. (1995). p16 gene homozygous deletions in acute lymphoblastic leukemia. Blood *85*, 657-663.

Raaijmakers, M.H., Mukherjee, S., Guo, S., Zhang, S., Kobayashi, T., Schoonmaker, J.A., Ebert, B.L., Al-Shahrour, F., Hasserjian, R.P., Scadden, E.O.*, et al.* (2010). Bone progenitor dysfunction induces myelodysplasia and secondary leukaemia. Nature *464*, 852-857.

Raynaud, S., Cave, H., Baens, M., Bastard, C., Cacheux, V., Grosgeorge, J., Guidal-Giroux, C., Guo, C., Vilmer, E., Marynen, P.*, et al.* (1996). The 12;21 translocation involving TEL and deletion of the other TEL allele: two frequently associated alterations found in childhood acute lymphoblastic leukemia. Blood *87*, 2891-2899.

Revilla, I.D.R., Bilic, I., Vilagos, B., Tagoh, H., Ebert, A., Tamir, I.M., Smeenk, L., Trupke, J., Sommer, A., Jaritz, M.*, et al.* (2012). The B-cell identity factor Pax5 regulates distinct transcriptional programmes in early and late B lymphopoiesis. The EMBO journal *31*, 3130-3146.

Reya, T. (2003). Regulation of hematopoietic stem cell self-renewal. Recent progress in hormone research *58*, 283-295.

Reynaud, D., Demarco, I.A., Reddy, K.L., Schjerven, H., Bertolino, E., Chen, Z., Smale, S.T., Winandy, S., and Singh, H. (2008). Regulation of B cell fate commitment and immunoglobulin heavy-chain gene rearrangements by Ikaros. Nature immunology *9*, 927-936.

Rieger, M.A., and Schroeder, T. (2012). Hematopoiesis. Cold Spring Harbor perspectives in biology *4*.

Rompaey, L.V., Potter, M., Adams, C., and Grosveld, G. (2000). Tel induces a G1 arrest and suppresses Ras-induced transformation. Oncogene *19*, 5244-5250.

Rubnitz, J.E., Behm, F.G., Wichlan, D., Ryan, C., Sandlund, J.T., Ribeiro, R.C., Rivera, G.K., Hancock, M.L., Relling, M.V., Evans, W.E.*, et al.* (1999). Low frequency of TEL-AML1 in relapsed acute lymphoblastic leukemia supports a favorable prognosis for this genetic subgroup. Leukemia *13*, 19-21.

Rubnitz, J.E., Shuster, J.J., Land, V.J., Link, M.P., Pullen, D.J., Camitta, B.M., Pui, C.H., Downing, J.R., and Behm, F.G. (1997). Case-control study suggests a favorable impact of TEL rearrangement in patients with B-lineage acute lymphoblastic leukemia treated with antimetabolite-based therapy: a Pediatric Oncology Group study. Blood *89*, 1143-1146.

Sabbattini, P., Lundgren, M., Georgiou, A., Chow, C., Warnes, G., and Dillon, N. (2001). Binding of Ikaros to the lambda5 promoter silences transcription through a mechanism that does not require heterochromatin formation. The EMBO journal *20*, 2812-2822.

Sanchez, P.V., Perry, R.L., Sarry, J.E., Perl, A.E., Murphy, K., Swider, C.R., Bagg, A., Choi, J.K., Biegel, J.A., Danet-Desnoyers, G.*, et al.* (2009). A robust xenotransplantation model for acute myeloid leukemia. Leukemia *23*, 2109-2117.
Schindler, J.W., Van Buren, D., Foudi, A., Krejci, O., Qin, J., Orkin, S.H., and Hock, H. (2009). TEL-AML1 corrupts hematopoietic stem cells to persist in the bone marrow and initiate leukemia. Cell stem cell *5*, 43-53.

Schmitz, M., Breithaupt, P., Scheidegger, N., Cario, G., Bonapace, L., Meissner, B., Mirkowska, P., Tchinda, J., Niggli, F.K., Stanulla, M.*, et al.* (2011). Xenografts of highly resistant leukemia recapitulate the clonal composition of the leukemogenic compartment. Blood *118*, 1854-1864.

Schofield, R. (1978). The relationship between the spleen colony-forming cell and the haemopoietic stem cell. Blood cells *4*, 7-25.

Seeger, K., Adams, H.P., Buchwald, D., Beyermann, B., Kremens, B., Niemeyer, C., Ritter, J., Schwabe, D., Harms, D., Schrappe, M.*, et al.* (1998). TEL-AML1 fusion transcript in relapsed childhood acute lymphoblastic leukemia. The Berlin-Frankfurt-Munster Study Group. Blood *91*, 1716-1722.

Seet, C.S., Brumbaugh, R.L., and Kee, B.L. (2004). Early B cell factor promotes B lymphopoiesis with reduced interleukin 7 responsiveness in the absence of E2A. The Journal of experimental medicine *199*, 1689-1700.

Shah, N.P., Nicoll, J.M., Nagar, B., Gorre, M.E., Paquette, R.L., Kuriyan, J., and Sawyers, C.L. (2002). Multiple BCR-ABL kinase domain mutations confer polyclonal resistance to the tyrosine kinase inhibitor imatinib (STI571) in chronic phase and blast crisis chronic myeloid leukemia. Cancer cell *2*, 117-125.

Shah, S.J., Taub, J.W., Witt, T.L., Pollock, B.H., Ding, B.C., Moore, D.S., Amylon, M., Pullen, J., Ravindranath, Y., and Matherly, L.H. (2001). Relationship of p15 and p16 gene alterations to elevated dihydrofolate reductase in childhood acute lymphoblastic leukaemia. British journal of haematology *113*, 746-756.

Shah, S.P., Morin, R.D., Khattra, J., Prentice, L., Pugh, T., Burleigh, A., Delaney, A., Gelmon, K., Guliany, R., Senz, J.*, et al.* (2009). Mutational evolution in a lobular breast tumour profiled at single nucleotide resolution. Nature *461*, 809-813.

Shah, S.P., Roth, A., Goya, R., Oloumi, A., Ha, G., Zhao, Y., Turashvili, G., Ding, J., Tse, K., Haffari, G.*, et al.* (2012). The clonal and mutational evolution spectrum of primary triple-negative breast cancers. Nature *486*, 395-399.

Shurtleff, S.A., Buijs, A., Behm, F.G., Rubnitz, J.E., Raimondi, S.C., Hancock, M.L., Chan, G.C., Pui, C.H., Grosveld, G., and Downing, J.R. (1995). TEL/AML1 fusion resulting from a cryptic t(12;21) is the most common genetic lesion in pediatric ALL and defines a subgroup of patients with an excellent prognosis. Leukemia *9*, 1985-1989.

Siolas, D., and Hannon, G.J. (2013). Patient-derived tumor xenografts: transforming clinical samples into mouse models. Cancer research *73*, 5315-5319.

Sloma, I., and Eaves, C.J. (2009). TEL me all. Cell stem cell *5*, 5-6.
Smith, E.M., Gisler, R., and Sigvardsson, M. (2002). Cloning and characterization of a promoter flanking the early B cell factor (EBF) gene indicates roles for E-proteins and autoregulation in the control of EBF expression. J Immunol *169*, 261-270.

Spangrude, G.J., Heimfeld, S., and Weissman, I.L. (1988). Purification and characterization of mouse hematopoietic stem cells. Science *241*, 58-62.

Suda, T., Arai, F., and Hirao, A. (2005). Hematopoietic stem cells and their niche. Trends in immunology *26*, 426-433.
Szymanska, B., Wilczynska-Kalak, U., Kang, M.H., Liem, N.L., Carol, H., Boehm, I., Groepper, D., Reynolds, C.P., Stewart, C.F., and Lock, R.B. (2012). Pharmacokinetic modeling of an induction regimen for in vivo combined testing of novel drugs against pediatric acute lymphoblastic leukemia xenografts. PLoS One *7*, e33894.

Taussig, D.C., Vargaftig, J., Miraki-Moud, F., Griessinger, E., Sharrock, K., Luke, T., Lillington, D., Oakervee, H., Cavenagh, J., Agrawal, S.G.*, et al.* (2010). Leukemia-initiating cells from some acute myeloid leukemia patients with mutated nucleophosmin reside in the CD34(-) fraction. Blood *115*, 1976-1984.

Teitell, M.A., and Pandolfi, P.P. (2009). Molecular genetics of acute lymphoblastic leukemia. Annual review of pathology *4*, 175-198.

Thirlwell, C., Will, O.C., Domingo, E., Graham, T.A., McDonald, S.A., Oukrif, D., Jeffrey, R., Gorman, M., Rodriguez-Justo, M., Chin-Aleong, J.*, et al.* (2010). Clonality assessment and clonal ordering of individual neoplastic crypts shows polyclonality of colorectal adenomas. Gastroenterology *138*, 1441-1454, 1454 e1441-1447.

Tsapogas, P., Zandi, S., Ahsberg, J., Zetterblad, J., Welinder, E., Jonsson, J.I., Mansson, R., Qian, H., and Sigvardsson, M. (2011). IL-7 mediates Ebf-1-dependent lineage restriction in early lymphoid progenitors. Blood *118*, 1283-1290.

Tsuzuki, S., Seto, M., Greaves, M., and Enver, T. (2004). Modeling first-hit functions of the t(12;21) TEL-AML1 translocation in mice. Proceedings of the National Academy of Sciences of the United States of America *101*, 8443-8448.

Uchida, H., Downing, J.R., Miyazaki, Y., Frank, R., Zhang, J., and Nimer, S.D. (1999). Three distinct domains in TEL-AML1 are required for transcriptional repression of the IL-3 promoter. Oncogene *18*, 1015-1022.

Uckun, F.M., Sather, H., Reaman, G., Shuster, J., Land, V., Trigg, M., Gunther, R., Chelstrom, L., Bleyer, A., Gaynon, P.*, et al.* (1995). Leukemic cell growth in SCID mice as a predictor of relapse in high-risk B-lineage acute lymphoblastic leukemia. Blood *85*, 873-878.

Urbanek, P., Wang, Z.Q., Fetka, I., Wagner, E.F., and Busslinger, M. (1994). Complete block of early B cell differentiation and altered patterning of the posterior midbrain in mice lacking Pax5/BSAP. Cell *79*, 901-912.

van Delft, F.W., Horsley, S., Colman, S., Anderson, K., Bateman, C., Kempski, H., Zuna, J., Eckert, C., Saha, V., Kearney, L.*, et al.* (2011). Clonal origins of relapse in ETV6-RUNX1 acute lymphoblastic leukemia. Blood *117*, 6247-6254.

van der Weyden, L., Giotopoulos, G., Rust, A.G., Matheson, L.S., van Delft, F.W., Kong, J., Corcoran, A.E., Greaves, M.F., Mullighan, C.G., Huntly, B.J.*, et al.* (2011). Modeling the evolution of ETV6-RUNX1-induced B-cell precursor acute lymphoblastic leukemia in mice. Blood *118*, 1041-1051.

van Galen, P., Kreso, A., Wienholds, E., Laurenti, E., Eppert, K., Lechman, E.R., Mbong, N., Hermans, K., Dobson, S., April, C.*, et al.* (2014). Reduced lymphoid lineage priming promotes human hematopoietic stem cell expansion. Cell stem cell *14*, 94-106.

von Freeden-Jeffry, U., Vieira, P., Lucian, L.A., McNeil, T., Burdach, S.E., and Murray, R. (1995). Lymphopenia in interleukin (IL)-7 gene-deleted mice identifies IL-7 as a nonredundant cytokine. The Journal of experimental medicine *181*, 1519-1526.

Wagner, W., Horn, P., Bork, S., and Ho, A.D. (2008). Aging of hematopoietic stem cells is regulated by the stem cell niche. Experimental gerontology *43*, 974-980.

Walter, M.J., Shen, D., Ding, L., Shao, J., Koboldt, D.C., Chen, K., Larson, D.E., McLellan, M.D., Dooling, D., Abbott, R.*, et al.* (2012). Clonal architecture of secondary acute myeloid leukemia. N Engl J Med *366*, 1090-1098.

Wang, J.H., Nichogiannopoulou, A., Wu, L., Sun, L., Sharpe, A.H., Bigby, M., and Georgopoulos, K. (1996a). Selective defects in the development of the fetal and adult lymphoid system in mice with an Ikaros null mutation. Immunity *5*, 537-549.

Wang, L., and Hiebert, S.W. (2001). TEL contacts multiple co-repressors and specifically associates with histone deacetylase-3. Oncogene *20*, 3716-3725.

Wang, L.C., Kuo, F., Fujiwara, Y., Gilliland, D.G., Golub, T.R., and Orkin, S.H. (1997). Yolk sac angiogenic defect and intra-embryonic apoptosis in mice lacking the Ets-related factor TEL. The EMBO journal *16*, 4374-4383.

Wang, L.C., Swat, W., Fujiwara, Y., Davidson, L., Visvader, J., Kuo, F., Alt, F.W., Gilliland, D.G., Golub, T.R., and Orkin, S.H. (1998). The TEL/ETV6 gene is required specifically for hematopoiesis in the bone marrow. Genes & development *12*, 2392-2402.

Wang, L.D., and Wagers, A.J. (2011). Dynamic niches in the origination and differentiation of haematopoietic stem cells. Nature reviews Molecular cell biology *12*, 643-655.

Wang, Q., Stacy, T., Binder, M., Marin-Padilla, M., Sharpe, A.H., and Speck, N.A. (1996b). Disruption of the Cbfa2 gene causes necrosis and hemorrhaging in the central nervous system and blocks definitive hematopoiesis. Proceedings of the National Academy of Sciences of the United States of America *93*, 3444-3449.

Wasylyk, B., Hahn, S.L., and Giovane, A. (1993). The Ets family of transcription factors. European journal of biochemistry / FEBS *211*, 7-18.

Woiterski, J., Ebinger, M., Witte, K.E., Goecke, B., Heininger, V., Philippek, M., Bonin, M., Schrauder, A., Rottgers, S., Herr, W.*, et al.* (2013). Engraftment of low numbers of pediatric acute lymphoid and myeloid leukemias into NOD/SCID/IL2Rcgammanull mice reflects individual leukemogenecity and highly correlates with clinical outcome. International journal of cancer Journal international du cancer *133*, 1547-1556.

Woo, H.Y., Kim, D.W., Park, H., Seong, K.W., Koo, H.H., and Kim, S.H. (2005). Molecular cytogenetic analysis of gene rearrangements in childhood acute lymphoblastic leukemia. J Korean Med Sci *20*, 36-41.

Wu, X., Northcott, P.A., Dubuc, A., Dupuy, A.J., Shih, D.J., Witt, H., Croul, S., Bouffet, E., Fults, D.W., Eberhart, C.G.*, et al.* (2012). Clonal selection drives genetic divergence of metastatic medulloblastoma. Nature *482*, 529-533.

Yachida, S., Jones, S., Bozic, I., Antal, T., Leary, R., Fu, B., Kamiyama, M., Hruban, R.H., Eshleman, J.R., Nowak, M.A.*, et al.* (2010). Distant metastasis occurs late during the genetic evolution of pancreatic cancer. Nature *467*, 1114-1117.

Yates, L.R., and Campbell, P.J. (2012). Evolution of the cancer genome. Nature reviews Genetics *13*, 795-806.

Yeoh, E.J., Ross, M.E., Shurtleff, S.A., Williams, W.K., Patel, D., Mahfouz, R., Behm, F.G., Raimondi, S.C., Relling, M.V., Patel, A.*, et al.* (2002). Classification, subtype discovery, and prediction of outcome in pediatric acute lymphoblastic leukemia by gene expression profiling. Cancer cell *1*, 133-143.

Zhang, J., Niu, C., Ye, L., Huang, H., He, X., Tong, W.G., Ross, J., Haug, J., Johnson, T., Feng, J.Q.*, et al.* (2003). Identification of the haematopoietic stem cell niche and control of the niche size. Nature *425*, 836-841.

Zhuang, Y., Soriano, P., and Weintraub, H. (1994). The helix-loop-helix gene E2A is required for B cell formation. Cell *79*, 875-884.

Zuna, J., Hrusak, O., Kalinova, M., Muzikova, K., Stary, J., and Trka, J. (1999). TEL/AML1 positivity in childhood ALL: average or better prognosis? Czech Paediatric Haematology Working Group. Leukemia *13*, 22-24.